SYNTHESIS OF CONDUCTING POLYMERS

CENTRE FOR NEWFOUNDLAND STUDIES

TOTAL OF 10 PAGES ONLY
MAY BE XEROXED

(Without Author's Permission)

FANG HUANG

National Library
of Canada

Acquisitions and
Bibliographic Services

395 Wellington Street
Ottawa ON K1A 0N4
Canada

Bibliothèque nationale
du Canada

Acquisisitons et
services bibliographiques

395, rue Wellington
Ottawa ON K1A 0N4
Canada

Your file Votre référence
ISBN: 0-612-93033-5
Our file Notre référence
ISBN: 0-612-93033-5

The author has granted a non-exclusive licence allowing the National Library of Canada to reproduce, loan, distribute or sell copies of this thesis in microform, paper or electronic formats.

The author retains ownership of the copyright in this thesis. Neither the thesis nor substantial extracts from it may be printed or otherwise reproduced without the author's permission.

L'auteur a accordé une licence non exclusive permettant à la Bibliothèque nationale du Canada de reproduire, prêter, distribuer ou vendre des copies de cette thèse sous la forme de microfiche/film, de reproduction sur papier ou sur format électronique.

L'auteur conserve la propriété du droit d'auteur qui protège cette thèse. Ni la thèse ni des extraits substantiels de celle-ci ne doivent être imprimés ou aturement reproduits sans son autorisation.

In compliance with the Canadian Privacy Act some supporting forms may have been removed from this dissertation.

While these forms may be included in the document page count, their removal does not represent any loss of content from the dissertation.

Conformément à la loi canadienne sur la protection de la vie privée, quelques formulaires secondaires ont été enlevés de ce manuscrit.

Bien que ces formulaires aient inclus dans la pagination, il n'y aura aucun contenu manquant.

Canada

Synthesis of Conducting Polymers

by

Fang Huang

B. Sc., Huazhong University of Science and Technology
Wuhan, Hubei, China 1997

A thesis submitted to the School of Graduate
Studies in partial fulfillment of the
Requirements for the degree of
Master of Science

Department of Chemistry
Memorial University of Newfoundland
St. John's, Newfoundland, Canada
June, 2003

Abstract

A series of novel electronic conducting polymers has been prepared as potential low band gap materials. Stille coupling reactions were employed for the polymerization of 2,7-dibromospiro[4',4'-dioctyl-2',6'-dioxocyclohexane]-1',9-fluorene (**2-9**) with 1,4-bis(trimethylstannyl)benzene (**2-20**), 2,5-bis(trimethylstannyl)-furan (**2-28**) and 2,5-bis(trimethylstannyl)thiophene (**2-5**) to yield precursor polymers poly(2,7-spiro[4',4'-dioctyl-2',6'-dioxocyclohexane]-1',9-fluorene-*co*-1,4-benzene) (**PFKB**), poly(2,7-spiro[4',4'- dioctyl-2',6'-dioxocyclohexane]-1',9-fluorene-*co*-2,5-furan) (**PFKF**) and poly(2,7-spiro[4',4'-dioctyl-2',6'-dioxocyclohexane]-1',9-fluorene-*co*-2,5-thiophene) (**PFKT**). The precursor polymers have been converted to target fluorenone-based polymers by deacetylisation of the acetal substituents to the ketones. Model compounds have been synthesized as compounds **2-15** and **2-16**. Compound **2-15** was converted to **2-16** to explore the method for conversion of the precursor polymers. The fluorenone-thiophene copolymer, **PFT**, gave the lowest band gap as ca. 1.6 eV.

The known ionic conducting polymers poly[2,2'-(4,4'-oxydiphenylene)-5,5'-bibenzimidazole] (**PBI-1**), poly[2,2'-(4,4'-sulfonyldiphenylene)-5,5'-bibenzimidazole] (**PBI-2**), poly[2,2'-(4,4'-oxydiphenylene)sulfonyl-5,5'-bibenzimidazole] (**PBI-3**) have been synthesized. **PBI-1** was cast as a thin film and doped with phosphoric acid. The ionic conductivity was 2.06 x 10^{-2} s cm^{-1} at 80 °C.

Acknowledgments

I would like to express my gratitude to my supervisor, Dr. Peter Pickup for his guidance, advice, help and assistance.

I extend my gratitude to my supervisory committee, Dr. Bob Helleur and Dr. Paris Georghiou for their advice on my research and thesis. I am grateful to Dr. Chaojie Song and Ms. Kavithaa Loganathan for electrochemical testing and my other colleagues in the Pickup research group for their kindly help. I appreciate the help from technical and support staff, as are those of Mr. Dave Miller and Ms. Rosemarie Harvey for NMR, Ms. Linda Winsor for MADLI and HPLC. I am grateful to the Chemistry Department, the School of Graduate Studies, Memorial University of Newfoundland and NSTRC for financial support.

Finally I would like to express my gratitude to my parents for having given me the gift of life.

Table of contents

Glossary of Abbreviations

PLED	polymer light-emitting diode
M_w	weight average molar mass
M_n	number average molar mass
HOMO	highest occupied molecular orbital
LUMO	lowest unoccupied molecular orbital
E_g	band gap
SPEM	solid polymer electrolyte membrane
PEMFC	polymer electrolyte membrane fuel cell
PBI	polybenzimidazole
PPA	poly(phosphoric acid)
GPC	gel permeation chromatography
THF	tetrahydrofuran
MALDI-TOF MS	matrix-assisted laser desorption / ionization time-of-flight mass spectrometry
IR	infrared (spectroscopy)
Uv-vis	ultraviolet-visible
NMR	nuclear magnetic resonance (spectroscopy)
Mp	melting point
DMF	*N,N*-dimethyl formamide
CB	conduction band
VB	valence band
DMSO	dimethyl sulfoxide
DMAc	*N,N*-dimethyl acetamide
COD	1,5-cyclooctadiene

List of figures

List of tables

List of schemes

Chapter 1

Introduction

1.1 Electrical conduction

Electrical conduction is a term used to describe the transport of charge carriers under the effect of an electrical field. In the phenomenon of electronic conduction, the electric current is due to the flow of electrons. For example, metals are excellent electronic conductors. On the other hand, electric current can also be produced by the flow of ions. It is then termed as ionic conduction. Typical ionic conductors are electrolytes.

Electronic conduction and ionic conduction are both observed in polymers [1, 2].

1.1.1 Electronic conduction in polymers

The electronic conductivity of polymers is related to their oxidation or reduction states [3]. Although intrinsic conductivity is observed in electronic conducting polymers, it is generally very low. When polymers are oxidized or reduced, their conductivity increases dramatically. These processes are also described as doping. The polymer is electronically charged by the loss (oxidation) or gain (reduction) of electrons. Counter ions (dopants) in the solvent are extracted by the positively or negatively charged polymer to maintain electrostatic neutrality.

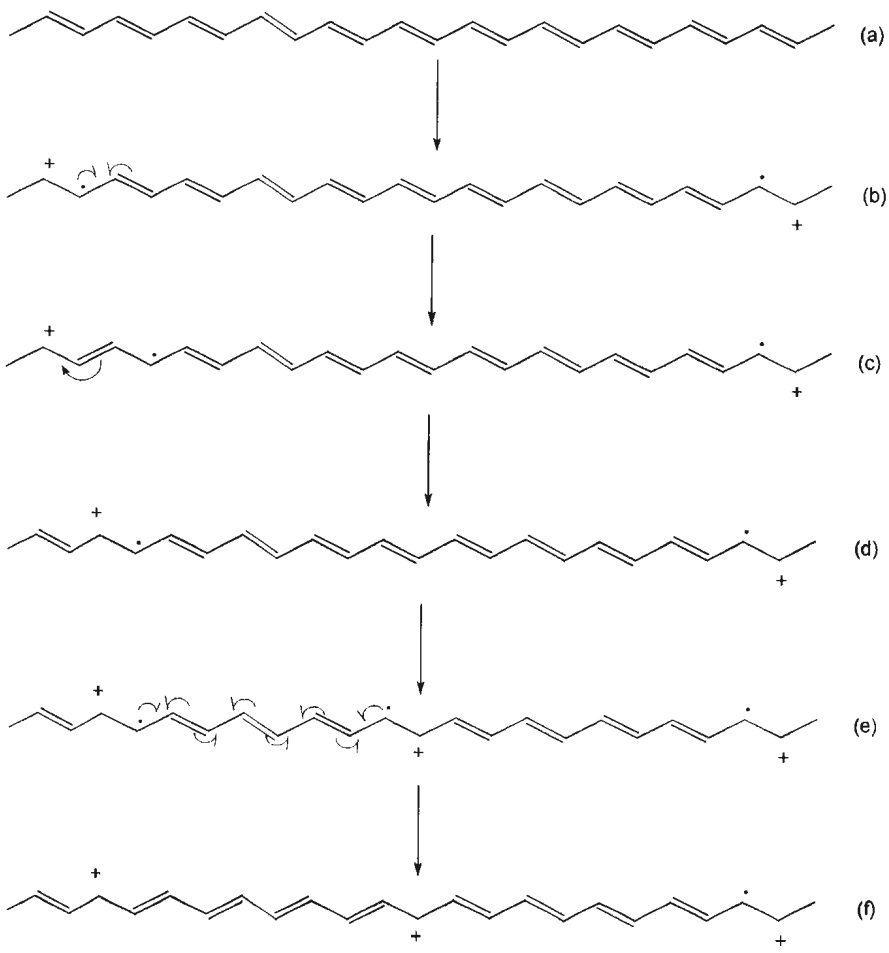

Scheme 1-1. Polaron and bipolaron formation

The terms polaron and bipolaron, in terminology from physics, are used to explain the electronic conductivity of organic polymers. For example, in the oxidation of polyacetylene (a), double bonds on the conjugated π-backbone are broken to form polarons (b) (Scheme 1-1) [3]. A polaron is a radical cation in chemical terminology. Polarons are partially delocalized. They can move over several double bonds by

rearrangements along conjugated chain [4]. At low oxidation levels, two polarons are kept away from each other by coulombic repulsion. With increasing oxidation level, the polarons become crowded and begin to interact when they get closer than about eight bond lengths on the conjugated π-backbone. Then two polarons can combine to form a bipolaron (d). A bipolaron is a conjugated dication. The remaining positive charges are free to move along the conjugated chains. Electronic conductivity arises from the mobility of polaron and bipolaron charge carriers.

1.1.2 Ionic conduction in polymers

The ionic conductivity of polymers depends on the formation and transport of ionic charge carriers. For example, in perfluorosulfonic acid polymers (such as Nafion), protons act as charge carriers [5]. Nafion consists of a highly hydrophobic backbone and highly hydrophilic sulfonic acid terminated side chains. Hydrophobic and hydrophilic domains are formed respectively by hydrophobic / hydrophilic nano-separation. This process is facilitated by the presence of water between the macromolecules. After hydration, protons are produced by the dissociation of sulfonic acid functional groups. Then protonic charge carriers are present in the inner space of the hydrophilic domains, and their mobility is increased by the assistance of water. As a result, electric current may be obtained with the application of an electrical field.

1.2 Electronic conducting polymers

1.2.1 History [6-17]

The investigation of organic electronic conducting polymers started with the discovery of the high conductivity of doped polyacetylene by Shirakawa *et al.* in 1977. Actually, at the beginning of the last century, Schlenk had suggested that some organic substances were possibly conductors. Their conductivities are possibly close to those of some metals.

The synthesis of polyacetylene can be traced back to the first approach by Natta's group in 1958. They had used the now-famous Ziegler-Natta catalyst to achieve a highly conjugated polyene structure at room temperature. Unfortunately, the resulting polymer only had low intrinsic conductivity. Berets and Smith found that exposure to acids or bases could improve the conductivity of pressed pellets of polyacetylene. The conductivity could be varied over the range of 10^{-9} to 10^{-2} S cm $^{-1}$. Further investigations showed that polyacetylene films had conductivities as high as 10^{2} to 10^{3} S cm $^{-1}$ after doping with strong donor or acceptor species. Later Naarman reported a conductivity of doped polyacetylene similar to that of copper and thus can be considered to be an organic metal.

After these 1970s milestones, the family of conducting polymers rapidly expanded. Many other π-conjugated systems have been investigated, including polyphenylenes, polythiophenes, polypyrroles, polyanilines, polyimides, polyperinaphthalenes and so on.

1.2.2 Polyfluorenes and their derivatives: prospective materials for light-emitting diode (LEDs)

Currently, many research groups are focusing on the development of effective materials for polymer light-emitting diodes (PLEDs) [18-23]. Compared with inorganic LEDs, polymer LEDs combine electronic and photonic activities with the advantages of plastics. Polymers are generally low cost materials with good mechanical flexibility and processibility. The energy gaps of PLEDs can be easily tuned through the use of various organic synthetic methods. Fusing with thin-film technology, the development of PLEDs opens up the possibility to miniaturize the size of electrical devices to molecular dimensions [6].

Polyfluorenes, as potential materials for PLEDs, have been under the spotlight for more than twenty years [24, 25]. The attraction mainly comes from their excellent luminescence properties [26-30]. Their light emissions cover the whole visible range and they exhibit high efficiency at low operating voltages [31]. By introduction of substituents at the C9 position or copolymerization with various compounds, polyfluorenes are modified to diversify their chemical, electrochemical and mechanical properties [32-40]. For example, a series of esterified polyfluorenes were reported by Ranger's group [41, 42]. These new acidic conducting polymers show electronic conductivities of 10^{-6} - 10^{-5} S cm^{-1} when doped with base.

Another successful modification of polyfluorenes leads to 2,7-poly(9-fluorenone) [43]. Due to the strongly electron-withdrawing carbonyl functional group at the C9 position, polyfluorenone is highly electron-deficient. Thus electron injection is enhanced and hole migration is blocked [43]. As a result, polyfluorenone is a good n-type conductor [43]. It is believed that it is a suitable material for ultrathin, light, flexible, full-color LEDs. Its reduction potential is as low as the work function of magnesium [44].

1.2.3 Synthesis of polyfluorenes and their derivatives: polymerization methodology

The synthesis of polyfluorenes involves the coupling of multiple aromatic moieties. Various powerful reactions, including Grignard, Stille, Yamaoto, Heck and Suzuki coupling, have been employed to synthesize diverse fluorene-based polymers or copolymers [29].

1.2.3.1 Stille coupling

The Stille coupling reaction [17] is considered a simple and powerful method to prepare novel conducting polymers. It is a commonly used polymerization methodology not only for the synthesis of polymers or copolymers with aromatic backbones but also for the synthesis of monomers.

Stille coupling reactions usually use organic tin compounds and organic halides as starting materials. They offer an excellent pathway to prepare alternating copolymers. The advantage of Stille coupling reactions include very mild reaction conditions, usually high yields and tolerance to many functional groups, such as alcohols, esters, amines and ethers [45].

Larmat *et al.* reported the synthesis of a monomer, bis(2-thienyl)-9,9-didecyl-fluorene **(1-3)**, using Stille coupling. **1-3** was obtained in 70 % yield from tributylthienyltin **(1-1)** and 2,7-dibromofluorene derivatives **(1-2)** (Scheme 1-2) [46].

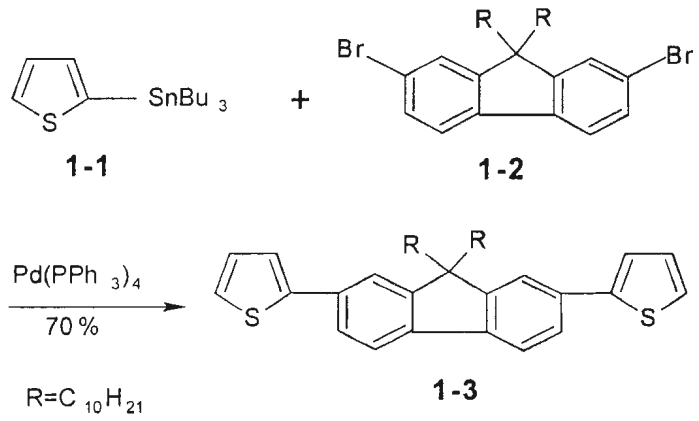

Scheme 1-2. Larmat's synthesis of bis(2-thienyl)-9,9-didecyl-fluorine

Palladium-catalyzed Stille coupling reactions are also used extensively in the synthesis of other types of conducting polymers, such as poly(2,5-dialkoxyhenylene-1,4-thiophene), poly(2,5-dialkylphenylene-1,4-thiophene) [47, 48] and a series of

copolymers from 9,9-dialkyl-2,7-dibromofluorene with thiophene, pyrrole, furan or 3,4-ethylenedioxythiophene [45]. Copolymerizations of aromatic compounds with organozinc, Grignard and organotin reagents (Stille coupling reaction) respectively were investigated by Bochmann *et al.* The results showed that the Stille coupling reaction led to the highest molar mass products [49].

1.2.3.2 Yamamoto coupling

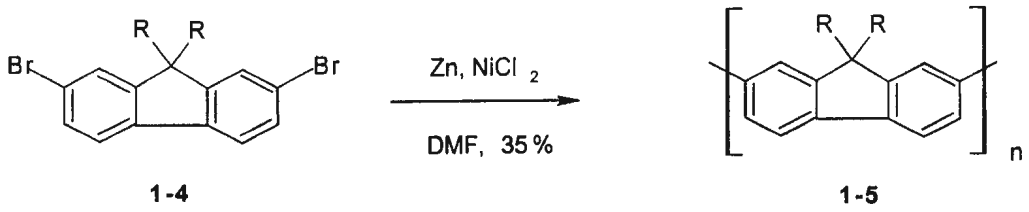

1-4 **1-5**

R=$CH_2CH_2OCH_2CH_2OCH_3$

Scheme 1-3. Pei's synthesis of **1-5**

Pei *et al.* reported the synthesis of poly[9,9-bis(3,6-dioxaheptyl)-fluorene-2,7-diyl] (**1-5**), a high-efficiency luminescent polymer, using a Yamamoto coupling reaction (Scheme 1-3) [50]. This reductive polymerization used zinc as the reductant and nickel(0) as the catalyst. It produced **1-5** from the dibrominated monomer **(1-4)** in 35 % yield. Based on gel permeation chromatography (GPC), weight average molar mass (M_w) was 215,000 g mol^{-1} and number average molar mass (M_n) was 94,000 g mol^{-1}. The onset of the absorption spectrum gave a 2.8 eV band gap for the target polymer.

Yamamoto-type copolymerization has been employed to prepare poly(fluorene-*co*-perylene) **(1-9)**, reported by Klärner *et al.* in 1999 (Scheme 1-4) [51]. This method used arylene dibromides as moieties and zero-valent nickel as a catalyst. Based on GPC, M_n was 55,000 g mol^{-1} when the ratio of monomers of 2,7-dibromo-9,9-di-2'-ethyl-hexylfluorene **(1-7)** and an isomeric mixture of 3,4 and 3,10-dibromoperylene **(1-6)** was 85:15. The resulting polymer showed good solubility and processibility.

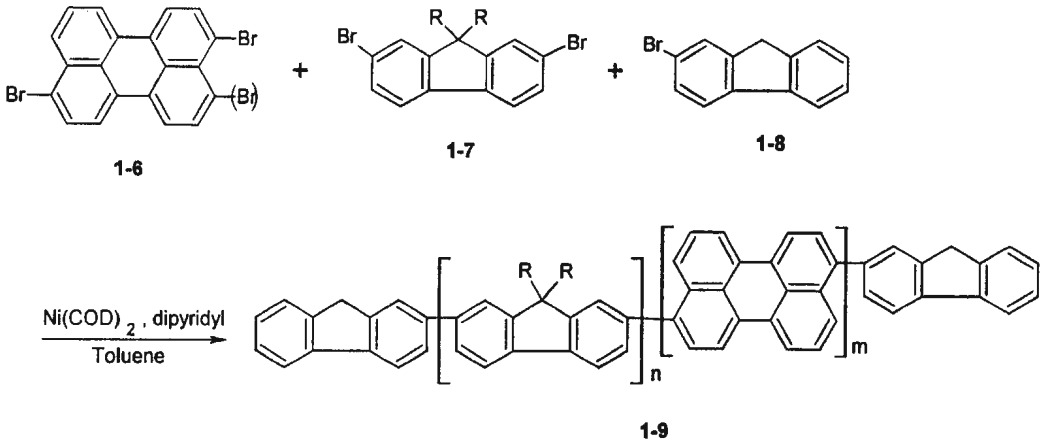

Scheme 1-4. Klärner's synthesis of poly(fluorene-*co*-perylene)

1.2.3.3 Suzuki coupling

Suzuki coupling reactions were used in the syntheses of a series of poly(2,7-fluorenylene) derivatives by Ranger *et al.*. One of them, poly[2,7'-(ethyl-9,9-dioctyl-2,7'-bifluorene-9'-carboxylate)] **(1-12)**, was synthesized for the first time (Scheme 1-5) [52]. This reaction gave 65 % yield of the desired polymer. M_w was 8000 g mol^{-1} based on

GPC. The polymer had a conductivity of 10^{-6}-10^{-5} S cm^{-1} when doped with base.

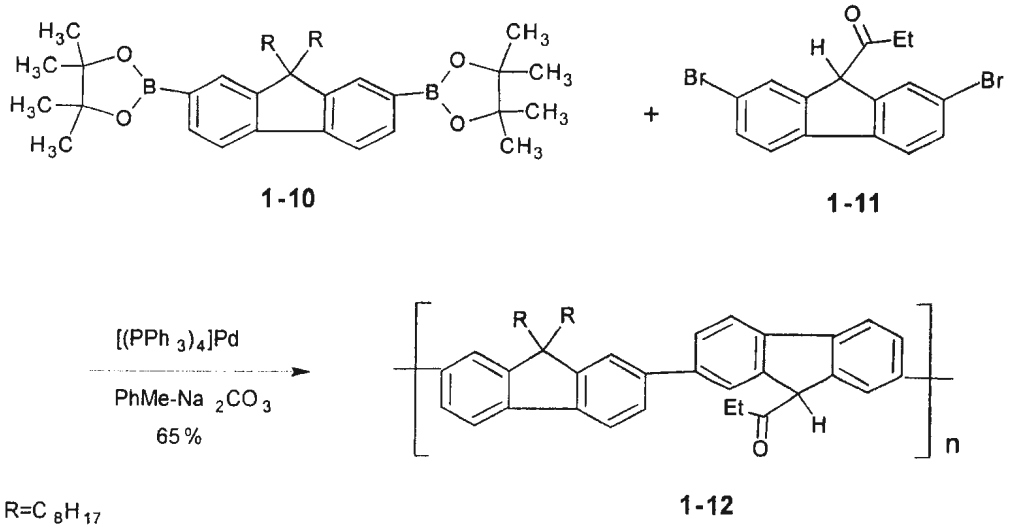

Scheme 1-5. Ranger's synthesis of poly[2,7'-(ethyl-9,9-dioctyl-2,7'-bifluorene-9'-carboxylate)]

1.2.3.4 Others

Ahn *et al.* reported the synthesis of poly[9,9-*n*-dihexyl-2,7-fluorenediylvinylene-*alt*-2,5-bis(trimethylsilyl)-*p*-phenlenevinylene] (**1-15**) using a Wittig reaction (Scheme 1-6) [53]. The product (**1-15**) was obtained in 43 % yield. M_n was 8800 g mol^{-1} and M_w was 16900 g mol^{-1} based on GPC. Polymer (**1-15**) is an efficient photo- and electroluminescent polymer in the blue and greenish-blue range.

A series of poly(fluorene-9,9-diyl-*alt*-alkan-α,ω-diyl)s (**1-18**) was reported by Inaoka *et al.* in 2002. These polymers were synthesized using a modified nucleophilic substitution and then chemical oxidation (Scheme 1-7) [54]. This route included dilithiation of

fluorene and then polymerization with α,ω-dibromoalkanes to give the precursor polymer **(1-17)**. The precursor polymers **(1-17)** underwent oxidative cross-linking to produce the desired network. Based on GPC, M_n was in the range of 7620 g mol^{-1} to 10700 g mol^{-1}.

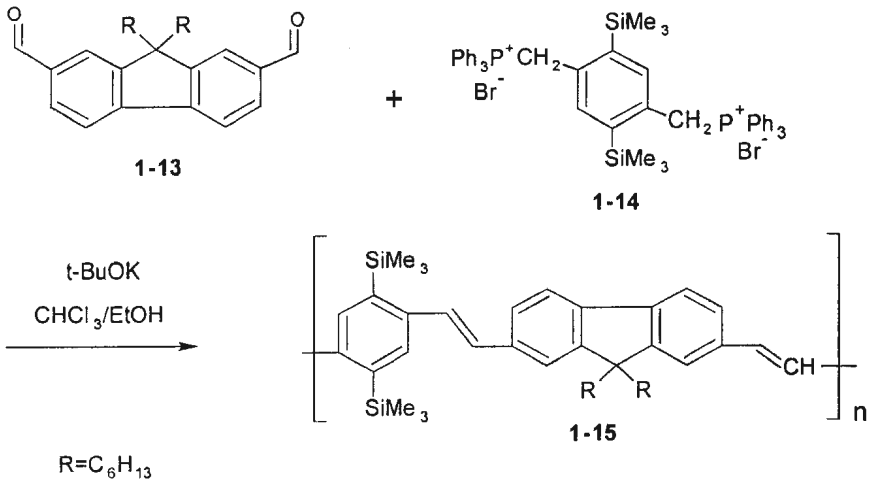

Scheme 1-6. Ahn's synthesis of **1-15**

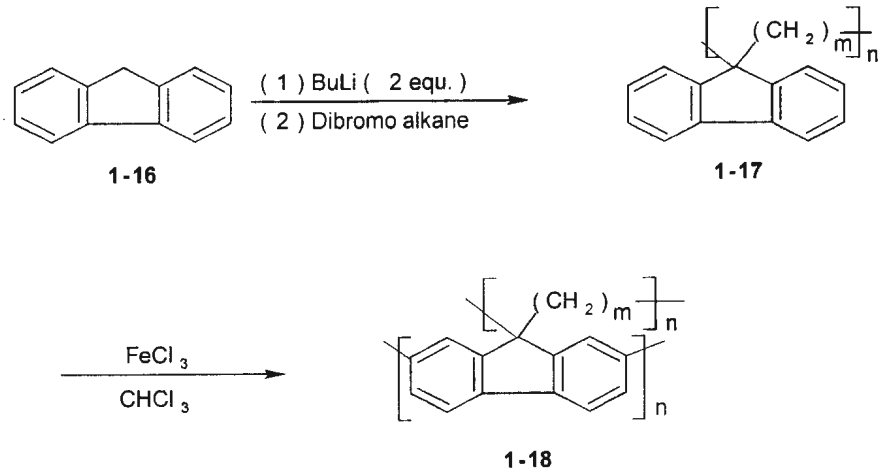

Scheme 1-7. Inaoka's synthesis of poly(fluorene-9,9-diyl-*alt*-alkan-α,ω-diyl)s

Friedländer's quinoline synthesis has been used as a polymerization reaction to prepare polyquinoline-fluorene copolymers reported by Kim *et al.*, in 1999 [55]. One of them, **1-21**, was obtained in 89 % yield. This method connects 2 moieties, 4,4'-diamino-3,3'-dibenzoyldiphenyl ether **(1-19)** and 2,7-diacetyl-9,9-*n*-dihexylfluorene **(1-20)** in the presence of phosphorous pentoxide (Scheme 1-8) [55]. Based on GPC, M_w was 60100 g mol^{-1} and M_n was 27300 g mol^{-1}. Polymer **(1-21)** is a thermally stable polymer with a decomposition temperature of over 420 °C.

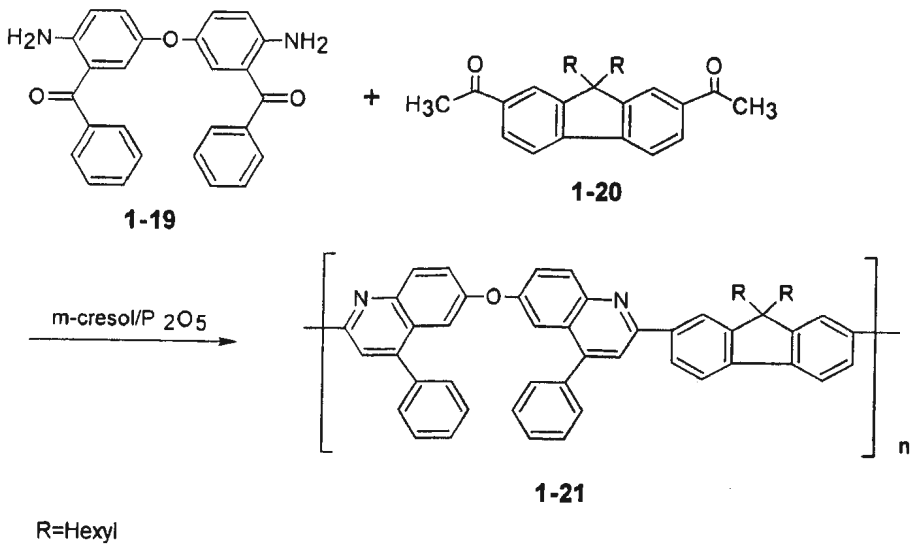

Scheme 1-8. Kim's synthesis of **1-21**

Pschirer *et al.* reported the syntheses of poly[(9,9-dialkyl)fluoren-2,7-ylene-ethynylene]s **(1-23)** using alkyne metathesis in 2000 [56]. These homopolymerizations used 9,9-dialkynefluorenes as monomers and $Mo(CO)_6$ as a catalyst. When R=hexyl, the

yield was 23 % (Scheme 1-9). M_n was 14100 g mol^{-1} and M_w was 59900 g mol^{-1} based on GPC.

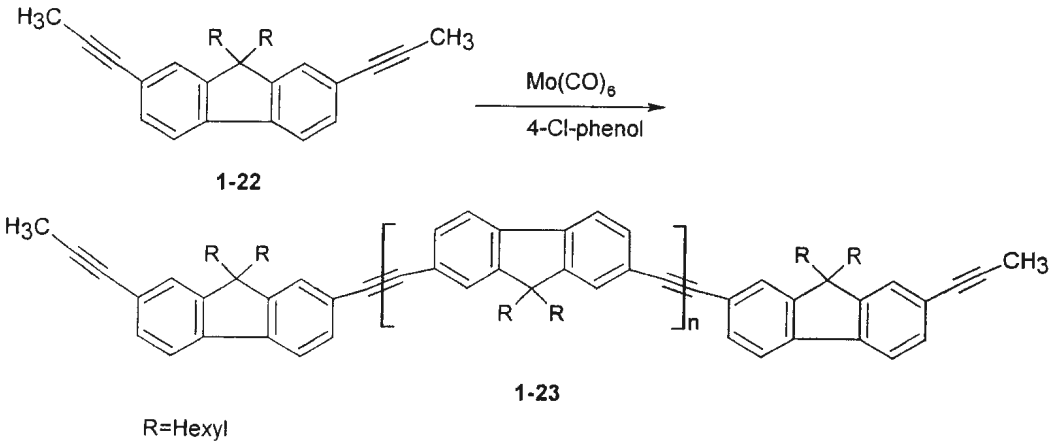

Scheme 1-9. Pschirer's synthesis of poly[(9,9-dihexyl)fluoren-2,7-yleneethynylene]s

The syntheses of fluorene-based poly(iminoarylene)s **(1-26)** were reported by Jung *et al.* in 2002 (Scheme 1-10) [57]. A palladium-catalyzed polycondensation was employed to prepare the nitrogen-containing structures.

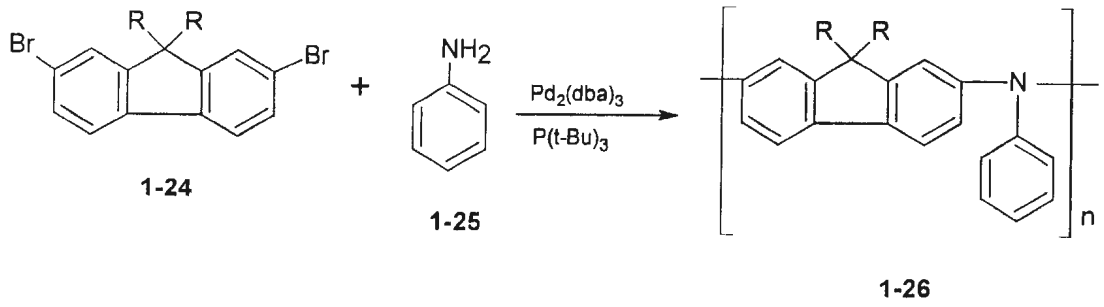

Scheme 1-10. Jung's synthesis of fluorene-based poly(iminoarylene)s

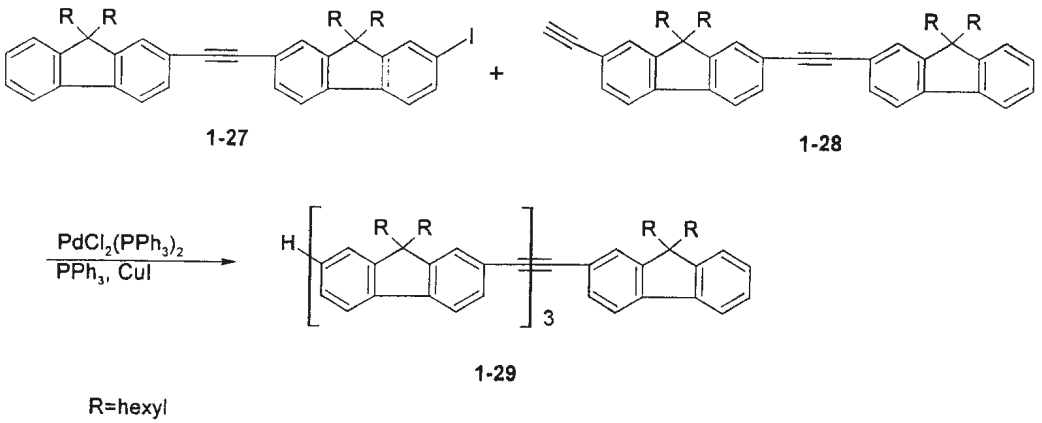

Scheme 1-11. Lee's synthesis of oligo(9,9-dihexyl-2,7-fluorene ethynylene)

A Sonogashira coupling has been used to prepare oligo(9,9-dihexyl-2,7-fluorene ethynylene) **(1-29)** from iodinated moieties **(1-27)** and alkynyl moieties (1-28) reported by Lee *et al.* in 2001 (Scheme 1-11) [58]. This methodology is a facile way to produce polymers with alkynyl linkages in the backbone.

1.2.4 Low band gap polymers

Band theory is considered to be the most reasonable explanation of electronic structures in the solid state [1]. Molecular orbitals are formed due to the overlap of the atomic orbitals between neighboring atoms in all directions. Although the energy levels of molecular orbitals are discrete based on quantum mechanics, they appear to be continuous in some ranges and to form energy bands [2].

At low temperature, electrons prioritize from the lowest energy level to the highest

energy level. The highest energy level occupied by electrons is derived from the HOMO and is called the valence band. The next higher band derived from the LUMO is called the conduction band. The energy difference between the valence band and the conduction band is called the band gap. The intrinsic conductivity of a polymer is determined by the mobility of charge carriers and the band gap (E_g) between the HOMO and LUMO.

In the case of insulators (a), the valence band is completely filled with electrons (Figure 1-1). The conduction band is empty. Neither a filled band nor an empty band can generate electrical current. In order to produce electrical current, electrons have to be excited from the valence band to the conduction band. Insulators all have big band gaps. For example, diamond has a band gap of 5.6 eV, which is so great as to make thermal excitation negligible at room temperature. As a result, diamond is a perfect insulator at room temperature.

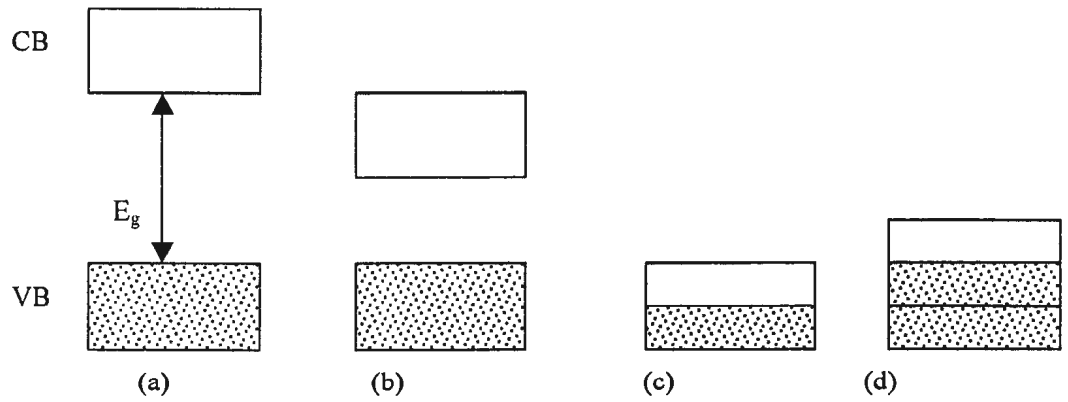

Figure 1-1. Energy band structures of an insulator (a), semiconductor (b) and conductors (c and d), Conduction band (CB), Valence band (VB)

The band gap of a semiconductor (b) is much smaller than that of an insulator. At room temperature, electrons can be excited from the valence band to the conduction band. As a result, both electrons in the conduction band and holes in the valence band produce electrical current in an electric field. The high conductivity of metal arises from either a partially filled valence band, such as an alkali metal (c) or overlap of the valence band with the 2^{nd} Brillouin band, such as an alkaline earth metal (d). These phenomena also can be summarized as zero band gaps. Most polymers have large band gaps. They are excellent insulators at room temperature. Narrowing the band gap will increase the intrinsic conductivity of the polymer to produce polymer semiconductors or even polymer conductors. Moreover, reduction of the band gap stabilizes the doped states, and can make the polymer transparent to light [17].

Several strategies, such as increasing electron density along the polymer chain, have been developed to reduce the band gap. Introduction of electron-donating substituents raises the HOMO level. Although the LUMO will generally increase at the same time, the net result can lead to modification of the band gap with properly chosen structures. Another strategy, electron donor-acceptor alternation, has been employed recently [48]. This strategy uses electron-rich moieties as donors and electron-deficient moieties as acceptors.

1.3 Ionic conducting polymers: solid polymer electrolytes

Solid polymer electrolytes have been investigated widely. They have been employed as ionic conductors in batteries, sensors, electrochromic devices and fuel cells.

Solid polymer electrolyte membranes (SPEM) can serve as proton conductors [2, 59]. Compared with liquid electrolytes, they are chemically and electrochemically stable [2]. As solid-state electrolytes, SPEMs preserve uniform electrolyte content and prevent regional drying due to high electrolyte transport. More importantly, they have high ionic conductivity and produce good performance with low voltage losses due to resistance and electronic conductivity. Moreover, SPEMs maintain good mechanical strength under operating conditions. The permeability of reactants separated by SPEMs is extremely low [59]. By replacing liquid electrolytes with solid electrolytes, electrochemical systems can be prepared as solid state devices with better stability and reliability [2].

1.3.1 Application of ionic conducting polymers in fuel cell technology

The applications of ionic conducting polymers especially in the energy conversion areas have always interested chemists and physicists [60]. For example, they are used as solid electrolyte membranes, which are essential components in polymer electrolyte membrane fuel cells (PEMFC).

1.3.1.1 General consideration of fuel cells

A fuel cell is an apparatus in which chemicals (*e.g.* H_2 and O_2) react together to convert chemical energy to electrical energy [61]. The two chemicals are stored separately outside the cell and flow into the cell continuously. One chemical (*e.g.* H_2) reacts at the anode and the other (usually O_2) is reduced at the cathode. The direct reaction of the two chemicals must be prevented because direct reaction only creates thermal energy [61].

The attraction of fuel cells is mainly due to their high efficiency. Moreover, fuel cells are quiet and produce very little pollution. With proper design and clean fuels, the pollution can be lowered to zero [62].

The investigation of fuel cells has persisted over 160 years since Grove's invention. In the early stages, the driving force came from the poor efficiencies of other power generating technologies. For example, in 1882, only about 2.5 % of the energy was converted to electricity in a coal burning electrical generating station [63]. With the improvement of other energy conversion technologies, the development of fuel cells slowed down. In the late 1950s, the development of fuel cells was renaissant promoted by applications in spacecraft [63]. In the last thirty years, under the cloud of the energy crisis, research on fuel cells has boomed. Today the potential commercial applications of fuel cells not only focuses on power stations and spacecraft, but also extend to personal vehicles, buses, trucks, locomotives and consumer electronics [64].

After a long period of development in the nineteenth and twentieth centuries, many types of fuel cells have been invented. Diverse classifications have been introduced to describe various fuel cells, based on the fuel, operating conditions, apparatus and so on [65]. According to the electrolyte employed, fuel cells are classified as alkaline fuel cells, molten-carbonate fuel cells, phosphoric-acid fuel cells, solid-oxide fuel cells and polymer electrolyte membrane fuel cells [63, 65].

1.3.1.2 Polymer electrolyte membrane fuel cells (PEMFC)

PEMFCs use polymer membranes as their electrolytes. The membrane, which is typically 50 to 250 μm thick [65], not only acts as an electrolyte to conduct protons from the anode to the cathode, but also separates the fuel from the oxidant (oxygen or air). A sandwich structure consisting of a polymer membrane and two platinum- catalyzed electrodes is employed.

The most widely investigated PEMFCs are H_2 / O_2 cells. They are considered possibly the most elegant in design and operation of all fuel cells. H_2 is used as the fuel gas which is oxidized on the platinum catalyst of the anode (Equation 1-1).

Anode $\quad H_2 \longrightarrow 2H^+ + 2e^-$

Cathode $\quad O_2 + 4H^+ + 4e^- \longrightarrow 2\,H_2O$

Equation 1-1. Electrochemical reactions of H_2 / O_2 PEMFCs

The conductivity of the polymer electrolyte and the reactivity of the electrocatalyst are both essential for the performance of PEMFCs. Moreover, excess liquid water on the surface between catalyst and the oxidant can occupy the pores of the catalyst. The performance may decrease due to the decrease of the effective area.

The applications of PEMFCs can be traced back to the Gemini space missions in the 1960's. PEMFCs are suitable for space technology due to their high-power densities. For example, the power density of a methanol PEMFC can be as high as 350 $mWcm^{-2}$ [65].

1.3.2 Polymer membranes

The polymer membrane is one of the key components in a PEMFC. It should be thin with high proton conductivity and high stability. It has to operate with aggressive fuels (*e.g.* methanol) and strong oxidants (oxygen) for many thousands of hours at elevated temperature (typically 30-200 °C). These harsh operating requirements challenge the lifetime of all membranes [64]. Improvement of membranes which are available has continued throughout the development of PEMFCs.

1.3.2.1 Nafion

The first polymer membrane used in PEMFCs was sulfonated polystyrene, but it only has a short lifetime due to chemical degradation. Further investigation showed that the

degradation is probably due to the peroxide intermediate produced by the cathode reaction [66]. Oxygen is reduced to produce H_2O_2 as an intermediate, which can be further converted to more reactive HO· and HO_2· radicals in the presence of trace metal ions [66]. C-H bonds are not stable enough to withstand these excessive oxidative conditions.

A much more oxidation-stable sulfonated polytetrafluoroethylene (Nafion) was developed by DuPont (Figure 1-2) [66, 67]. It is now by far the most commonly used membrane in PEMFCs [68].

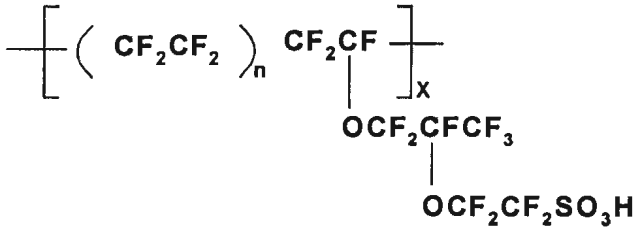

1-30

Figure 1-2. Structure of Nafion

Nafion has a completely fluorinated carbon backbone, perfluorinated-vinyl- polyether side chains and sulfonate functional groups on the termini of the side chains. Because of the absence of C-H bonds, Nafion does not suffer rapid degradation under the fuel cell operation environment. When hydrated, Nafion displays fair ionic conductivity, good oxygen solubility, thermal stability and mechanical strength [59,65, 69, 70].

The disadvantages of Nafion are, first, its high cost. The current price is US$ 800 m^{-2}

[60]. Second, Nafion has a large electro-osmotic drag number [60]. Water transport from the anode to the cathode is a severe problem in fuel cells. In combination with the water formation in the cathode reaction, it can cause flooding of the cathode. At the same time, the membrane can become dehydrated on the anode side. As a result, there is a large loss of cell voltage [66]. Third, Nafion limits the operating temperature. The best conductivity and thermal stability of Nafion membranes occurs at temperatures below 85 °C [65]. At these temperatures, the electrode catalysts are easily poisoned by only traces of CO [60,71]. In the methanol fuel cell, methanol crossover also causes losses of cell voltage.

1.3.2.2 Polybenzimidazoles (PBIs): prospective polymer membranes

Due to the shortcomings of Nafion, alternative polymer membranes are being developed, including perfluorinated polymer membranes, grafted fluorinated membranes, fluorinated copolymers, nonfluorinated ionomers, high-molar mass/ low-molar mass blend membranes and organic / inorganic blend membranes [64, 72-77]. Among them, polybenzimidazoles (PBIs) are particularly attractive as potential membrane materials.

PBIs were widely investigated in the early years due to their outstanding thermal stability (Figure 1-3). The early work shows that PBIs can keep their excellent mechanical strength, strength retention, toughness, chemical inertness and radiative stability after exposure to high temperature environments (250-300 °C) for long periods [78]. Since the

1960s, the applications of PBI were focused on structural engineering materials, thermo- or electro- insulation materials and osmotic membranes [79].

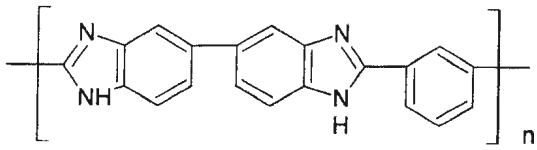

1-31

Figure 1-3. Structure of PBI

Undoped PBI shows an intrinsic resistance of 10^{12} ohm-cm [78]. Its ionic conductivity is too low to be applied in fuel cells. As a basic polymer, PBI can be easily doped with various acids [80,81]. In the cases of phosphoric acid or sulfuric acid doping, PBI displays good proton conductivity over a wide range of temperatures [64].

The most attractive advantage of PBI membranes is their high operating temperatures (80-180 °C). At these temperatures, the tolerance of precious metal catalysts (Pt) to CO increases dramatically [78]. Moreover, the permeability of methanol vapor at 80 °C is 80,000 barrer* for Nafion-117, but it is only 270 barrer for PBI / H_3PO_4 [78]. Raising the temperature to the range of 150-200 °C increases performance. Thus PBI is especially suitable for direct methanol fuel cells.

PBI shows an almost negligible water-drag number. By using a PBI / H_3PO_4 membrane in a hydrogen fuel cell, dehydration is avoided. Thus the fuel cell is allowed to run at low

* 1 Barrer = 10^{-10} cm^3 (STP) cm / cm^2 s cmHg

operating gas humidity. For example, Wang *et al.* reported that a power density of 0.25 Wcm^{-2} was obtained at low gas humidification [73, 81].

1.3.3 Synthesis of PBIs

PBIs are obtained by polymerization of aromatic tetraamines with dialdehydes or dicarboxylates, including acids, amides and esters [82, 83]. Melt and solution techniques have been developed to achieve this task as described below.

1.3.3.1 Melt polymerization

Melt polymerization was the first method developed to achieve high molar mass PBIs. Marvel *et al.* first described a melt procedure to prepare a series of all aromatic PBIs (Scheme 1-12) [84, 85].

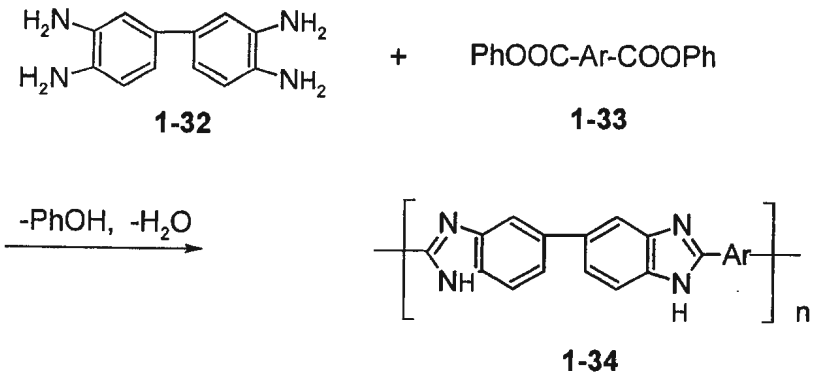

Scheme 1-12. Marvel's synthesis of PBIs

In Marvel's synthesis, an equimolar mixture of a tetraamine **(1-32)** and a dicarboxylate (**1-33**) is heated under a nitrogen atmosphere [84, 85]. The temperature is gradually increased to 300 °C to melt the starting materials and it allows the reactions to take place. Following a short period under vacuum, the reaction is completed by heating the prepolymers for several hours at 350-400 °C. The conversion to PBIs is nearly quantitative.

The melt polymerization technique has been extensively used to prepare various PBIs with introduction of oxygen, sulfone groups, vinylene *etc.* into the backbone (Figure 1-4) [85-91].

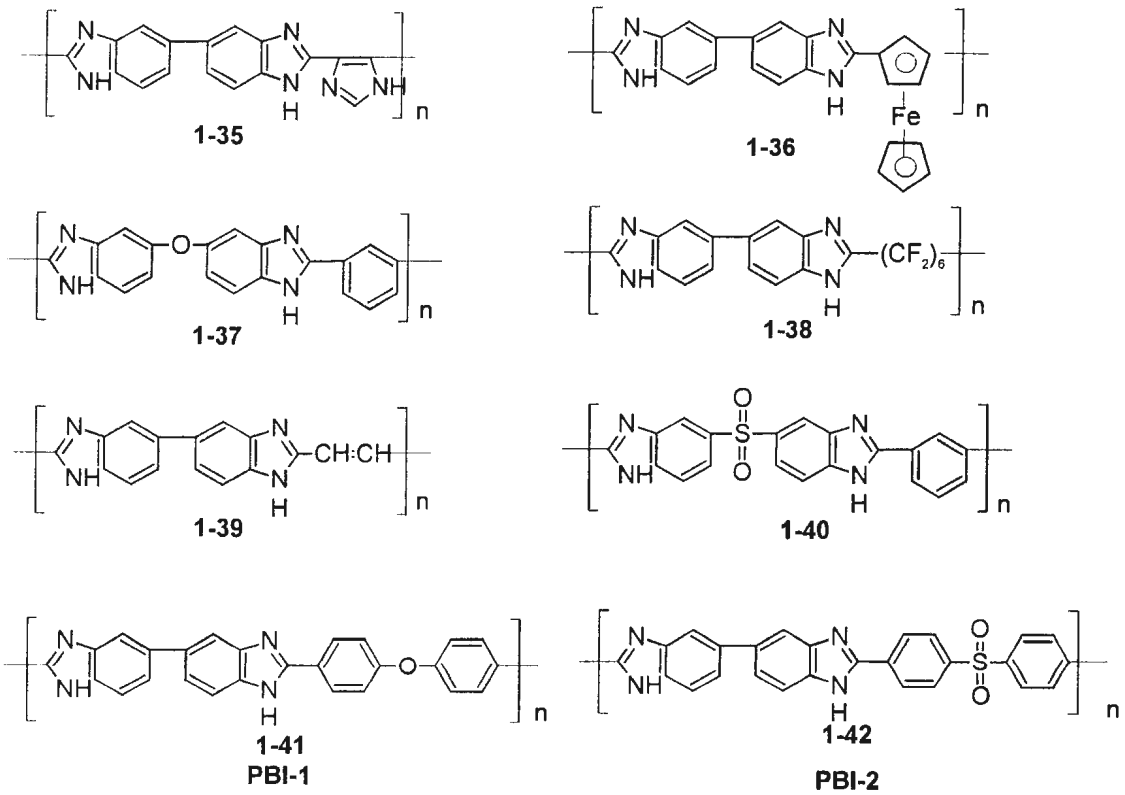

Figure 1-4. Structures of various PBIs

Further investigation has revealed some shortcomings of melt polymerization due to the fact that monomers must melt to react. For example, Iwakura *et al.* reported melt polymerizations of diphenyl esters of diquinazolinylmethane derivatives with tetraamines. The results showed that at 250-270 °C, the starting materials remained as powders due to their high melting points. The polymers obtained had low viscosity. When the temperature was increased above 270 °C, undesired crosslinked polymers formed [92].

Melt polymerization is a two-step procedure carried out under harsh conditions (high temperature) and it often fails to produce well-defined polymers [84]. Small molecules eliminated in the condensation, such as water and phenols, may be trapped in the solid and can retard the reaction [93]. Reactive end groups can also be trapped away from their counterparts.

1.3.3.2 Solution polymerizations in poly(phosphoric acid) (PPA)

In order to avoid the problems encountered in the melt condensation, solution polymerizations have been developed. Various solvents have been investigated, including 1-methyl-2-pyrrolidine [94], veratrole, *N,N*-dimethylaniline, various amide solvents [95], sulfolane solvents [93] and ethylated polyphosphoric acid [96]. Poly(phosphoric acid) (PPA) has emerged as the most widely used solvent.

PPA, a high-temperature solution, was first introduced into the syntheses of PBIs by

Iwakura *et al.* [97]. Since then, many kinds of PBIs have been synthesized in PPA solution [98-103].

Although PPA can have different polymerization degrees and compositions, the general structure can be drawn as shown below (figure 1-5) [104].

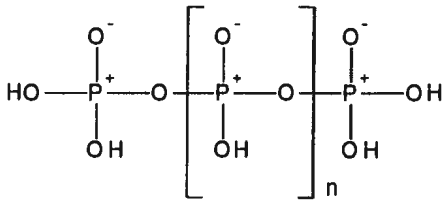

1-43

Figure 1-5. General structure of PPA

PBI synthesis in PPA is usually conducted at 180-200 °C. These relatively low temperatures allow dicarboxylic acids to be starting materials. Most dicarboxylic acids cannot be used in melt polymerizations because of their decarboxylation at high temperature [84]. Another advantage of PPA is that tetraamine hydrochlorides can be employed instead of air-sensitive tetraamines [84].

1.3.3.3 Polymerization mechanism

There are two mechanistic routes in the formation of PBIs (Scheme 1-13) [84, 104]. For a specific reaction, the mechanism depends on the conditions.

Route A involves a nucleophilic addition to the carboxylate as the first step, followed by dehydration. PBIs are obtained by cyclization and final elimination of ROH [84,104].

In route B, the first step is amide formation to form poly(aminoamide) by loss of ROH. And then the intermediates undergo cyclization and dehydration to give PBIs [84, 104].

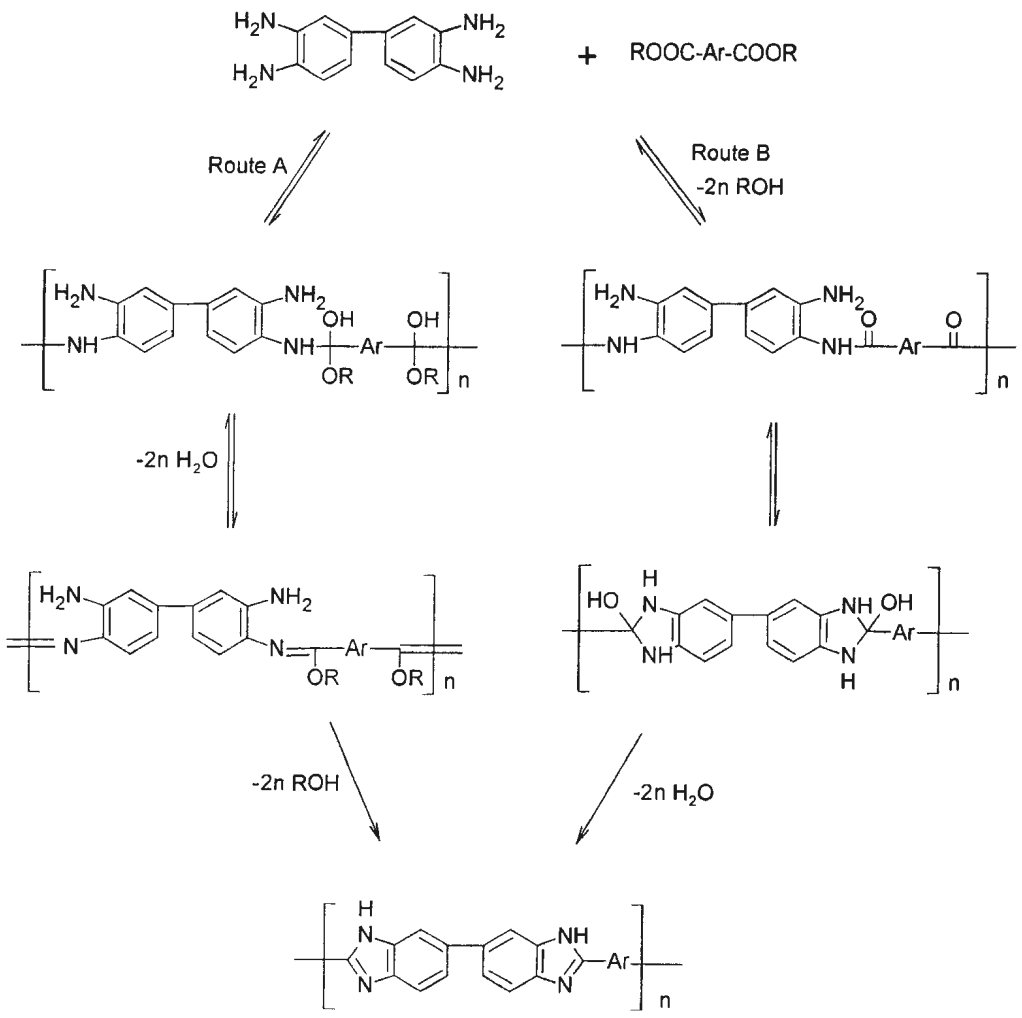

Scheme 1-13. Mechanisms of PBIs formation

1.4 Aim of this work

The first goal of this work was the synthesis of new electronic conducting polymers, which is described in chapter 2. Fluorenone, which is electron-poor, based copolymers with electron-rich moieties: benzene, furan and thiophene have been prepared. These were designed to be low band gap copolymers based on the electron donor-acceptor alternation strategy. The target polymers are expected to be potentially effective materials for PLEDs.

The synthesis of a family of PBI ionic conducting polymers was the second goal of this work, as described in chapter 3. Known compounds **PBI-1**, **PBI-2** and **PBI-3** were prepared using PPA solution polymerization. Although PBI has been reported to work well as a polymer electrolyte membrane, it is very brittle. Introducing hetero-atoms between the aromatic fragments will increase its flexibility. This will facilitate the film casting and increase mechanical strength. The resulting polymers were cast as thin films to investigate their application in PEMFCs. The target polymers were anticipated to have better processibility and performance than that of **1-31**, which has been used almost exclusively in fuel cell work.

Chapter 2

Synthesis of Electronic Conducting Polymers:

Copolymers of Fluorenone with Benzene, Furan and Thiophene

2.1 Introduction

This chapter is focused on the synthesis of electronic conducting copolymers of fluorenone with benzene **(PFB)**, furan **(PFF)** and thiophene **(PFT)** (Figure 2-1).

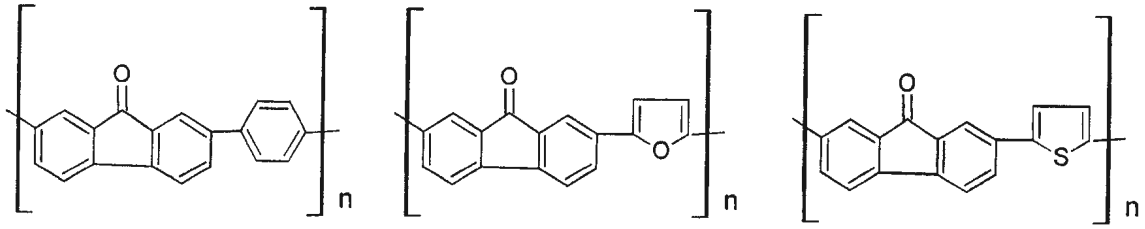

2-1
PFB

2-2
PFF

2-3
PFT

Figure 2-1. Structures of **PFB**, **PFF** and **PFT**

As a highly electron-deficient unit, fluorenone is a good electron acceptor. Thiophene and furan are electron-rich π donors, due to the contribution of the lone pairs on the S and O atoms to their respective π systems. Benzene is also an electron-rich aromatic molecule compare to fluorenone. **PFB**, **PFF** and **PFT** are expected to be low band gap polymers based on the donor-acceptor alternation strategy [48]. They also can be the potential materials for PLEDs.

The backbones of **PFB**, **PFF** and **PFT** all feature alternation of the two aromatic building blocks. Stille coupling reactions are especially suitable to synthesize these kinds of polymers.

2.2 Synthesis

2.2.1 Initial synthesis towards PFT

The initial attempt to prepare a fluorenone-thiophene copolymer **(PFT)** was conducted by Cammisa [105]. 2,7-Dibromo-9-fluorenone **(2-4)** and 2,5-bis(trimethly-stannyl)thiophene **(2-5)** were copolymerized using a Stille coupling reaction in the presence of a palladium (II) catalyst (Scheme 2-1).

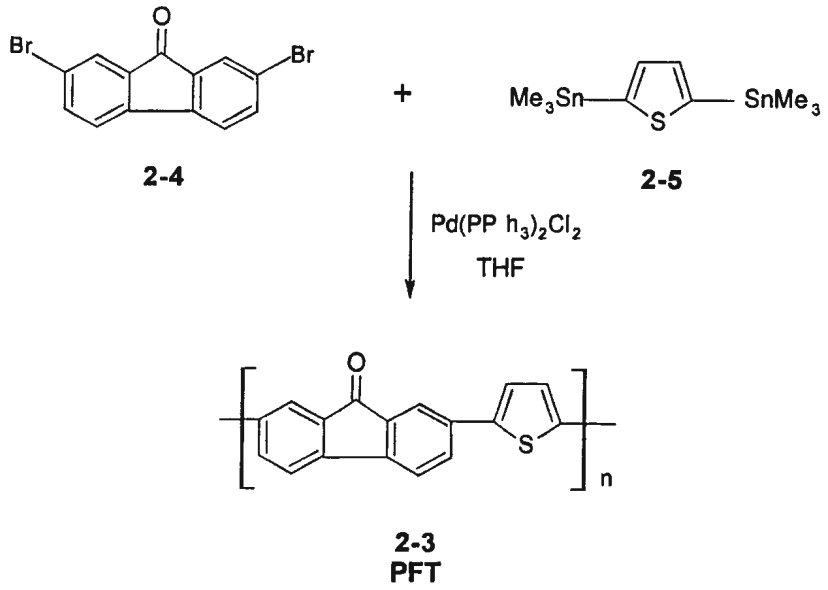

Scheme 2-1. Initial synthesis of **PFT**

Based on its MALDI-TOF mass spectrum, the product determined to be a mixture of monomer, dimer and trimer species. The poor solubility of the oligomers was assumed to be responsible for the low molar mass of the product.

2.2.2 Uckert's precursor route to polyfluorenone

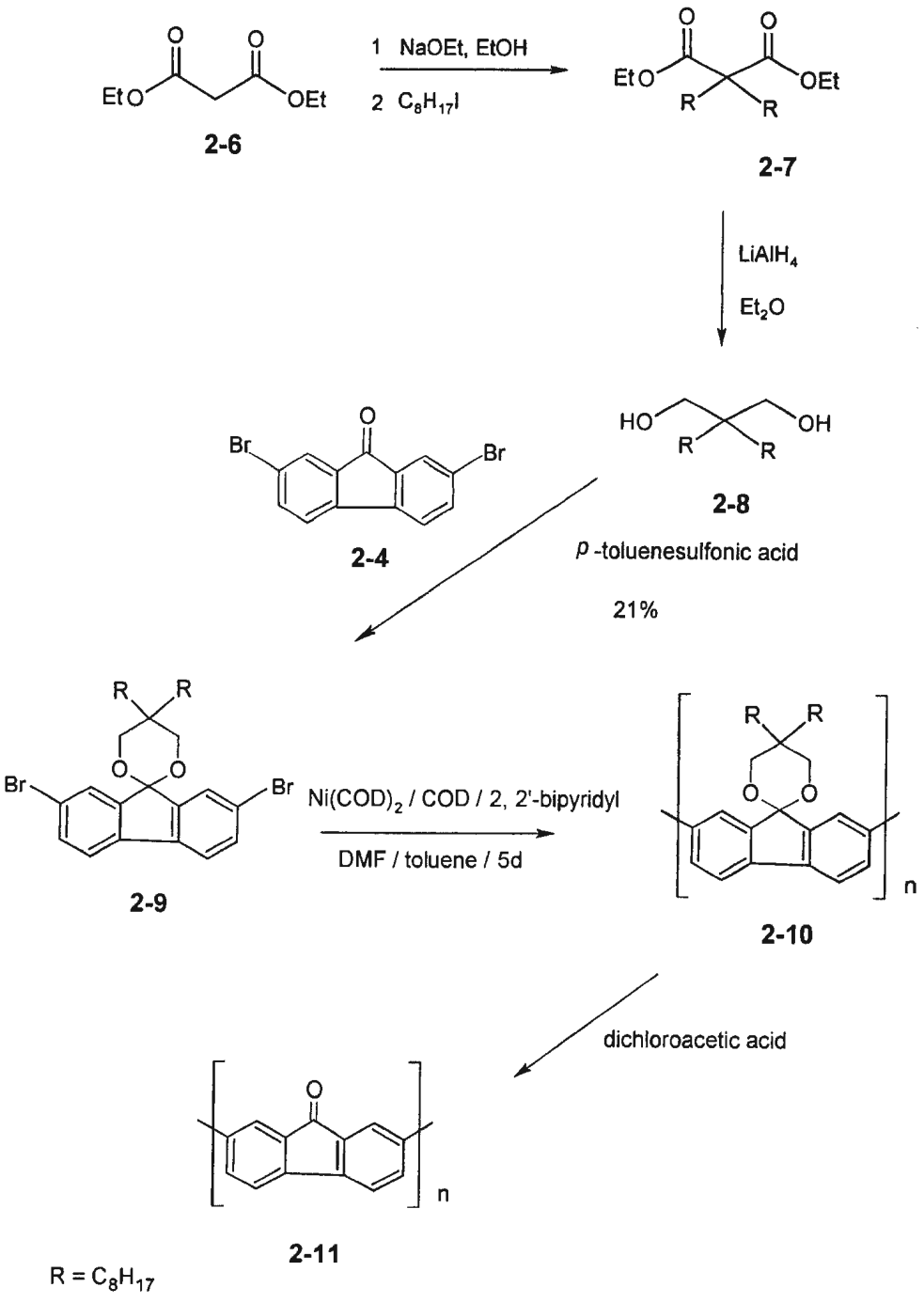

Scheme 2-2. Uckert's synthesis of 2,7-poly(9-fluorenone)

Uckert *et al.* reported a precursor route to polyfluorenone to avoid the solubility problem (Scheme 2-2) [43]. Their route used 2,7-dibromospiro[4,4'-dioctyl-2',6'-dioxocyclohexane]-1',9-fluorene **(2-9)** instead of 2,7-dibromo-9-fluorenone **(2-4)** as the dihalide fragment. Thus, long side chains were introduced to improve the solubility of oligomers and facilitate the formation of high molecular weight products. Based on GPC, M_w was as high as 200,000 g mol^{-1} [43]. The additional acetal groups could be easily removed by exposure of the precursor polymer to dichloroacetic acid.

2.2.3 Precursor polymers

In order to improve the solubility of oligomers, we employed Uckert's precursor strategy. The precursor copolymers: poly(2,7-spiro[4',4'-dioctyl-2',6'-dioxocyclohexane]-1',9-fluorene-*co*-1,4-benzene) **(PFKB)**, poly(2,7-spiro[4',4'-dioctyl-2',6'-dioxocyclohexane]-1',9-fluorene-*co*-2,5-furan) **(PFKF)** and poly(2,7-spiro[4',4'-dioctyl-2',6'-dioxocyclohexane]-1',9-fluorene-*co*-2,5-thiophene) **(PFKT)** were synthesized and characterized (Figure 2-2).

2,7-Dibromospiro[4,4'-dioctyl-2',6'-dioxocyclohexane]-1',9-fluorene **(2-9)** was used instead of 2,7-dibromofluorenone **(2-4)**. 2,5-bis(trimethyl)stannylthiophene, 2,5-bis(trimethyl)stannylfuran and 1,4-bis(trimethyl)stannylbenzene were used as the distannyl fragments. Palladium-catalysed Stille coupling reactions were used to prepare

the precursor copolymers. These could then be converted to the target copolymers through deacetalisation reactions.

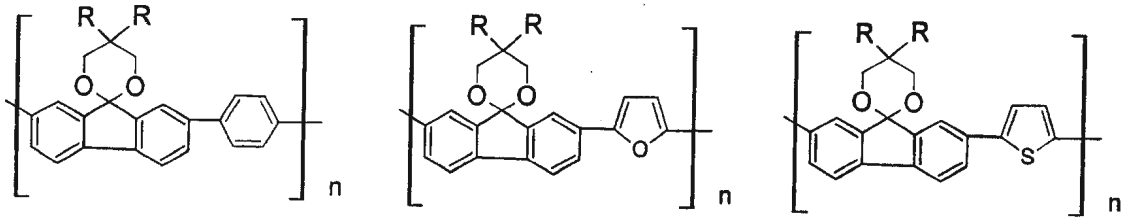

2-12
PFKB

2-13
PFKF

2-14
PFKT

$R=C_8H_{17}$

Figure 2-2. Structures of **PFKB**, **PFKF** and **PFKT**

In order to investigate the conversion of the precursor polymers to the target polymers, model compounds of **PFKT** and **PFT** were synthesized as 2,7-bis(2-thienyl)spiro[4',4'-dioctyl-2',6'-dioxocyclohexane]-1',9-fluorene **(2-15)** and 2,7-bis(2-thienyl)-9-fluorenone **(2-16)** (Figure 2-3). The same method was used to convert the model compound and precursor polymers to the targets.

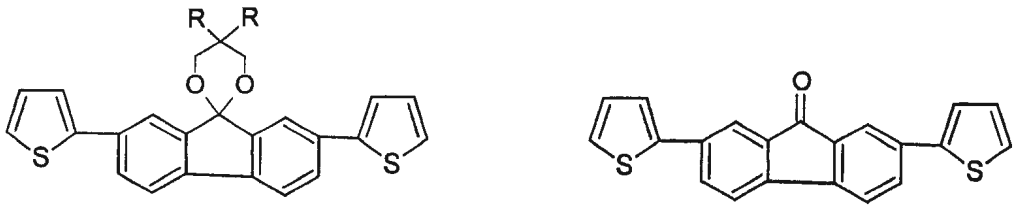

2-15

2-16

$R = C_8H_{17}$

Figure 2-3. Model compounds of **PFKT** and **PFT**

2.2.4 Synthesis of poly(2,7-spiro[4',4'-dioctyl-2',6'-dioxocyclo-hexane]-1',9-fluorene-*co*-1,4-benzene) (PFKB)

Poly(2,7-spiro[4',4'-dioctyl-2',6'-dioxocyclohexane]-1',9-fluorene-*co*-1,4-benzene) **(PFKB)** was prepared by copolymerization of 2,7-dibromospiro-[4',4'-dioctyl-2',6'-dioxocyclohexane]-1',9-fluorene **(2-9)** and 1,4-bis(trimethylstannyl)benzene **(2-20)** (Scheme 2-3). 2,7-Dibromospiro[4',4'-dioctyl- 2',6'-dioxocyclohexane-1',9-fluorene] **(2-9)** was synthesized according to Uckert's procedure from malonic acid diethyl ester **(2-6)** in three steps [43].

2.2.4.1 Synthesis of 2,7-dibromo-9-fluorenone (2-4)

2,7-Dibromo-9-fluorenone **(2-4)** is a commercially available compound but is very expensive. It can be prepared by oxidation of 2,7-dibromofluorene **(2-17),** a much cheaper material.

Huntress *et al.* reported a procedure in which fluorene was oxidized by sodium dichromate in acetic acid and water. In this reaction, fluorenone was obtained in 60-70 % yield (Scheme 2-4) [106]. Our first approach, following Huntress's procedure, used sodium dichromate as an oxidant in acetic acid and water. 2,7-Dibromo-9-fluorenone was prepared in very low yield (2 %). Postulating that the poor solubility of 2,7-dibromo-9-fluorene in acetic acid was probably responsible for the low yield, acetone was added in

the second attempt to dissolve the starting materials. The yield was improved to only 6 %.

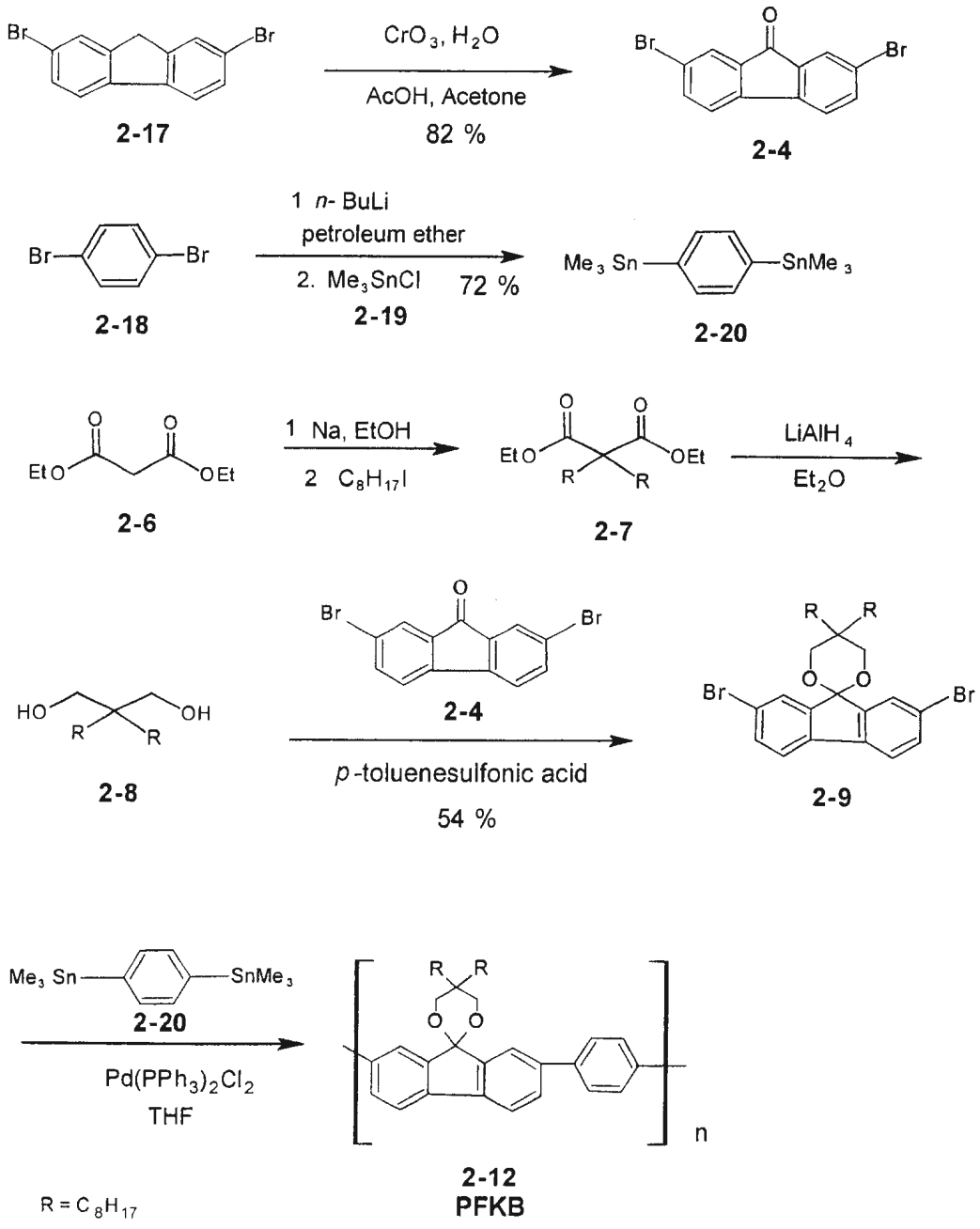

Scheme 2-3. Synthesis of **PFKB**

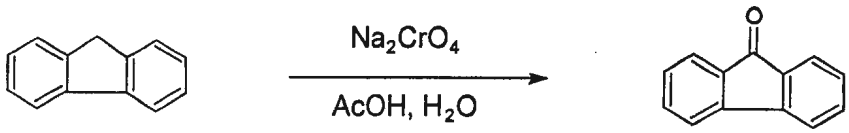

2-21 **2-22**

Scheme 2-4. Huntress's synthesis of 9-fluorenone

Use of the Jones reagent (chromium trioxide in aqueous sulfuric acid) [107] only improved the yield to 19 %. 2,7-Dibromofluorene has good solubility in benzene. The inorganic oxidant only dissolves in water. We expected that vigorous stirring could facilitate a two-phase reaction. Compound **(2-17)** was dissolved in benzene and then Jones reagent was added with mechanical stirring. However, the yield was reduced to 14 %.

Murahashi *et al.* reported the oxidation of 2,7-dibromofluorene with chromium oxide-acetic acid, but they did not give the procedure [108]. We therefore tried the method reported by Burnham *et al.* [109]. Chromium trioxide-acetic acid-water was used as oxidant, and acetic acid and acetone were used as solvents. 2,7-Dibromo-9-fluorenone was obtained in 82 % yield after stirring for 8 d at room temperature.

2.2.4.2 Synthesis of 2,2-dioctylmalonic acid diethyl ester (2-7)

Our first attempt to synthesize 2,2-dioctylmalonic acid diethyl ester **(2-7)** followed

Uckert's procedure (See Section 2.2.2). Malonic acid diethyl ester **(2-6)** was stirred with sodium ethoxide, and then 1-iodooctane was added dropwise. However, none of the desired product **(2-7)** was detected by NMR. The procedure was modified by using sodium. Sodium ethoxide was produced *in situ* to reduce the effect of moisture absorption by the reaction mixture. 2,2-Dioctylmalonic acid diethyl ester **(2-7)** was obtained in 57 % yield.

2.2.4.3 Synthesis of 2,2-dioctyl-1,3-propanediol (2-8)

2,2-Dioctyl-1,3-propanediol **(2-8)** was prepared by reduction of 2,2-dioctylmalonic acid diethyl ester **(2-7)** with lithium aluminum hydride under anhydrous conditions as described by Uckert [43]. After stirring for 6 h, the yield was 95 %.

2.2.4.4 2,7-Dibromospiro[4',4'-dioctyl-2',6'-dioxocyclohexane]-1',9-fluorene (2-9)

2,7-Dibromospiro[4',4'-dioctyl-2',6'-dioxocyclohexane]-1',9-fluorene **(2-9)** was prepared by ketalization of 2,7-dibromo-9-fluorenone **(2-4)**with 2,2-dioctyl-1,3-propanediol **(2-8)** in the presence of *p*-toluenesulfonic acid. Water is a byproduct in this reaction. Removing water shifts the equilibrium towards the direction of acetal formation. In our initial attempt, we used a Dean and Stark apparatus to remove the water produced in

the reaction. However, no target compound **(2-9)** was detected by NMR after refluxing for 2 days. The problem was probably the solvent. Toluene and water are partially miscible. A Soxhlet extractor containing 4Å molecular sieves was subsequently employed to remove the water. With effective water absorption by the activated molecular sieves, 2,7-dibromospiro[4',4'-dioctyl-2',6'-dioxocyclohexane]-1',9-fluorene **(2-9)** was obtained in 54 % of yield after purification by column chromatography.

2.2.4.5 Synthesis of 1,4-bis(trimethylstannyl)benzene (2-20)

Bao *et al.* reported a synthesis of 1,4-bis(trimethylstannyl)benzene **(2-20)** from the Grignard reagent of *p*-dibromobenzene **(2-18)** and magnesium powder. The Grignard reagent reacted with trimethyltin chloride **(2-19)** to give **(2-20)** in a poor yield of 30 % (Scheme 2-5) [47].

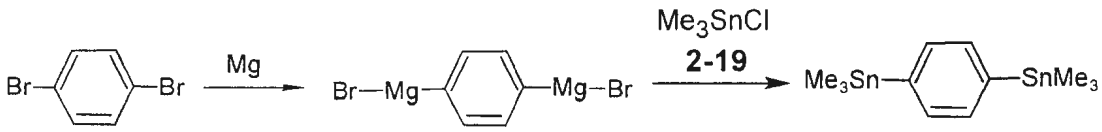

2-18 **2-23** **2-20**

Scheme 2-5. Bao's synthesis of 1,4-bis(trimethylstannyl)benzene

Gilman *et al.* reported an investigation of the conversion of aromatic halides to their organolithium compounds. Among them, *p*-dibromobenzene **(2-18)** was reacted with *n*-butyllithium for 24 h and then worked up with solid carbon dioxide to give terephthalic acid **(2-25)** in 89 % yield (Scheme 2-6) [110]. Gilman emphasized the advantages of petroleum ether as a solvent for alkyllithium reagents.

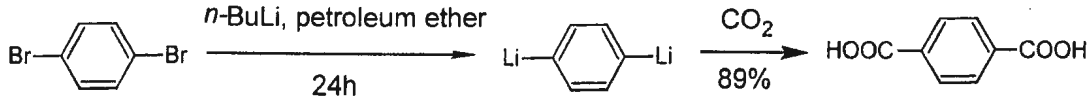

2-18 **2-24** **2-25**

Scheme 2-6. Gilman's synthesis of terephthalic acid

Comparison of Bao's synthesis of 1,4-bis(trimethylstannyl)benzene **(2-20)** to Gilman's synthesis of terephthalic acid **(2-25)** and the synthesis of 2,5-bis(trimethyl-stannyl)thiophene (See Section 2.2.6.1), we anticipated that an organolithium intermediate could give a better yield than the Grignard intermediate. Thus *n*-butyllithium was used to produce dilithium benzene from *p*-dibromobenzene **(2-18)** in petroleum ether through halogen-metal exchange. Then trimethyltin chloride **(2-19)** was added to the reaction mixture to produce the desired product in 72 % yield.

2.2.4.6 Synthesis of poly(2,7-spiro[4',4'-dioctyl-2',6'-dioxocyclo-hexane]-1',9-fluorene-*co*-1,4-benzene) (PFKB)

PFKB was prepared by a Stille coupling reaction in the presence of a palladium (II) catalyst. The reaction is sensitive to water and oxygen. Anhydrous conditions and an inert atmosphere are required.

2.2.5 Synthesis of poly(2,7-spiro[4',4'-dioctyl-2',6'-dioxocyclo-hexane]-1',9-fluorene-*co*-2,5-furan) (PFKF)

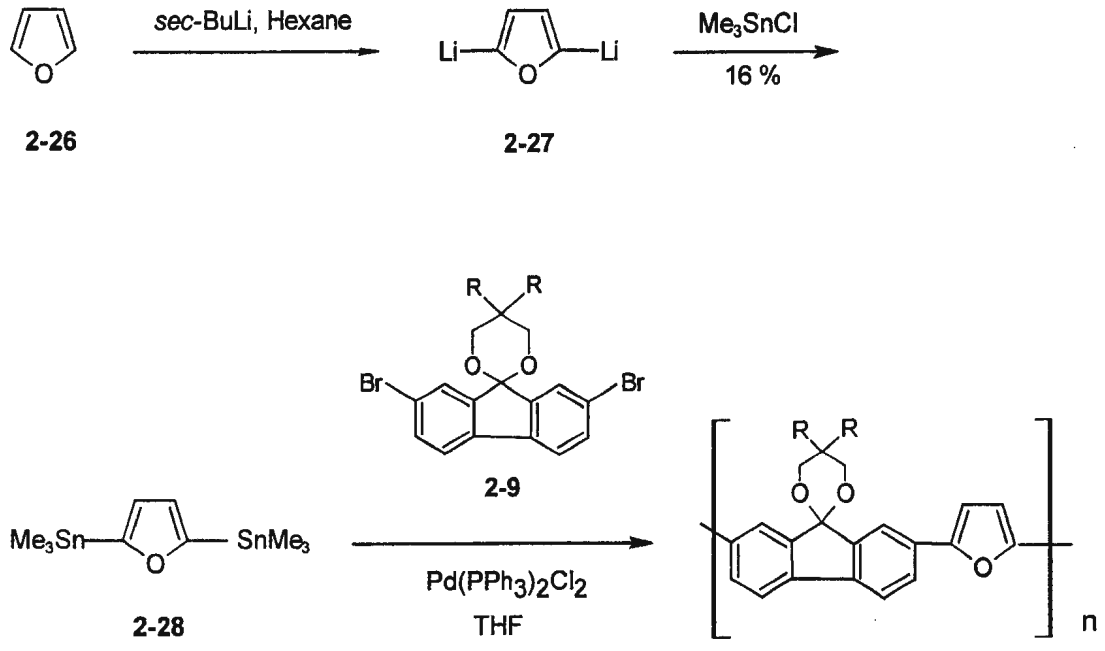

Scheme 2-7. Synthesis of **PFKF**

Poly(2,7-spiro[4',4'-dioctyl-2',6'-dioxocyclohexane]-1',9-fluorene-*co*-2,5-furan) **(PFKF)** was prepared by copolymerization of 2,7-dibromospiro[4',4'-dioctyl-2',6'-dioxocyclohexane]-1',9-fluorene **(2-9)** and 2,5-bis(trimethylstannyl)furan **(2-28)** (Scheme 2-7). 2,5-Bis(trimethylstannyl)furan **(2-28)** was synthesized according to Seitz's procedure from furan [111].

2.2.5.1 Synthesis of 2,5-bis(trimethylstannyl)furan (2-28)

Furan **(2-26)** is more difficult to metallate than thiophene [112]. Thus the synthesis of 2,5-bis(trimethylstannyl)furan **(2-28)** started with metallation with a stronger base, *sec*-butyllithium. The dilithiofuran intermediate was prepared by stirring the reaction mixture at room temperature for 4 h. Then trimethyltin chloride was added dropwise to the reaction mixture. After stirring overnight under a nitrogen atmosphere, the target compound was obtained in 16 % yield. This procedure had been developed by Seitz *et al.* in 1983 [111].

2.2.5.2 Synthesis of poly(2,7-spiro[4',4'-dioctyl-2',6'-dioxocyclohexane]-1',9-fluorene-*co*-2,5-furan) (PFKF)

The synthesis of **PFKF** is similar to the polymerization of **PFKB**, which is described in Section 2.2.4.6.

2.2.6 Synthesis of poly(2,7-spiro[4',4'-dioctyl-2',6'-dioxocyclo-hexane]-1',9-fluorene-*co*-2,5-thiophene) (PFKT)

Poly(2,7-spiro[4',4'-dioctyl-2',6'-dioxocyclohexane]-1',9-fluorene-*co*-2,5-thiophene) **(PFKT)** was synthesized by polymerization of 2,7-dibromospiro-[4',4'-dioctyl-2',6'-dioxocyclohexane]-1',9-fluorene **(2-9)** and 2,5-bis(trimethylstannyl)thiophene **(2-5)** (Scheme 2-8). 2,5-Bis(trimethylstannyl)thiophene **(2-5)** was prepared based on Seitz's procedure from thiophene [111].

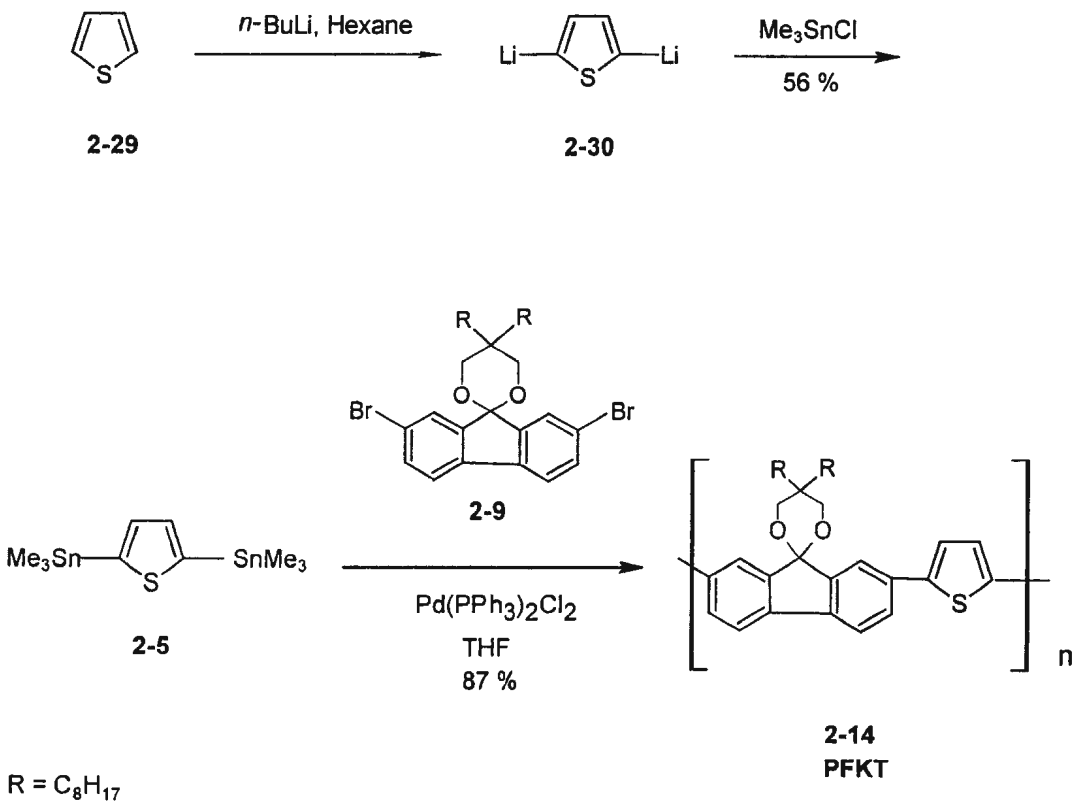

Scheme 2-8. Synthesis of **PFKT**

2.2.6.1 Synthesis of 2,5-bis(trimethylstannyl)thiophene

The synthesis of 2,5-bis(trimethylstannyl)thiophene **(2-5)** followed the procedure developed by Seitz *et al.* in 1983 [111]. The reaction started by metallation of thiophene by *n*-butyllithium to produce the dilithium intermediate **(2-30)**. Without isolation, **2-30** was reacted with trimethyltin chloride under a nitrogen atmosphere to give the desired product **(2-5)** in 82 % yield.

2.2.6.2 Synthesis of poly(2,7-spiro[4',4'-dioctyl-2',6'-dioxocyclohexane]-1',9-fluorene-*co*-2,5-thiophene) (PFKT)

The synthesis of **PFKT** is similar to the polymerization of **PFKB**, which is described in Section 2.2.4.6.

2.2.7 Synthesis of 2,7-bis(2-thienyl)spiro[4',4'-dioctyl-2',6'-dioxocyclohexane]-1',9-fluorene: a model compound of precusor polymer PFKT

The model compound of **PFKT** was prepared as bis(2-thienyl)spiro[4',4'-dioctyl-2',6'-dioxocyclohexane]-1',9-fluorene **(2-15)** using a Stille coupling reaction of 2,7-dibromospiro[4',4'-dioctyl-2',6'-dioxocyclohexane-1',9-fluorene] **(2-9)** and 2-(trimethylstannyl)thiophene **(2-32)** (Scheme 2-9).

2.2.7.1 Synthesis of 2-(trimethylstannyl)thiophene (2-32)

The synthesis of 2-(trimethylstannyl)thiophene **(2-32)** started with the metallation of thiophene by *n*-butyllithium. A reduced amount of base was used to favor the monosubstituted intermediate. Intermediate **(2-31)** was reacted with trimethyltin chloride to give the desired product **(2-32)** in 99 % yield.

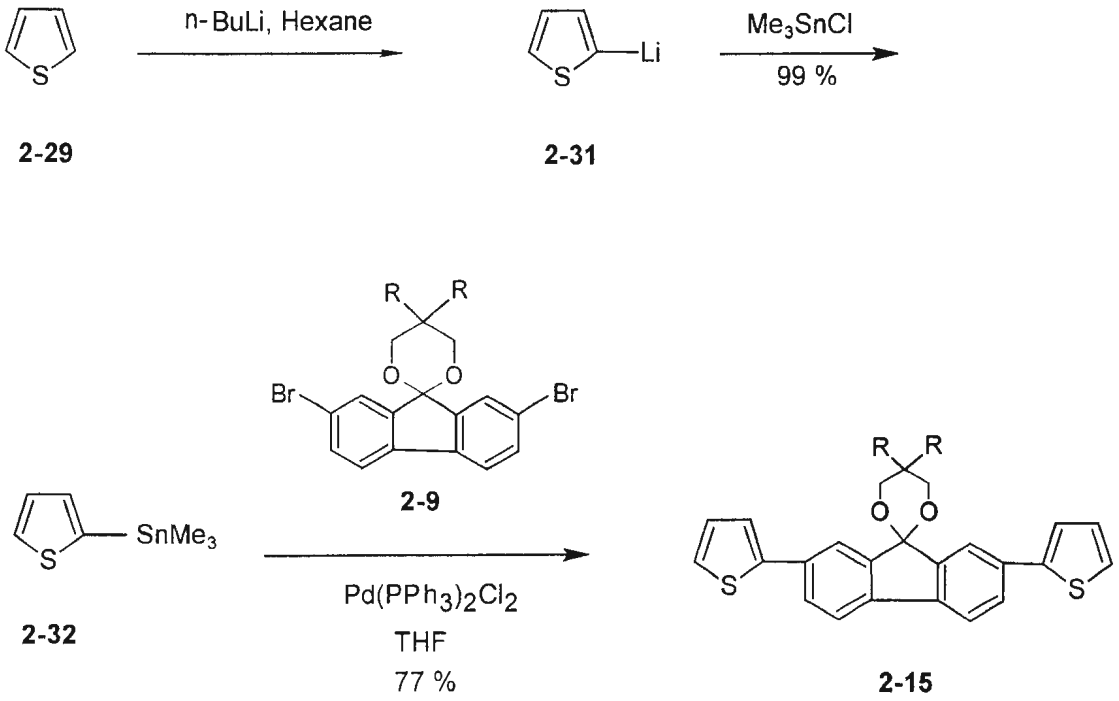

Scheme 2-9. Synthesis of 2,7-bis(2-thienyl)spiro[4',4'-dioctyl-2',6'-dioxocyclohexane]-1',9-fluorene

2.2.8 Synthesis of 2,7-bis(2-thienyl)-9-fluorenone: a model compound of target polymer PFT

The model compound of **PKF** was prepared as 2,7-bis(2-thienyl)-9-fluorenone (**2-16**). The Stille coupling reaction was used in this synthesis. 2,7-Dibromo-9- fluorenone **(2-9)** reacted with 2-trimethylstannylthiophene **(2-32)** to give the desired product **(2-16)** in the presence of a palladium catalyst (Scheme 2-10).

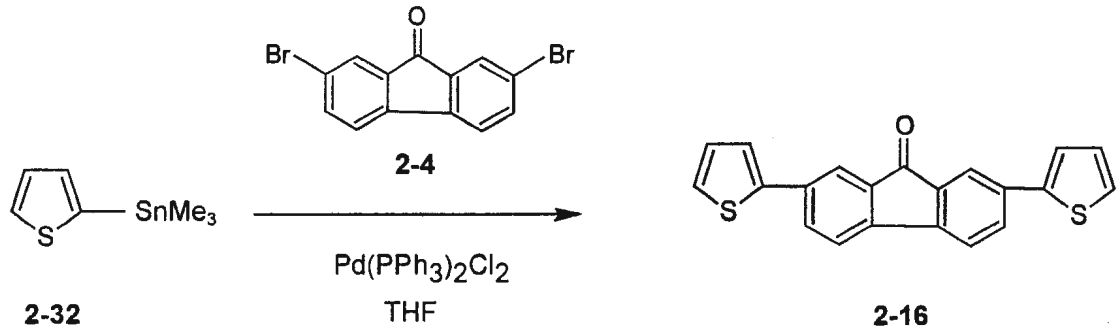

2-32 **2-16**

$R = C_8H_{17}$

Scheme 2-10. Synthesis of 2,7-bis(2-thienyl)-9-fluorenone

2.3 Results and discussion

2.3.1 Precursor polymers

2.3.1.1 PFKT

The synthesis of **PFKT** was conducted three times with different amounts of catalyst (Table 2-1). The molar masses of the resulting copolymers were measured by GPC using polystyrene standards.

Tsuie *et al.* reported the synthesis of a dialkyl substituted fluorene and thiophene copolymer (**2-34**) with small amounts of catalyst (Scheme 2-11) [45]. In the first approach to **PFKT**, we followed Tsuie's method with 0.13 % molar equivalents catalyst based on 2,7-dibromospiro[4',4'-dioctyl-2',6'-dioxocyclohexane]-1',9-fluorene (**2-9**). After heating at reflux overnight, the product marked as **PFKT-1** was isolated in 96 % yield as a yellow powder. GPC showed a bimodal distribution with median molar masses at 18,900 g mol^{-1} and 3,600 g mol^{-1}.

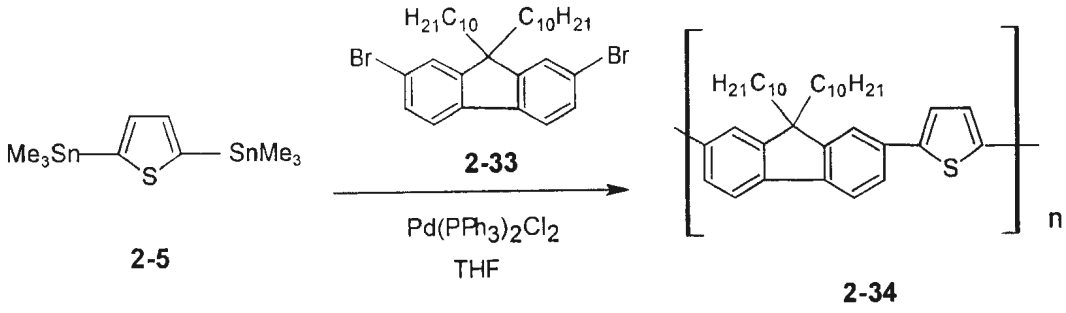

Scheme 2-11. Tsuie's synthesis of fluorene-thiophene-based hybrids

The use of 5 % molar equivalents of palladium catalyst is a more typical amount used for Stille coupling-type polymerizations. For example, Bao *et al.* reported the synthesis of a series of benzene-thiophene alternating copolymers **(2-36)** with 5 % catalyst. M_n was as high as 14,000 g mol^{-1} (Scheme 2-12) [47, 48]. Thus in the second synthesis, the amount of catalyst was increased to 5 % molar equivalents to improve the molar mass of polymer. The product marked, **PFKT**, was isolated as a brown solid in 87 % yield. Median molar masses were 40,400 g mol^{-1} and 4,500 g mol^{-1} with a bimodal distribution based on GPC analysis.

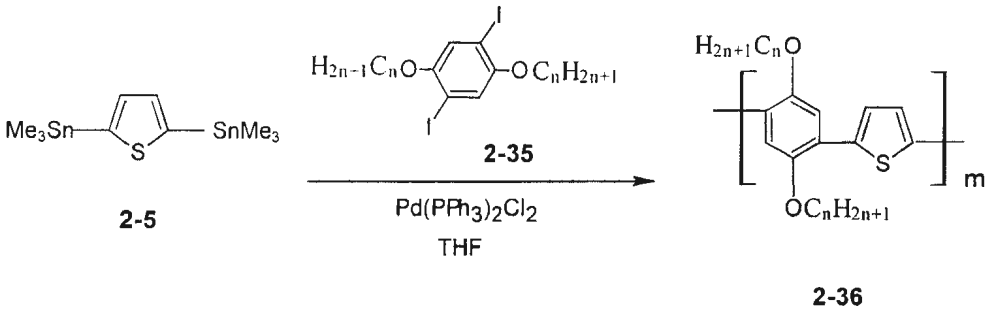

Scheme 2-12. Bao's synthesis of benzene-thiophene alternating copolymers

Bao *et al.* also investigated the influence of % molar equivalents of the catalyst in the synthesis of dialkyl substituted benzene and thiophene copolymers using Stille coupling reactions from a diiodobenzene and 2,5-bis(trimethylstannyl)thiophene [48]. The result showed that 2 % molar equivalents of Pd (II) catalyst gave the highest M_n. In the third synthesis of **PFKT**, the amount of catalyst was reduced to 2 % molar

equivalents based on **2-9**. The resulting copolymer was marked as **PFKT-2**. **PFKT-2** was isolated as a yellow solid in 25 % yield. GPC showed a bimodal molar mass distribution with median molar masses at 27,500 g mol^{-1} and 2,400 g mol^{-1}.

Table 2-1. **PFKT-1**, **PFKT-2** and **PFKT**

Polymer	Amount of $Pd(PPh_3)_2Cl_2$ (mol %)	Yield %	Median molar mass based on GPC / g mol^{-1} (approx. peak % area)[1]	
PFKT-1	0.13	96	18,900 (50 %)	3,600 (50 %)
PFKT-2	2.0	25	27,500 (30 %)	2,400 (70 %)
PFKT	5.0	87	40,400 (55 %)	4,500 (45 %)

1 Detection was based on absorption at 340nm; peak areas were broad.

Based on these three experiments, the median molar mass of the higher molar mass part increased with the increasing % molar equivalents of the catalyst from 0.13 % to 5 % in the polymerization of fluorenone-thiophene precursor copolymers.

2.3.1.2 Molar mass measured by MALDI-TOF MS

MALDI-TOF MS was attempted to measure the molar mass of fluorenone-thiophene precursor copolymers, **PFKT-1** and **PFKT**.

For **PFKT-1**, a molecular mass distribution ranging from 3,900 g mol^{-1} (n=7) to 600 g mol^{-1} (n=1) was clearly seen in the spectrum (Figure 2-4). The base peak was at

2,200 g mol^{-1} (n=4). Thus, the mass spectrum displays a major series of molar masses corresponding to **PFKT** oligmers. This result is consistent with the expected repeat unit structure. Between the major signals corresponding to **PFKT** oligmers, another series of peaks of less intensity are observed. These peaks may be due to **PFT** oligmers where the acetal side chains of the precursor copolymers have been cleaved during MS laser desorption. This side chain loss behavior was also observed in other rigid backbone polymers [113].

We expected the main molar mass of GPC to be close to the molar mass from data obtained from the MALDI-TOF MS spectrum. The experiments showed that there was a little deviation. There were two median molar masses showed in the GPC due to the bimodal distribution, in which the lower median molar mass was 3,600 g mol^{-1}. This deviation may be caused by the inaccuracy of GPC (See Section 2.3.1.3). The higher molar mass product (18,900 g mol^{-1}) measured by GPC was not observed in the MALDI spectrum, possibly due to insolubility in the matrix solvent.

For **PFKT**, MALDI-TOF MS spectra only showed low intensity signals, with none significantly above the high background. As was mentioned above results of GPC indicated that **PFKT** had a much higher main molar mass than **PFKT-1**. Again the solubility of the polymer in the matrix solvent used in MALDI analysis maybe the problem.

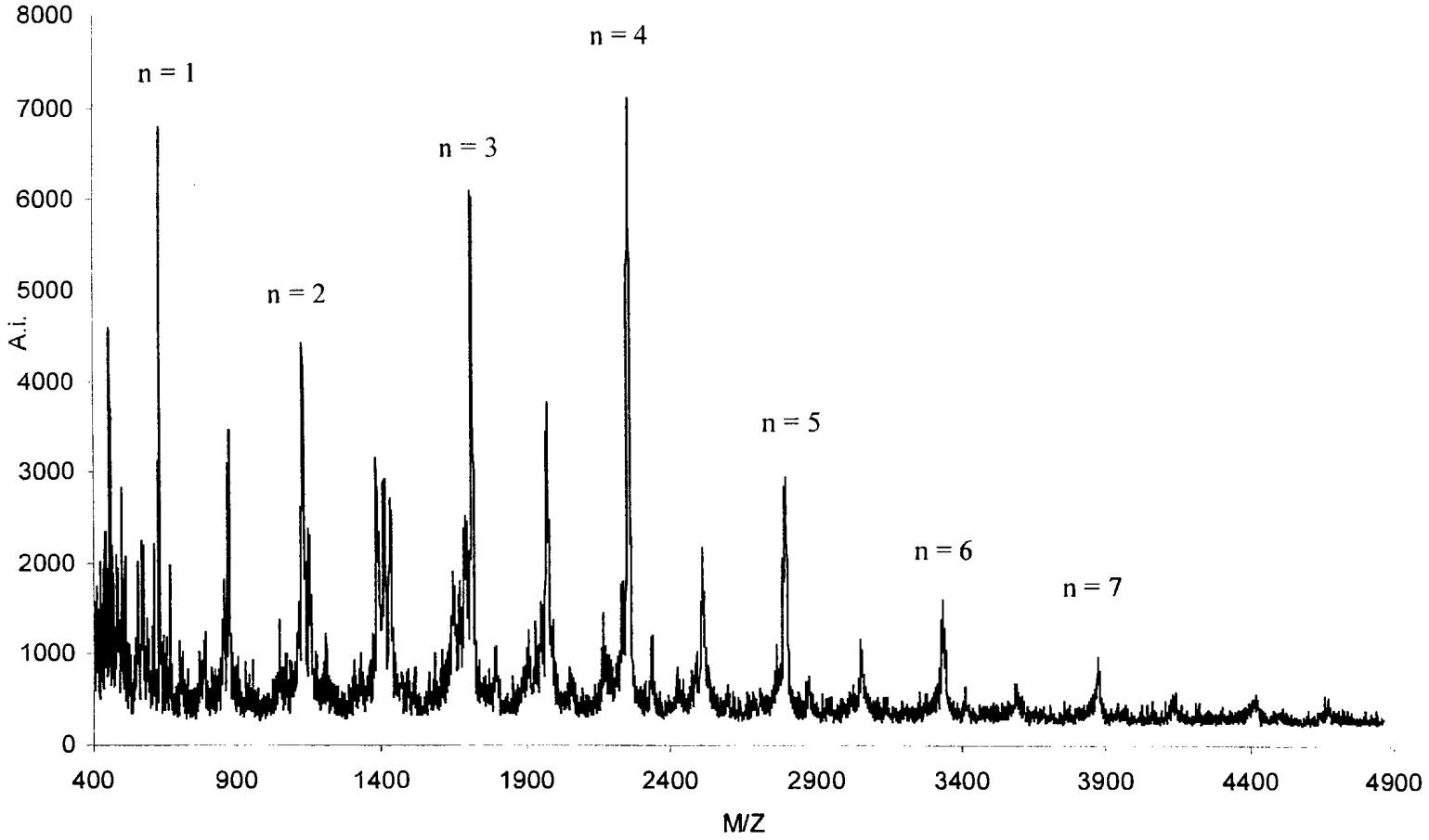

Figure 2-4. MALDI mass spectrum of **PFKT-1**

2.3.1.3 Molar mass averages and the structures of the precursor polymers

The weight-average molar mass, M_w, was determined based on GPC, the number-average molar mass, M_n, was calculated from GPC and also from % Br of end groups found by elemental analysis (Table 2-2) [114].

The precursor polymer, **PFKT**, gave the highest molar mass averages in both GPC and end group analysis. Based on the end group analysis, when the structure was assumed to have one bromine atom at the end of the backbone (A) (Figure 2-5). M_n was calculated as 9,100 g mol^{-1}. When the structure was assumed to contain two bromine atoms (B), M_n was calculated as 18,200 g mol^{-1}. Based on GPC, M_n was 4,600 g mol^{-1}. Comparing the results from the two methods, the single bromine structure (A) was a reasonable prediction for **PFKT**. Based on GPC, M_w was found to be 45,000 g mol^{-1}, which is much higher than M_n. As the molar mass averages, M_w was more dependent on the amounts of high molar mass fraction than M_n. Thus M_w was always equal or higher than M_n [115].

For precursor copolymer **PFKB**, M_n was 4,600 g mol^{-1} based on the end group analysis when the structure was assumed to be A (Figure 2-5). If we expected two bromines in the end of the backbone (B), M_n was calculated as 9,300 g mol^{-1}. M_n was 3,800 g mol^{-1} based on GPC. Comparing the result of end group analysis to GPC, the value of M_n based on structure A was closer than that of structure B. We expect A to be the structure of **PFKB**. A little higher value of M_w, 5,100 g mol^{-1} was obtained based on

GPC. It is very close to the value of M_n.

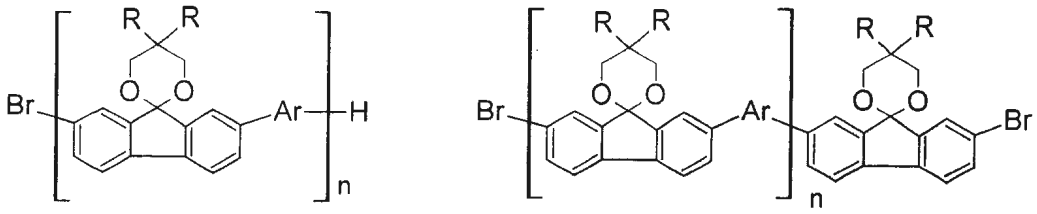

2-37
A

2-38
B

R=C_8H_{17}

Ar= 

Figure 2-5 End groups of precursor polymers

For the precursor copolymer **PFKF**, M_n was found to be 4,700 g mol^{-1} from end group analysis when the structure was assumed to contain one bromine end group (A) (Figure 2-5). M_n was calculated as 9,500 g mol^{-1} if we expected two bromine atoms at the end of the backbone (B). M_n was 1,900 g mol^{-1} based on GPC. Comparing the results of end group analysis to GPC, the value of M_n based on one bromine atom was closer to the GPC result than that based on two bromine atoms. Thus **PFKF** probably only had one bromine end group (A).

All values of M_n and M_w are summarized in Table 2-2. Comparing the average molar mass based on GPC with end group analysis, we concluded that all three precursor copolymers, **PFKB**, **PFKF** and **PFKT**, only contain one bromine in their structures.

All values based on end group analysis were higher than those of GPC. There were perhaps three reasons. First, bromine was probably not estimated accurately because of its low mass %. Second, GPC is a relative method for molar mass determination. All calculations were conducted based on polystyrene standards. Here we assumed that copolymers, **PFKB**, **PFKF** and **PFKT** have the same character in the GPC experiment as polystyrene. This assumption probably causes the deviation from the true molar mass averages. Third, maybe there are some polymers without Br end groups due to the reduction in the Stille reaction.

PFKB and **PFKF** showed monodisperse distribution curves and **PFKT** showed a bimodal distribution curve in GPC. **PFKB** had the smallest polydispersity (M_w / M_n) based on GPC. The polydispersity of **PFKB** was 1.3. The polydispersity of **PFKF** was 2.4, and the polydispersity of **PFKT** was as high as 6.7. The high polydispersity of **PFKT** is caused by its bimodal distribution.

Table 2-2 Molar mass averages of **PFKB, PFKF** and **PFKT**

Polymers	M_n based on End Group Analysis		Based on GPC	
	One Br end group g mol^{-1}	Two Br end groups g mol^{-1}	M_w g mol^{-1}	M_n g mol^{-1}
PFKB	4,600	9,300	5,100	3,800
PFKF	4,700	9,500	4,600	1,900
PFKT	9,100	18,200	45,000	4,600

2.3.2 Deacetylisation of the precursors

2.3.2.1 Deacetylisation of the precursor model compound 2-15 to 2-16

Uckert *et al.* reported the conversion of precursor polymer **(2-10)** to corresponding polymer **(2-11)** by exposing a film of the precursor polymer to dichloroacetic acid vapor at about 50°C (Scheme 2-2) [43].

Following Uckert's procedure, 2,7-bis(2-thienyl)spiro[4',4'-dioctyl-2',6'-dioxo-cyclohexane]-1',9-fluorene **(2-15)** was dissolved in THF and drop cast onto a KBr plate. This film was then exposed to trifluoroacetic acid vapor (Scheme 2-13). The cleavage of the acetal can be observed as a color change immediately from yellow to red. Figure 2-6 shows the IR spectrum of **2-15** on a KBr plate. Figure 2-7 shows the IR spectrum of the precursor model compound treated with trifluoroacetic acid. The conversion was confirmed by the reduced C-H absorptions at 2,927 $cm^{-1}$and 2,856 cm^{-1}. Moreover, the disappearance of the acetal's absorptions at 1,071 cm^{-1} and 1,028 cm^{-1} and the appearance of a group of new intense absorption peaks around 1,677 cm^{-1} due to the carbonyl functional group were both evidence of the cleavage. Figure 2-7 shows the same characteristic peaks in the IR spectrum of 2,7-bis(2-thienyl)-9-fluorenone **(2-16)** synthesized from 2,7-dibromo-9-fluorenone and 2-(trimethylstannyl)thiophene (See Section 2.2.8) with that of **2-16** prepared from **2-15**.

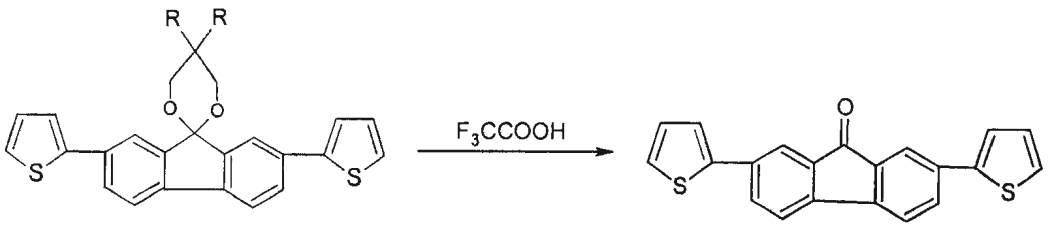

2-15 **2-16**

Scheme 2-13. Conversion of the precursor model compound

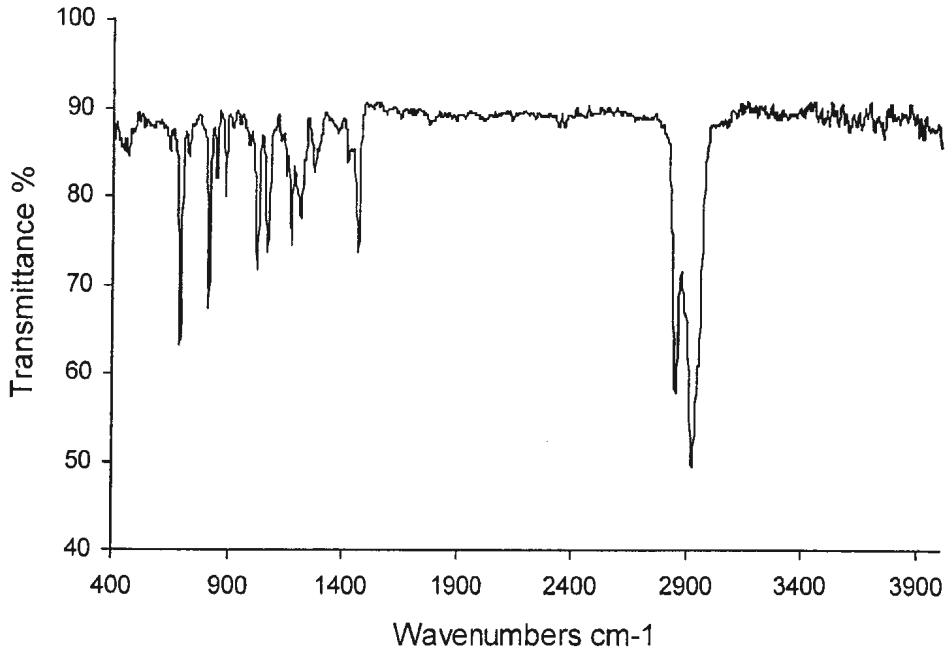

Figure 2-6. IR spectrum of 2,7-bis(2-thienyl)spiro[4',4'-dioctyl-2',6'-dioxocyclo-hexane]-1',9-fluorene on a KBr plate

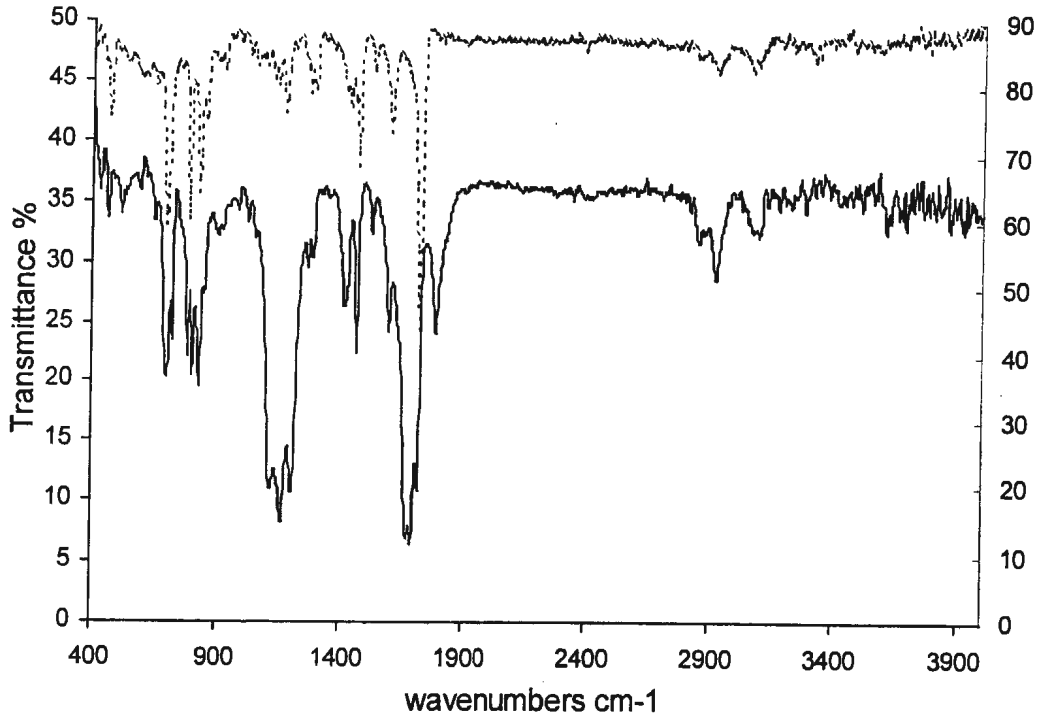

——— The film of 2,7-bis(2-thienyl)spiro[4',4'-dioctyl-2',6'-dioxocyclohexane]-1',9-fluorene exposured to trifluoroacetic acid vapor for 30 min

------ **2-16** Synthesized from 2,7-dibromo-9-fluorenone and 2-(trimethylstannyl)thiophene

Figure 2-7. IR spectra of **2-16** and trifluoroacetic acid treated **2-15**

The IR spectrum of the product obtained from deacetylisation of **2-15** shows broad and strong absorptions at 1,789 cm^{-1}, 1692 cm^{-1} and 1167cm^{-1}. These are very likely due to residual trifluoroacetic acid, which, on its own, exhibits absorptions similar to these [116].

2.3.2.2 Deacetylisation of the precursor polymers to target polymers

2.3.2.2.1 Deacetylisation by *p*-toluenesulfonic acid

The deacetylisation of the precursor polymers followed a general method in which the acetal side chains were exchanged with acetone in the presence of an acid catalyst [117] [118]. The precursor polymers were dissolved in acetone and THF and then *p*-toluenesulfonic acid was added (Scheme 2-14). The reaction mixtures were stirred overnight at room temperature. Sodium carbonate was added to neutralize the acid. The precipitated products were collected by filtration, washed with water and acetone, and dried under vacuum.

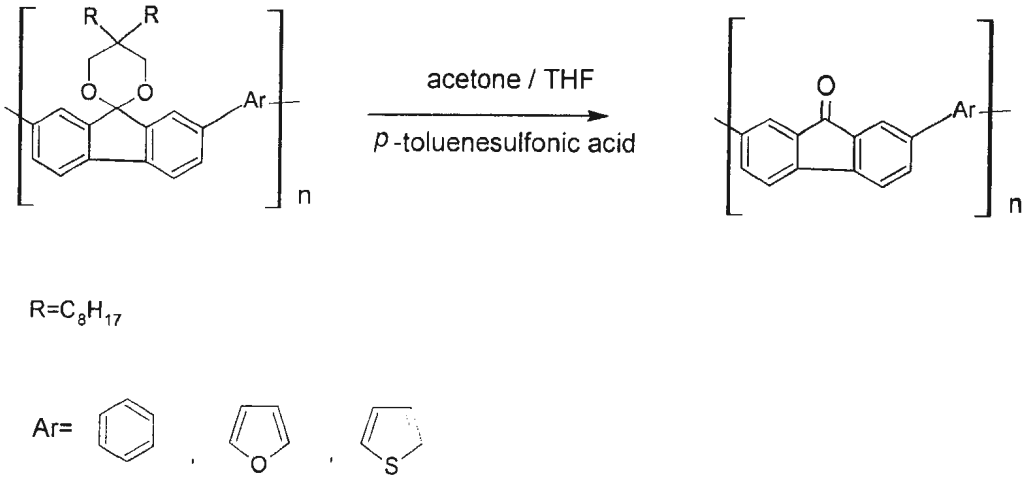

Scheme 2-14. Deacetylisation of precursor copolymers by *p*-toluenesulfonic acid

IR spectra were used to characterize the products. The hydrolysed product from **PFKT** showed two weak peaks at 1,723 cm^{-1} and 1,645 cm^{-1}. The IR spectrum of the

product from **PFKF** also showed two weak peaks at 1,718 cm^{-1} and 1,672 cm^{-1}. These new peaks can be attributed to carbonyl groups. Thus, it was believed that **PFKT** and **PFKF** to be partly converted to their corresponding polyfluorenones.

As a result of the cleavage of the solubilizing side chains, the resulting target fluorenone-based copolymers had poor solubilities and were therefore difficult to characterize further.

2.3.2.2.2 Deacetylisation of the precursor copolymers by acid vapor

The successful conversion of precursor model compound **2-15** to **2-16** suggested another method from precursor polymers to target polymers.

The precursor copolymer **PFKT** was drop coated onto glassy carbon electrodes. After drying, they were exposed to trifluoroacetic acid vapor at room temperature by hanging them in a capped conical flask containing trifluoroacetic acid (5 mL) on the bottom. The cleavage can be observed as a color change from yellow to red over a 10 min period. After the acetals were converted back to the ketones, the target copolymer could be used directly for electrochemical characterization. **PFKB** and **PFKT** were conversted to **PFB** and **PFF** by the same method [105].

2.3.3 Band gaps

Band gaps were determined by cyclic voltammetry and uv-vis spectroscopy by Ms. Kavithaa Loganathan (Table 2-3) [105].

Table 2-3. Electrochemical and optical band gaps [1]

Polymer	$E^{o'}$ (p-doping)[2] / V	$E^{o'}$ (n-doping)[2] / V	Electrochemical band gap / eV	Optical band gap / eV
PFKB	1.4	< -2.0	-	2.4
PFB	1.4	-1.3	1.9	1.9
PFKT	1.2	< -2.0	-	2.3
PFT	1.0	-1.2	1.6	1.9
PFKF	1.0	< -2.0	-	2.3
PFF	1.1	-1.3	1.7	1.9

1. Data copied from [105].
2. Average peak of formal potential vs Ag / AgCl

2.3.3.1 Electrochemical band gaps

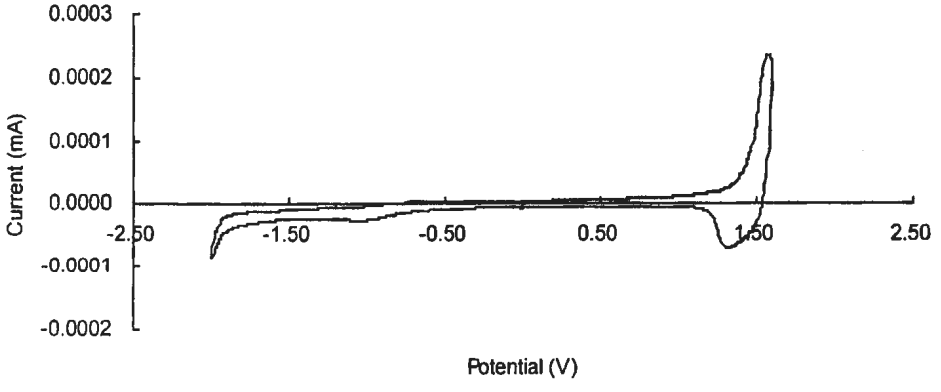

Figure 2-8. Cyclic voltammogram of a **PFKB** film [105]

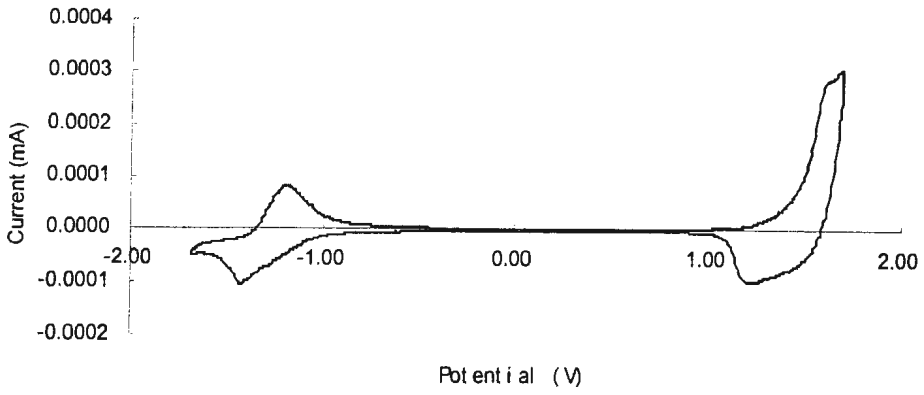

Figure 2-9. Cyclic voltammogram of a **PFB** film [105]

A cyclic voltammogram of a **PFKB** film showed the onset p-doping at *ca.* +1.2 V (Figure 2-8). The formal potential is *ca.* +1.4 V. In the potential range of the experiment (< -2.0 V), n-doping of the **PFKB** film was not observed.

A **PFKB** film was converted to **PFB** by treatment with TFA vapor (Figure 2-9). A cyclic voltammogram of the **PFB** film showed that the formal potentials were *ca.* +1.4 V and *ca.* -1.3 V. The p- and n-doping onset potentials were *ca.* +1.0 V and *ca.* -0.9 V respectively. The band gap between the onsets of p- and n-doping was 1.9 eV. As expected, **PFKB** has a bigger band gap than **PFB**. When **PFKB** was converted to **PFB**, the n-doping formal potential was reduced from over *ca.* -2.0 V to *ca.* -1.3 V. The p-doping potential was unchanged. With a strong electron-withdrawing carbonyl group in 9-position, fluorenone is highly electron deficient. This results in a large stabilizing effect on the LUMO energy level [105].

PFKF, **PFF**, **PFKT** and **PFT** showed very similar electrochemical characteristics to **PFKB** and **PFB**. Formal potentials and band gaps are summarized in Table 2-3.

The band gap of **PFF** is *ca.* 0.2 eV lower than that of **PFB** and the band gap of **PFT** is 0.3 eV lower than that of **PFB**. These results confirm the strategy that increasing the electron density in the electron-deficient conjugated systems could reduce band gaps. The electron-rich furan and thiophene moieties increased the HOMO energy of the polymer significantly relative to benzene moieties. The LUMO energy remains unchanged. We considered that the LUMO energy was determined by the fluorenone moiety [105].

2.3.3.2 Optical band gaps

Optical band gaps were calculated from uv-vis spectra (Table 2-3) [105]. **PFB**, **PFF** and **PFK** had the same optical band gaps, 1.9 eV, due to their close onset absorptions of uv-vis spectra. The optical band gaps of **PFB**, **PFF** and **PFT** were roughly consistent with their electrochemical band gaps.

The optical band gaps of precursor copolymers, **PFKB**, **PFKF** and **PFKT** are 2.4 eV, 2.3 eV and 2.3 eV respectively. These results are all considerably lower than those estimated from cyclic voltammetry.

PFB, **PFF** and **PFT** all have lower band gaps than their precursor copolymers. These results are also consistent with the electrochemical results.

2.4 Experimental

2.4.1 General procedures

Unless otherwise stated, all chemicals were used as received. Absolute ethanol was distilled from sodium directly into the reaction flask. Toluene and tetrahydrofuran (THF) were distilled from sodium-benzophenone. *n*-Hexane and furan were distilled from sodium. *N,N,N',N'*-Tetramethylethylenediamine was distilled from potassium hydroxide. A 30 mL of aqueous 10 % chromium trioxide solution in acetic acid was prepared by dissolving 3.65 g of chromium trioxide in 28.5 mL acetic acid and 1.5 mL water [109].

^{1}H NMR spectra were obtained with a 300 MHz General Electric GN-300NB spectrometer and a 500 MHz Bruker Avance spectrometer. Chemical shifts were recorded in ppm relative to internal standard (Me_4Si) or deuterated solvent. In all cases individual signals were reported as chemical shift, multiplicity (s=singlet, d=doublet, dd=doublet of doublets, t=triplet, q=quartet, m=multiplet), number of hydrogens and coupling constants. Melting points were recorded on Fisher-Johns apparatus. Uv-vis data were recorded on a Hewlett Packard 8452A diode array spectrophotometer. GPC analysis was performed on a Model 5000 LC system in THF with a Perkin-Elmer LC-95UV/Vis spectrophotometer (λ = 340 nm) as detector and a Waters styragel HR 4E column. Molar masses were calibrated with polystyrene standards. MALDI mass spectra were collected on an Applied Biosystems Voyager System 2026 (N_2 laser, λ = 337 nm) with dithanol as the matrix, operating at a pulse rate of 3 Hz. The ions were

accelerated by a voltage of 25,000 V, and 50 shots were accumulated for each spectrum.

2.4.2 2,7-Dibromo-9-fluorenone (2-4)

2,7-Dibromofluorene (1.03 g, 3.09 mmol) was dissolved with mechanical stirring in acetic acid (90 mL) and acetone (30 mL). Aqueous 10 % chromium trioxide / acetic acid solution (75 mL) was added over a period of 7 d. The reaction mixture was then stirred for another 24 h at room temperature. After concentrating the reaction mixture to 30 mL under vacuum, ice water (100 mL) was added carefully. The yellow precipitate was collected by filtration, washed with aqueous 2 % sulfuric acid (20 mL x 2) and water (20 mL x 3), and dried overnight in air. The filter cake was dissolved in benzene, washed with water (10 mL x 3) and dried over magnesium sulfate. The title product was purified by column chromatography (silica gel, hexane: benzene= 4:1) to provide 0.86 g (82 %) as a yellow solid: m.p. 202-205°C, (lit [20]: 198 °C); ^{1}H NMR ($CDCl_3$): δ 7.78 (2H, d, *J*=1.6 Hz), 7.64 (2H, dd, *J*=8.4, 2.0 Hz), 7.40 (2H, d, *J*=8.0 Hz); IR (KBr, Nujol): ν (cm^{-1}) 2925, 2855, 1708, 1592, 1460, 1377, 903, 821, 780, 471.

2.4.3 2,2-Dioctylmalonic acid diethyl ester (2-7)

Sodium (8.28 g, 0.36 mol) was cut into small pieces and added gradually into absolute alcohol (130 mL). After the solution became clear, malonic acid diethyl ester

(5.00 g, 0.0312 mol) was added dropwise. The reaction mixture was heated under reflux, and then 1-iodooctane (35.75 g, 0.1489 mol) in absolute ethanol (30 mL) was added dropwise over a 50 min period. The reaction mixture was kept at reflux for 4 d. After evaporating the solvent, ice was added gradually. The mixture was extracted with diethyl ether (10 mL x 3). The combined organic layers were washed with water and dried over magnesium sulfate. The solvent was evaporated and the low-boiling point byproducts were distilled out under reduced pressure. The title product was purified by column chromatography (silica gel, ethyl acetate: hexane= 1:4) to provide 0.88 g (57 %) as a colorless oil: ^{1}H NMR ($CDCl_3$): δ 4.16 (4H, q, *J*=7.3 Hz), 1.88-1.83 (4H, m), 1.26-1.21 (30H, m), 0.90-0.85 (6H, m); IR (KBr): ν (cm^{-1}) 2956, 2926, 2856, 1734, 1464, 1368, 1252, 1228, 1205, 1178, 1132, 1097, 1032, 723.

2.4.4 2,2-Dioctyl-1,3-propanediol (2-8)

To a suspension of lithium aluminum hydride (2.73 g, 0.0719 mol) in diethyl ether (28 mL) was added dropwise a solution of 2,2-dioctylmalonic acid diethyl ester (5.3 g, 0.0177 mol) in diethyl ether (28 mL) over 1 h. The reaction mixture was then heated to reflux for 6 h. After cooling to room temperature, ice (20 g) and then aqueous 10 % sulfuric acid (20 mL) were added carefully. The organic layers were separated and the water layer was extracted with diethyl ether (20 mL x 3). The organic layers were combined, washed with water (10 mL x 3) and dried over magnesium sulfate. After evaporating the solvent and drying under vacuum, the title product was obtained as

3.94 g (95 %) of a colorless oil: ^{1}H NMR ($CDCl_3$): δ 3.53 (4H, s), 3.07 (2H, s), 1.27-1.04 (28H, m), 0.90 (6H, t, *J*=7.0 Hz); IR (KBr): ν (cm^{-1}) 3350, 2926, 2856, 1464, 1378, 1031, 722.

2.4.5 2,7-Dibromospiro[4',4'-dioctyl-2',6'-dioxocyclohexane]-1',9-fluorene (2-9)

This compound was prepared according to the literature procedure but with improved water removal. A solution of 2,7-dibromo-9-fluorenone (1.00 g, 2.96 mmol), 2,2-dioctyl-1,3-propanediol (2.09 g, 6.97 mmol) and *p*-toluenesulfonic acid (0.30 g 1.6 mmol) in toluene (170 mL) was heated for 1 d under reflux, equipped with a soxhlet extractor containing 4Å molecule sieves. Additional 2,2-dioctyl-1,3-propanediol (1.05 g, 3.48 mmol) was added and the reaction mixture was kept under reflux for a further 24 h. After cooling, the title product was purified by column chromatography (basic alumina, petroleum ether: ethyl acetate=50:1) to provide 0.97 g (54 %) as a light yellow solid: mp. 68-70 °C (lit [10]: 74 °C); ^{1}H NMR ($CDCl_3$): δ 7.83 (4H, s), 7.53 (2H, d, *J*=8.2 Hz), 7.43 (2H, d, *J*=8.0 Hz), 4.03 (4H, s), 1.64-1.57 (4H, m), 1.38-1.27 (24H, m), 0.92-0.90 (6H, m); IR (KBr, Nujol): ν (cm^{-1}) 2953, 2925, 2854, 1462, 1378, 1281, 1243, 1178, 1164, 1133, 1097, 1075, 1081, 989, 873, 807, 720.

2.4.6 1,4-Bis(trimethylstannyl)benzene (2-20)

To a solution of 1,4-dibromobenzene (1.00 g, 4.24 mmol) in petroleum ether was

added dropwise a solution of *n*-butyllithium in hexane (2.38 M, 14.0 mL, 33.3 mmol). The reaction mixture was heated for 24 h under reflux and then cooled to 0 °C using an ice bath. Trimethyltin chloride in hexane (1 M, 33.3 mL, 33.3 mmol) was added dropwise. The reaction mixture was then stirred for 40 h at room temperature under a nitrogen atmosphere. Aqueous saturated ammonium chloride (20 mL) was added. The water layer was separated and extracted with ether (10 mL x 3). The combined organic layers were washed with water (10 mL x 3), and dried over magnesium sulfate. The title product was purified by column chromatography (silica gel, hexane) and dried under vacuum to provide 1.24 g (72 %) as white crystals: m.p. 113-115 °C; ^{1}H NMR ($CDCl_3$) δ 7.49 (4H, s), 0.29 (18H, s); IR (KBr, Nujol): ν (cm^{-1}) 3030, 2924, 2856, 1462, 1371, 1237, 1187, 1095, 1015, 767, 530 471.

2.4.7 Poly(2,7-spiro[4',4'-dioctyl-2',6'-dioxocyclohexane]-1',9-fluorene-*co*-1,4-benzene) (PFKB)

2,7-Dibromospiro[4',4'-dioctyl-2',6'-dioxocyclohexane]-1',9-fluorene (0.42 g, 0.68 mmol) and 1,4-bis(trimethylstannyl)benzene (0.29 g, 0.71 mmol) were dried for 1 h under vacuum and dissolved in THF (10 mL). The solution was added into a flask containing dichlorobis(triphenylphosphine)palladium (II) (0.024 g, 0.034 mmol). The reaction mixture was shielded from light and was heated at reflux under a nitrogen atmosphere for 24 h. After cooling to room temperature, the reaction mixture was poured into methanol (100 mL). The light yellow precipitate was collected by filtration,

dissolved into dichloromethane and filtered to remove impurities. The filtrate was concentrated to 10 mL and poured into methanol (100 mL). The precipitate was collected and dried under vacuum. The title polymer was obtained as 0.23 g (63 %) of a light yellow solid: Anal. (%): calculated for $C_{38}H_{48}O_2Br_{0.12}$: Br, 1.72; C, 83.55; H, 8.88; O, 5.86; Found: Br. 1.72; C, 83.34; H, 9.45; O, 5.47; ^{1}H NMR ($CDCl_3$): δ 8.04 (2H, s), 7.59-7.83 (8H, m), 4.20 (4H, s), 1.70 (4H, s), 1.56-1.25 (24H, m), 0.88 (6H, s); IR (KBr): ν (cm^{-1}) 3030, 2955, 2926, 2853, 1600, 1460, 1258, 1211, 1168, 1077, 1020, 892, 813; GPC: Median molar mass = 5,000 g mol^{-1}; uv-vis (THF): λ_{max} (nm) = 360.

2.4.8 2,5-Bis(trimethylstannyl)furan (2-28)

sec-Butyllithium in hexane (1.3 M, 28.8 mL, 37.5 mmol) was added to an 0 °C solution of *N,N,N',N'*-tetramethylethylenediamine (4.39 g, 37.5 mmol), furan (1.02 g, 15.0 mmol) and hexane (37.5 mL). The reaction mixture was stirred for 1 h at 0 °C and 4 h at room temperature. After cooling the reaction mixture to 0 °C again, trimethyltin chloride (1.00 M, 40.5 mL, 40.5 mmol) was added. The reaction mixture was stirred for 24 h at room temperature. Saturated ammonium chloride (40 mL) was added. The organic layer was separated, washed with 3 % copper sulfate and water, and dried over sodium sulfate. After vacuum distillation, the title product was purified by column chromatography (basic alumina, hexane: chloroform = 1:1) to provide 0.7 g (16 %) as a colorless liquid: ^{1}H NMR ($CDCl_3$): δ 6.65 (2H, s), 0.33 (18H, s); IR (KBr): ν (cm^{-1}) 3097, 2983, 2916, 1526, 1441, 1286, 1192, 1164, 1142, 1081, 1000, 904, 733, 532.

2.4.9 Poly(2,7-spiro[4',4'-dioctyl-2',6'-dioxocyclohexane]-1',9-fluorene-*co*-2,5- furan) (PFKF)

2,7-Dibromospiro[4',4'-dioctyl-2',6'-dioxocyclohexane]-1',9-fluorene (0.42 g, 0.68 mmol) and 2,5-bis (trimethylstannyl)furan (0.28 g, 0.71 mmol) were dried for 1 h under vacuum and dissolved in THF (30 mL). Dichlorobis(triphenylphosphine)-palladium (II) (0.024 g, 0.034 mmol) was added to that solution. The reaction mixture was heated for 7 d under reflux under a nitrogen atmosphere and shielded from light. After cooling to room temperature, the reaction mixture was poured into methanol (100 mL). The yellow precipitate was collected by filtration. The filter cake was dissolved in THF and filtered again. The filtrate was precipitated into methanol (100 mL) and the precipitate was collected by filtration and dried under vacuum. The title polymer was provided as 0.18 g (48 %) of a yellow solid: Anal. (%): calculated for $C_{36}H_{46}O_3Br_{0.11}$: Br, 1.69, C, 80.51; H, 8.65; O, 8.94. Found: Br, 1.69, C, 80.18; H, 8.98; O, 9.30; ^{1}H NMR ($CDCl_3$): δ 8.10-8.07 (2H, m), 7.84-7.83 (2H, m), 7.65-7.62 (2H, m), 6.84-6.83 (2H, m), 4.23-4.18 (4H, m), 1.77 (4H, s), 1.46-1.22 (24H, m), 0.91-0.86 (6H, m); IR (KBr): ν (cm^{-1}) 2925, 2854, 1601, 1459, 1304, 1213, 2266, 1083, 1023, 989, 884, 823, 780; GPC: Median molar mass = 4,400 g mol^{-1}; uv-vis (THF): λ_{max} (nm) = 422.

2.4.10 2,5-Bis(trimethylstannyl)thiophene (2-5)

A solution of thiophene (1.05 g, 0.0125 mol), *N,N,N',N'*-tetramethyl-

ethylenediamine (2.82 g, 0.0243 mol) and hexane (4.6 mL) was cooled in ice water and *n*-butyllithium in hexane (2.38 M, 10.20 mL, 0.0243 mol) was added dropwise over 1 h. The reaction mixture was then heated for 30 min under reflux. After cooling to 0 °C, trimethyltin chloride (1 M, 26.4 mL, 0.0264 mol) in hexane was added dropwise. The reaction mixture was stirred overnight at room temperature. Saturated ammonium chloride (40 mL) was added. The organic layer was separated and the water layer was extracted with diethyl ether. The organic layers were combined, washed with aqueous 3 % copper sulfate and water (10 mL x 3), and then dried with sodium sulfate. After evaporation of the solvent, the title product was purified by recrystallization from hexane and recrystallization again from hexane:ethanol = 1:1 to provide as 2.76 g (56 %) as white crystals: m.p. 97-97.5 °C; ^{1}H NMR ($CDCl_3$): δ 7.39 (2H, s), 0.38 (18H, s); IR (KBr, Nujol): ν (cm^{-1}) 3054, 2925, 2856, 1462, 1378, 1255, 1180, 953, 921, 711, 534, 487.

2.4.11 Poly(2,7-spiro[4',4'-dioctyl-2',6'-dioxocyclohexane]-1',9-fluorene-*co*-2,5-thiophene) (PFKT)

To a solution of 2,7-dibromospiro[4',4'-dioctyl-2',6'-dioxocyclohexane]-1',9-fluorene (0.4076 g, 0.670 mmol), 2,5-bis(trimethylstannyl)thiophene (0.2885 g, 0.704 mmol) in THF (30 mL) was added dichlorobis(triphenylphosphine)palladium (II) (0.0237 g, 0.0335 mmol). The reaction mixture was stirred for 24 h under reflux under a nitrogen atmosphere. After cooling to room temperature, the reaction mixture was

poured into methanol (100 mL). The precipitate was collected by filtration, washed with hexane and acetone. The title polymer was isolated after dried under vacuum overnight as 0.36 g (87 %) of a brown solid: Anal. (%): calculated for $C_{36}H_{46}O_2SBr_{0.06}$; Br, 0.88; C, 78.99; H, 8.49; O, 5.85; S, 5.86; Found: Br, 0.88, C, 78.61; H, 8.53; O, 6.07; S, 5.91; ^{1}H NMR ($CDCl_3$) δ 8.03 (2H, s), 7.73-7.55 (2H, m), 7.40-7.31 (2H, m), 4.26-4.11 (4H, m), 2.09-1.84 (4H, m), 1.69-1.11 (24H, m), 0.88 (6H, s); IR (KBr): ν (cm^{-1}) 2952, 2923, 2856, 1600, 1460, 1284, 1249, 1191, 1159, 1075, 1024, 990, 881, 792; GPC: Median molar mass = 40,400 and 4,500 g mol^{-1}; uv-vis (THF): λ_{max} (nm) = 438

2.4.12 2-(Trimethylstannyl)thiophene (2-32)

A solution of thiophene (1.051 g, 0.0125 mol) and *N,N,N',N'*-tetramethylene-diamine (1.44 g, 0.0125 mol) in hexane (15 mL) was cooled in an ice bath and *n*-butyllithium in hexane (2.38 M, 5.25 mL, 0.0125 mol) was added over a 30 min period. The reaction mixture was heated to reflux for 30 min. After cooling to 0 °C, trimethyltin chloride in hexane (1 M, 13.75 mL, 0.1375 mol) was added dropwise. Then the reaction mixture was warmed to room temperature and stirred for 20 h under a nitrogen atmosphere. Saturated ammonium chloride (20 mL) was added. The organic layer was separated, washed with aqueous 3 % copper sulfate solution and water (10 mL x 3), and dried over sodium sulfate. After evaporation of the solvent, the residue was dried under vacuum for 1 h to yield 2-(trimethylstannyl)thiophene 3.07 g (99 %)

as a light brown liquid: ^{1}H NMR ($CDCl_3$) δ 7.65 (1H, dd, *J*=4.5, 1.2 Hz), 7.27-7.25 (1H, m), 7.23-7.22 (1H, m), 0.37 (9H, s); IR (KBr): ν (cm^{-1}) 2981, 2914, 1494, 1396, 1319, 1213, 1076, 1044, 944, 773, 703, 533, 472.

2.4.13 2,7-Bis(2-thienyl)spiro[4',4'-dioctyl-2',6'-dioxocyclohexane]-1',9-fluorene (2-15)

2,7-Dibromospiro[4',4'-dioctyl-2',6'-dioxocyclohexane]-1',9-fluorene (0.2000 g, 0.3223 mmol) and 2-trimethlystannylthiophene (0.2533 g, 1.026 mmol) was dried under vacuum for 1 h and dissolved in THF (10 mL). A solution of dichlorobis-(triphenylphosphine)palladium (II) (0.0127 g, 0.0182 mmol) in THF was added. Then the reaction mixture was heated to reflux for 28 h. The solvent was evaporated and the residue was dissolved in hexane. Aqueous 2 % KF solution (10 mL) was added. The organic layer was separated, washed with water, and dried over magnesium sulfate. The residue was purified by column chromatography (hexane: chloroform=4:1) and dried under vacuum gave the desired product (0.1542 g, 77 %) as a yellow solid: m.p. 112 °C; ^{1}H NMR ($CDCl_3$): δ 7.99 (2H, s), 7.67 (2H, d, *J*=7.8 Hz), 7.60 (2H, d, *J*=7.8 Hz), 7.37 (2H, s), 7.32 (2H, s), 7.13 (2H, m), 4.17 (4H, s), 1.68 (4H, s), 1.41-1.27 (24H, m), 0.92-0.91 (6H, m); IR (KBr): ν (cm^{-1}) 3105, 3071, 3042, 2924, 2852, 1466, 1378, 1213, 1154, 1072, 1028, 989, 888, 815, 694, 413; uv-vis (THF): λ_{max} (nm) 352.

2.4.14 2,7-bis(2-thienyl)-9-fluorenone (2-16)

2,7-Dibromo-9-fluorene (0.50 g, 1.48 mmol), 2-trimethlystannylthiophene (0.44 g, 1.78 mmol) and dichlorobis(triphenylphosphine)palladium (II) (0.05 g, 0.071 mmol) were dissolved in THF (30 mL). The reaction mixture was heated at reflux for 9 h under a nitrogen atmosphere. After cooling to room temperature, the solvent was evaporated. The residue was washed with benzene, acetone, aqueous 2 % KF and water. The target compound was obtained 0.16 g (52 %) of a red solid after drying under vacuum for 2 h: m.p. 224-229 °C; ^{1}H NMR ($CDCl_3$): δ 7.93 (2H, d, *J*=1.74 Hz), 7.48 (2H, dd, *J*=7.8, 2.0 Hz), 7.53 (2H, d, *J*=7.8 Hz), 7.40 (2H, dd, *J*=3.5, 1.4 Hz), 7.34 (2H, dd, *J*=5.2, 1.3 Hz), 7.14-7.10 (2H, m); IR (KBr): ν (cm^{-1}) 3088, 3067, 2922, 2850, 1720, 1599, 1528, 1468, 1434, 1294, 1273, 1208, 1171, 1126, 824, 784, 694; uv-vis (THF): λ_{max} (nm) = 346.

2.4.15 2,7-bis(2-thienyl)-9-fluorenone (conversion from 2,7-bis(2-thienyl)spiro[4',4'-dioctyl-2',6'-dioxocyclohexane]-1',9-fluorene)

2,7-Bis(2-thienyl)spiro[4',4'-dioctyl-2',6'-dioxocyclohexane]-1',9-fluorene (10 mg) was dissolved in THF (1 mL) and then drop cast on a KBr plate. After drying in air for 30 min and vacuum for 1h, the KBr plate with film was hung in a capped 100 mL beaker containing trifloroacetic acid (5 mL) for 30 min. When the color had changed from orange to red, the cleavage was judged to be complete: IR (KBr): ν (cm^{-1}) 3102, 3079, 2926, 2857, 1789, 1720, 1692, 1675, 1600, 1528, 1468, 1420, 1294, 1271, 1206, 1167, 1117, 831, 785, 698; uv-vis (THF): λ_{max} (nm) 354.

Chapter 3

Synthesis of Ionic Conducting Polymers: Polybenzimidazoles

3.1 Introduction

This chapter is focused on the synthesis of the following ionic conducting polymers: poly[2,2'-(4,4'-oxydiphenylene)-5,5'-bibenzimidazole] **(PBI-1)**, poly[2,2'-(4,4'-sulfonyldiphenylene)-5,5'-bibenzimidazole] **(PBI-2)**, poly[2,2'-(4,4'-oxy-diphenylene)sulfonyl-5,5'-bibenzimidazole] **(PBI-3)** (Figure 3-1).

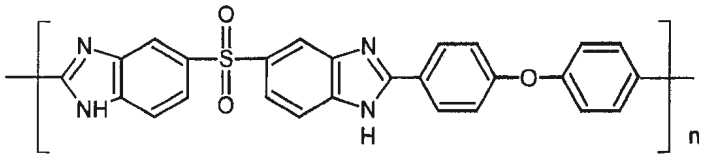

3 -1
PBI-3

Figure 3-1. Structure of **PBI-3**

As derivatives of PBI, **PBI-1**, **PBI-2** and **PBI-3** are considered to be thermally stable polymers. PBIs have been investigated extensively, especially in the 1960s and 1970s. Various PBIs had been synthesized using melt polymerization in the early years and solution polymerization methods more recently (See Section 1.3.3).

After doping with acid, PBI shows good ionic conductivity. This discovery extended the application of PBI to the fuel cell field. PBI membranes allow fuel cells to be operated at higher temperatures than with Nafion membranes.

In order to increase the flexibility of PBI, sulfone or oxygen linkages were introduced in **PBI-1**, **PBI-2** and **PBI-3**.

3.2 Synthesis

3.2.1 Synthesis of poly[2,2'-(4,4'-oxydiphenylene)-5,5'-bibenzimidazole] (PBI-1)

Poly[2,2'-(4,4'-oxydiphenylene)-5,5'-bibenzimidazole] **(PBI-1)** was prepared by polycondensation of 3,3'-diaminobenzidine **(1-32)** and diphenyl ether 4,4'-dicarboxylic acid **(3-2)** (Scheme 3-1)

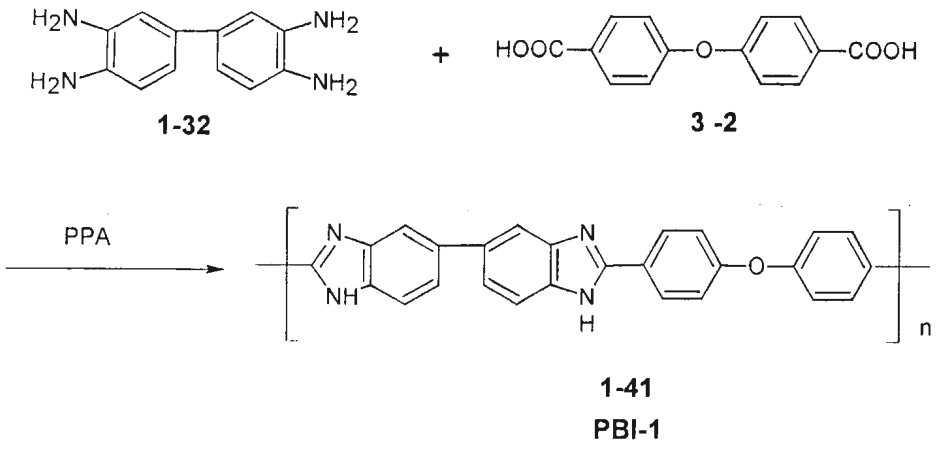

Scheme 3-1. Synthesis of **PBI-1**

PBI-1 has been synthesized by Marvel's group using melting polymerization [87]. Later, solution polymerizations, such as in PPA, were developed for the synthesis of PBIs (See Section 1.3.3.2). PPA offers a convenient single-step method, in which high temperature conditions (400 °C) are avoided.

In another study, Cameron synthesized poly[(5,5'-bibenzimidazole)-2,2'-diyl]-2,5-

pyridine using PPA as a solvent (Scheme 3-2) [119].

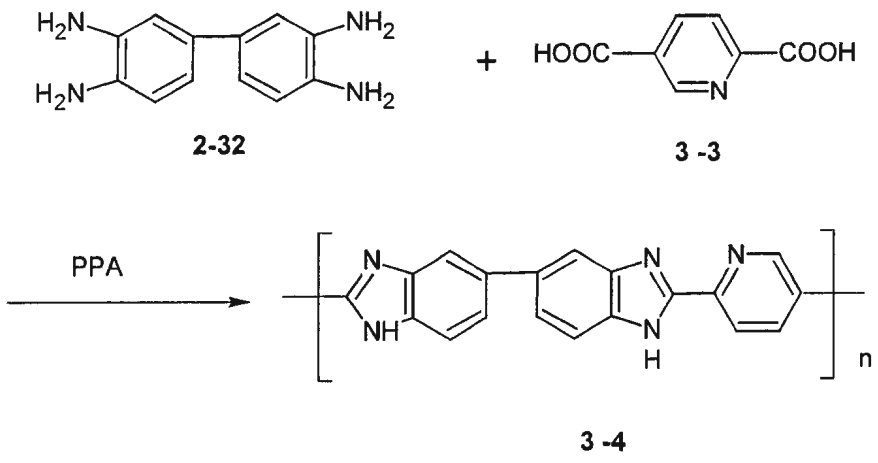

Scheme 3-2. Cameron's synthesis of 3-4

Following Cameron's procedure, 3,3'-diaminobenzidine **(1-32)** and diphenyl ether 4,4'-dicarboxylic acid **(3-2)** were mixed in freshly prepared PPA and heated for 3 d. Phosphorous pentoxide was added in the final stage to facilitate polymerization. The resulting polymer was washed with a large amount of water three times to remove PPA. The desired polymer was obtained in almost quantitative yield.

3.2.2 Synthesis of poly[2,2'-(4,4'-sulfonyldiphenylene)-5,5'-bibenz-imidazole] (PBI-2)

PBI-2 was prepared by polycondensation of 3,3'-diaminobenzidine **(1-32)** and

diphenyl sulfone 4,4'-dicarboxylic acid (**3-6**) (Scheme 3-3). Diphenyl sulfone 4,4'-dicarboxylic acid (**3-6**) was obtained by the oxidation of ditolyl sulfone (**3-5**).

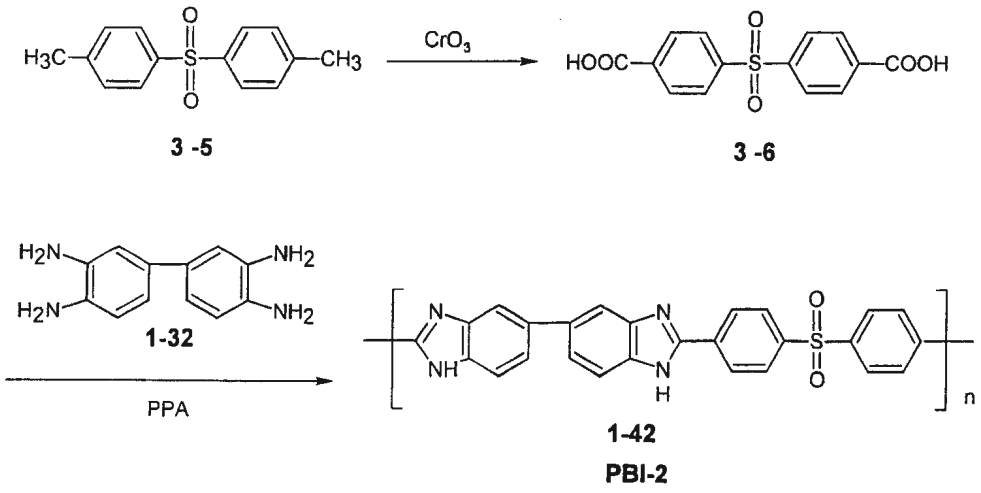

Scheme 3-3. Synthesis of **PBI-2**

3.2.2.1 Synthesis of diphenyl sulfone 4,4'-dicarboxylic acid (3-6)

Adámak *et al.* reported a comparison of two oxidants: $KMnO_4$ and CrO_3 for the synthesis of diphenyl sulfone 4,4'-dicarboxylic acid from ditolyl sulfone [120]. The results showed that the maximum yield was obtained with $KMnO_4$ after reacting for 31 h at 120 °C. However, they did not point out the yield. CrO_3 in glacial acetic acid, concentrated sulfuric acid and water gave a 92 % yield by maintaining the temperature at 100 °C for 15 min. This study considered that a 92 % yield was sufficient and the shorter reaction time using CrO_3 made the synthesis more efficient than that of

$KMnO_4$.

3.2.2.2 Synthesis of poly[2,2'-(4,4'-sulfonyldiphenylene)-5,5'-bibenzimidazole] (PBI-2)

The polymerization to PBI-2 was conducted in PPA, according to the procedure described for **PBI-1** in Section 3.2.1.

3.2.3 Synthesis of poly[2,2'-(4,4'-oxydiphenylene)sulfonyl-5,5'-bibenzimidazole] (PBI-3)

Initially, we planned the polymerization of 3,3',4,4'-tetraaminodiphenyl sulfone **(3-13)** and diphenyl ether 4,4'-dicarboxylic acid **(3-2)**. The final step to 3,3',4,4'-tetraaminodiphenyl sulfone **(3-13)** from 3,3',4,4'-tetraaminodiphenyl sulfone tetrahydrochloride **(3-12)** produced a very low yield (7 %).

Moreover, the PPA solution polymerization permitted the use of tetraamino hydrochlorides as starting materials (Scheme 3-4). Thus we employed 3,3',4,4'-tetraaminodiphenyl sulfone tetrahydrochloride **(3-12)** to shorten the synthesis route and avoid a low yield step. 3,3',4,4'-Tetraaminodiphenyl sulfone tetrahydrochloride **(3-12)** was prepared from 4,4'-diaminodiphenyl sulfone **(3-7)** in 4 steps.

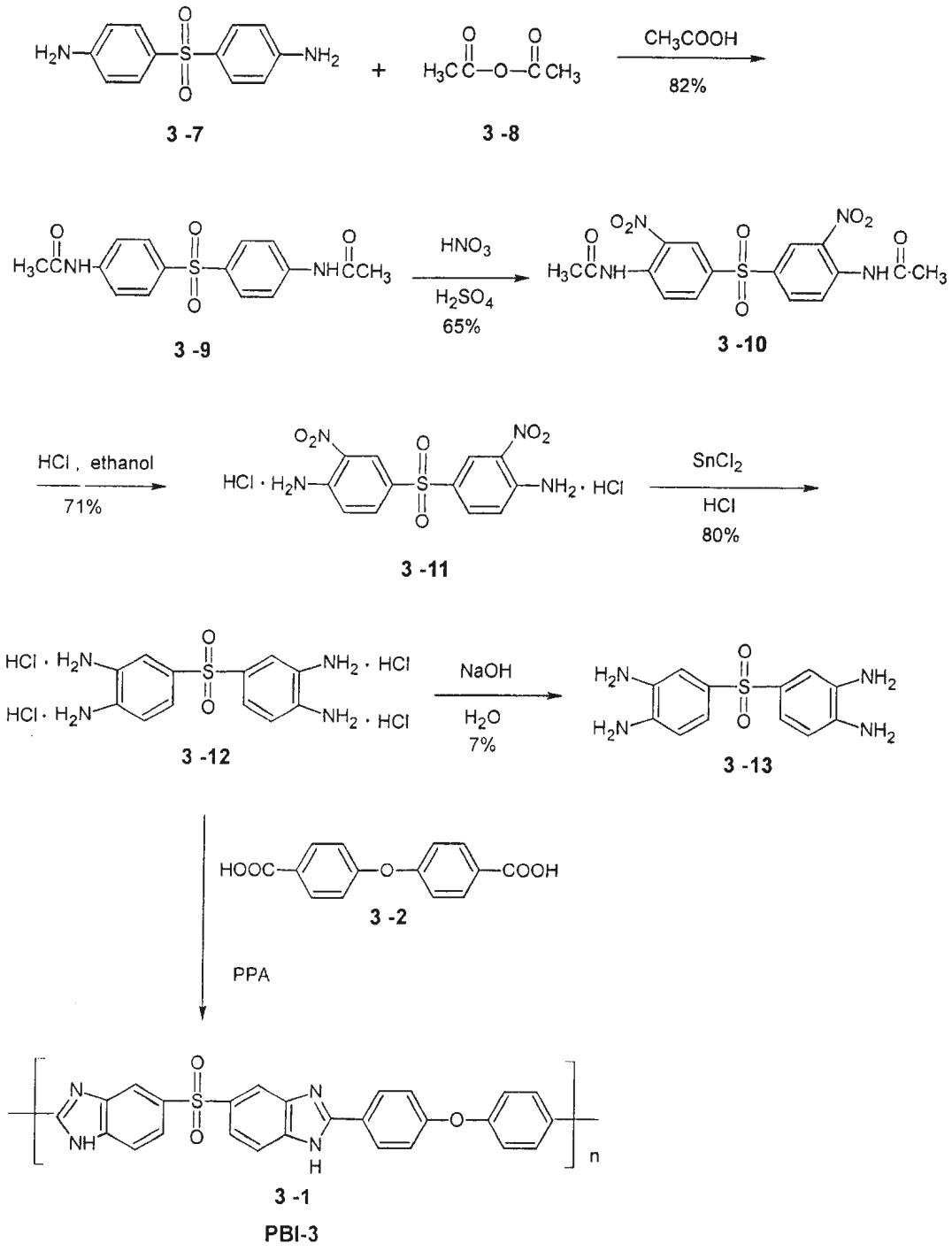

Scheme 3-4. Synthesis of **PBI-3**

3.2.3.1 Synthesis of 4,4'-diacetamidodiphenyl sulfone (3-9)

Stille *et al.* reported a synthesis of 4,4'-diacetamidodiphenyl sulfone **(3-9)** [121]. According to their procedure, we suspended 4,4'-diaminodiphenyl sulfone **(3-7)** in acetic acid and gradually added acetic anhydride over a 2 d period. The desired product was isolated in 83 % yield.

3.2.3.2 Synthesis of 3,3'-dinitro-4,4'-diacetamidodiphenyl sulfone (3-10)

The initial synthesis of 3,3'-dinitro-4,4'-diacetamidodiphenyl sulfone **(3-10)** followed the procedure reported by Stille *et al.* [121]. 4,4'-Diacetamidodiphenyl sulfone **(3-9)** was added gradually into fuming nitric acid. But the desired product was isolated in low yield (17 %). In order to increase the yield, the reaction was conducted at different temperatures for different reaction times. However, the highest yield obtained was only 19 %. The use of concentrated sulfuric acid to catalyse the nitration, increased the yield of the desired product to 65 %.

3.2.3.3 Synthesis of 3,3'-dinitro-4,4'-diaminodiphenyl sulfone hydrochloride (3-11)

The synthesis of 3,3'-dinitro-4,4'-diaminodiphenyl sulfone hydrochloride **(3-11)** was reported by Marvel's group [122] in 61 % yield using a 4 h reaction period. Using their procedure and hydrolyzing 3,3'-dinitro-4,4'-diacetamidodiphenyl sulfone **(3-10)**

in the presence of hydrochloric acid afforded a higher yield (71 %) by prolonging the reaction time to 15 h.

3.2.3.4 Synthesis of 3,3',4,4'-tetraaminodiphenyl sulfone tetrahydrochloride (3-12)

The synthesis of 3,3',4,4'-tetraaminodiphenyl sulfone tetrahydrochloride **(3-12)** followed a procedure reported by Marvel's group [122]. Stannous chloride dihydrate was employed to reduce the nitro functional groups to amines in concentrated hydrochloric acid. After refluxing under a nitrogen atmosphere for 3 d, the desired product was obtained in 80 % yield.

3.2.3.5 Synthesis of 3,3',4,4'-tetraaminodiphenyl sulfone (3-13)

3,3',4,4'-Tetraaminodiphenyl sulfone tetrahydrochloride **(3-12)** was dissolved in water. Aqueous 20 % sodium hydroxide solution was added dropwise. The desired product was isolated and purified in 7 % yield. This procedure has been reported by Marvel's group [122].

3.2.3.6 Synthesis of poly[2,2'-(4,4'-oxydiphenylene)sulfonyl-5,5'-bibenzimidazole] (PBI-3)

Iwakura *et al.* reported the synthesis of poly-2,2'-(*m*-phenylene)-5,5'-bibenzimidazole from 3,3'-diaminobenzidine tetrahydrochloride **(3-14)** and isophthalamide

(3-15) in PPA (Scheme 3-5) [97].

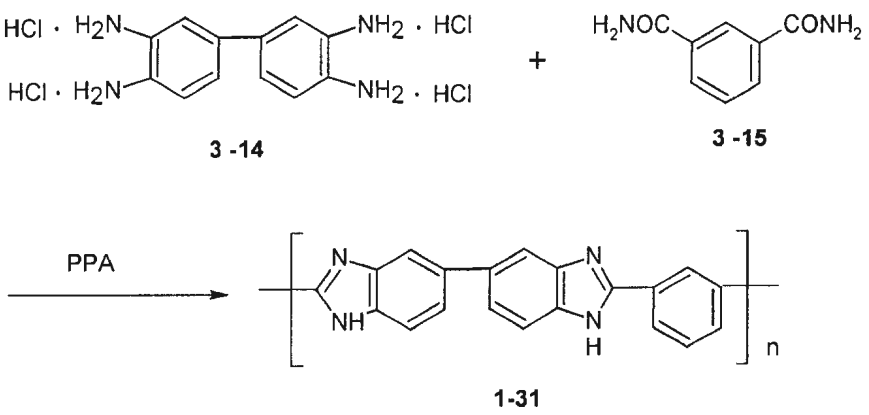

Scheme 3-5. Iwakura's synthesis of poly-2,2'-(*m*-phenylene)-5,5'-bibenzimidazole

The polymerization to **PBI-3** was conducted in PPA according to Iwakura's procedure. 3,3',4,4'-Tetraaminodiphenyl sulfone tetrahydrochloride (**3-12**) was first heated in PPA and then subjected to 3 vacuum / nitrogen cycles to remove hydrogen chloride gas. 3,3',4,4'-Tetraaminodiphenyl sulfone was produced *in situ*. The reaction mixture was allowed to cool to room temperature and then diphenyl ether 4,4'-dicarboxylic acid was added. The polymerization was complete after stirring at 100 °C for 24 h, 120 °C for 24 h and at 150 °C for another 24 h. After washing with water and precipitating in benzene, the product still contained impurities by NMR.

3.3 Results and discussion

3.3.1 Film casting

In order to evaluate the new PBIs for use in fuel cells, they were cast as thin films according to the literature procedure [123-126]. The general procedure involved dissolving the PBI in warm DMAc under a nitrogen atmosphere overnight. Undissolved particles were removed by filtration. The filtrate was concentrated under vacuum to 1-2 mL and then drop cast onto a glass plate. After drying under vacuum overnight at room temperature, the film was peeled off carefully. Longer drying times and higher temperatures would make the film drier, but it also made it more difficult to be peeled off from the glass. The film was washed in boiling water for 6 h and was then doped by immersion in aqueous 11 M phosphoric acid for 3 d.

Usually PBI films are very brittle and can be damaged at every step, even the washing step. The quick current of water (generated by stirring) can break it into pieces. **PBI-1** had much better flexibility than PBI. **PBI-1** films were easy to cast. This result confirms that the oxygen linkages on the backbone increase the flexibility of the polymer.

3.3.2 Conductivity measurements

The ionic conductivity of **PBI-1** was measured by Dr. Chaojie Song.

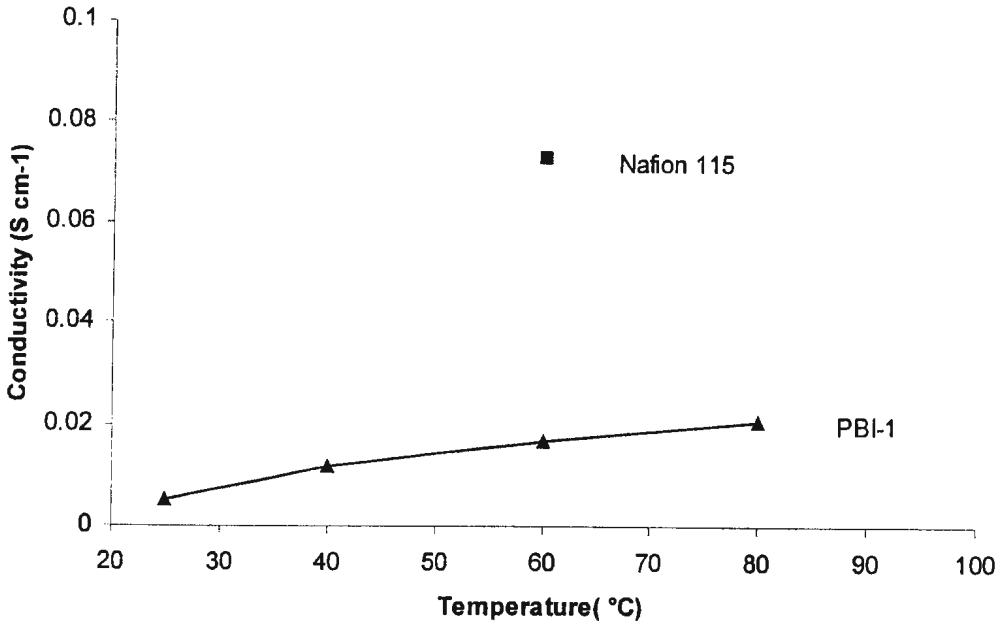

Figure 3-2. Conductivities of **PBI-1** vs Nafion 115

PBI-1 shows an ionic conductivity of 2.06 x 10^{-2} S cm^{-1} at 80 °C. Although the conductivity of **PBI-1** is lower than that of Nafion 115, **PBI-1** is expected to exhibit higher thermal stability, and low crossover of methanol and water [78].

3.4 Experimental

3.4.1 General procedures

3,3'-Diaminobenzidine was recrystallized from water twice under a nitrogen atmosphere. Polyphosphoric acid (PPA) was prepared according to Cameron's procedure [119], which required dissolving phosphorous pentoxide (18 g) into aqueous 85 % phosphoric acid (10 g), under a nitrogen atmosphere. This process required stirring at 100 °C for 24 h. When the solution becomes homogeneous, the PPA is ready to use. Other procedures were the same as those described in Section 2.4.1.

3.4.2 Poly[2,2'-(4,4'-oxydiphenylene)-5,5'-bibenzimidazole] (PBI-1)

3,3'-Diaminobenzidine (0.5000 g, 2.330 mmol) and diphenyl ether 4,4'-dicarboxylic acid (0.6026 g, 2.330 mmol) were added to freshly prepared PPA (28 g). The reaction mixture was stirred at 95 °C for 24 h and then at 110 °C for 47 h. Phosphorous pentoxide (1.5 g) was added. The reaction mixture was heated to 150 °C and stirred for 30 h. After cooling to room temperature, the reaction mixture was added to water (500 mL) and stirred overnight. The precipitate was collected by filtration and resuspended in water (500 mL). The wash procedure was repeated three times and then the polymer was washed with aqueous NH_4OH. After filtration, the filter cake was dried under vacuum. The dry product was dissolved in DMSO (150 mL) and precipitated into benzene. The solid was collected by filtration and dried under vacuum to give 0.92 g (98 %) of the polymer as a light brown solid: ^{1}H NMR (DMSO-d_6): δ 8.28 (4H, d,

J=8.1 Hz), 7.86 (2H, s), 7.70 (2H, d, *J*=7.3 Hz), 7.57 (2H, d, *J*=7.5 Hz), 7.31 (2H, d, *J*=8.7 Hz); IR (KBr): ν (cm^{-1}) 3430, 1629, 1483, 1245, 1173, 1102, 616; GPC: Median molar mass = 367,000 g mol^{-1} and 325,000 g mol^{-1}; uv-vis (DMF): λ_{max} (nm) = 348.

3.4.3 Diphenyl sulfone 4,4'-dicarboxylic acid (3-6)

Ditolyl sulfone (0.50 g, 2.0 mol) was dissolved in glacial acetic acid (8 mL) at 50 °C and added dropwise to a solution of chromium trioxide (1.50 g, 15.0 mmol), water (2.5 mL), concentrated sulfuric acid (2.5 mL) and glacial acetic acid (4 mL) at 60 °C. The reaction mixture was then heated under reflux for 1 h. After cooling to room temperature, the reaction mixture was poured into ice water (100 mL). The white precipitate was collected by filtration. The filter cake was washed with water (10 mL x 3) and dried in air. The product was purified by recrystallization from DMF : H_2O = 2 : 1. The desired product was obtained as 0.26 g (55 %) of a white solid after drying under vacuum: m.p. >350 °C; ^{1}H NMR (DMSO-d_6): δ 13.57 (2H, s), 8.13 (8H, s); IR (KBr, Nujol): ν (cm^{-1}) 2924, 2855, 1691, 1577, 1460, 1425, 1377, 1329, 1285, 1160, 1124, 1101, 933, 864, 770, 724, 621, 571, 548.

3.4.4 Poly[2,2'-(4,4'-sulfonyldiphenylene)-5,5'-bibenzimidazole (PBI-2)

3,3'-Diaminobenzidine (0.5000 g, 2.330 mmol) and 4,4'-sulfonyldibenzoic acid

(0.7130 g, 2.330 mmol) were added to PPA (28 g). The reaction mixture was stirred at 110 °C for 24 h and at 140 °C for 24 h. Phosphorous pentoxide (1.66 g) was added and the reaction mixture was stirred at 170 °C for 24 h. The reaction mixture was then cooled to room temperature and water (100 mL) was added to suspend the product. The solid was collected by filtration and then resuspended in water (100 mL). The wash procedure was repeated 3 times. After drying, the polymer was dissolved in DMSO (50 mL). The solution was concentrated to 10 mL and poured into toluene (100 mL). The precipitate was collected by filtration, washed with DMSO and dried under vacuum. The desired polymer was obtained as 1.4 g (100 %) of a yellow power: ^{1}H NMR (DMSO-d_6): δ 8.46 (4H, d, *J*=7.1 Hz), 8.24 (4H, d, *J*=7.8 Hz), 7.90 (2H, s), 7.74 (2H, d, *J*=7.7 Hz), 7.62 (2H, d, *J*=8.0 Hz), 3.93 (2H, s); IR (KBr, Nujol): ν (cm^{-1}) 2924, 2855, 1598, 1540, 1460, 1377, 1287, 1152, 1093, 843, 804, 759, 726, 624, 561.

3.4.5 4,4'-Diacetamidodiphenyl sulfone (3-9)

4,4'-Diaminodiphenyl sulfone (1.00 g, 4.03 mmol) was suspended in acetic acid (5 mL), which was then heated to reflux. Acetic anhydride (7.65 mL) was added in portions. After stirring for 2 d, ice water (20 mL) was added carefully. The white precipitate was collected by filtration and washed with water (10 mL x 3). The desired product was obtained as 1.10 g (83 %) of a white powder after drying under vacuum: m.p.: 294-297 °C; ^{1}H NMR (DMSO-d_6): δ 7.84 (4H, d, *J*=9.0 Hz), 7.76 (4H, d, *J*=9.1Hz), 2.06 (4H, s); IR (KBr, Nujol): ν (cm^{-1}) 3334, 3258, 2923, 2855, 1684, 1587,

1527, 1461, 1405, 1376, 1317, 1297, 1263, 1151, 1104, 841, 742, 716, 635, 598, 552.

3.4.6 3,3'-Dinitro-4,4'-diacetamidodiphenyl sulfone (3-10)

A mixture of fuming nitric acid (5 mL) and concentrated sulfuric acid (5 mL) was added dropwise to an ice cold solution of 4,4'-diacetamidodiphenyl sulfone (1.00 g, 3.11 mmol) in concentrated sulfuric acid (50 mL). The reaction mixture was then warmed to room temperature, stirred for 15 min and poured into ice water (400 mL). The precipitate was collected by filtration and washed with acetone (10 mL x 3). The desired product was obtained as 1.21 g (92 %) of a yellow solid. Combining the product of another experiment, 5.27 g of 3,3'-dinitro-4,4'-diacetamidodiphenyl sulfone was recrystallized from acetone and to give 3.46 g of a yellow solid: m.p. 240-245 °C; ^{1}H NMR (DMSO-d_6): δ 8.50 (2H, d, *J*=2.3 Hz), 8.30 (2H, dd, *J*=8.8, 2.7 Hz), 7.88 (2H, d, *J*=8.7 Hz), 2.10 (6H, s); IR (KBr, Nujol): ν (cm^{-1}) 3350, 2923, 2856, 1715, 1606, 1581, 1499, 1460, 1376, 1341, 1270, 1224, 1155, 1081, 893, 843, 763, 723, 657, 578.

3.4.7 3,3'-Dinitro-4,4'-diaminodiphenyl sulfone hydrochloride (3-11)

3,3'-Dinitro-4,4'-diacetamidodiphenyl sulfone (1.00 g, 2.37 mmol) was suspended in absolute ethanol (60 mL). Hydrochloric acid (9 mL) was added dropwise. The reaction mixture was heated under reflux overnight. After cooling to room temperature, the reaction mixture was concentrated to 10 mL. The precipitate was collected by filtration and washed with ethanol (10 mL x 3). The desired product was obtained as

0.69 g (71 %) of an orange powder after drying under vacuum: m.p. 288.5-290 °C; ^{1}H NMR (DMSO-d_6): δ 8.45 (2H, d, *J*=2.4 Hz), 8.09 (4H, s), 7.79 (2H, dd, *J*=9.1, 2.6 Hz), 7.13(2H, d, J=9.2 Hz); IR (KBr, Nujol): ν (cm^{-1}) 2924, 2854, 1622, 1557, 1513, 1460, 1413, 1376, 1351, 1305, 1259, 1155, 1075, 905, 839, 820, 745, 723, 667, 575.

3.4.8 3,3',4,4'-Tetraaminodiphenyl sulfone tetrahydrochloride (3-12)

Stannous chloride dihydrate (3.75 g, 19.8 mmol) was dissolved in concentrated hydrochloric acid (12.5 g). 3,3'-Dinitro-4,4'-diaminodiphenyl sulfone hydrochloride (0.50 g, 1.22 mmol) was added in small portions. The reaction mixture was heated under reflux under a nitrogen atmosphere for 3 d. After cooling to room temperature, the precipitate was collected by filtration and washed with hydrochloric acid and water. The desired product was obtained as 0.41 g (80 %) of a white solid after drying under vacuum for 1 h: m.p. 156-158 °C; ^{1}H NMR (D_2O): δ 7.69 (2H, d, *J*=2.1 Hz), 7.61-7.58 (2H, m), 6.78 (2H, dd, *J*=8.0, 1.5 Hz); IR (KBr): ν (cm^{-1}) 3327, 2924, 2855, 1775, 1618, 1460, 1377, 1144, 1100, 722, 591.

3.4.9 3,3',4,4'-Tetraaminodiphenyl sulfone (3-13)

Aqueous 20 % sodium hydroxide solution (12.5 mL) was added dropwise to a solution of 3,3',4,4'-tetraaminodiphenyl sulfone tetrahydrochloride (0.22 g, 0.52 mmol) in water (5 mL). The precipitate was collected by filtration. The filter cake was washed with water and dried under vacuum. The desired product was obtained as 0.01 g (7 %)

of a white powder: m.p. 180-181.5 °C; ^{1}H NMR (DMSO-d_6): δ 6.87 (2H, s), 6.83 (2H, d, *J*=8.2 Hz), 6.50 (2H, d, *J*=8.2 Hz), 5.25 (4H, s), 4.84 (4H, s).

3.4.10 Poly[2,2'-(4,4'-oxydiphenylene)sulfonyl-5,5'-bibenzimidazole (PBI-3)

3,3',4,4'-Tetraaminodiphenyl sulfone tetrahydrochloride (0.1306 g, 0.4717 mmol) was added to PPA (14 g) in small portions. The temperature was raised to 100 °C under a thin stream of nitrogen to remove hydrogen chloride gas. Then the reaction mixture was heated to 140 °C. The hydrogen chloride gas was removed by alternation of vacuum and nitrogen for 3 times. After the reaction mixture was cooled to 100 °C, diphenyl ether 4,4'-dicarboxylic acid (0.0795 g, 0.4717 mmol) was added. The reaction mixture was stirred at 100 °C for 24 h and at 120 °C for 24 h. Then phosphorous pentoxide (7 g) was added. The reaction mixture was stirred at 150 °C for 24 h. After the reaction mixture was cooled to room temperature, water (100 mL) was added and stirred for 24 h. The precipitate was collected by filtration and then resuspended in water (100 mL). The wash procedure was repeated 3 times. After drying, the polymer was dissolved in warm DMSO (30 mL). The solution was poured into benzene (50 mL). The precipitate was collected by filtration, washed with benzene and dried under vacuum to give 0.17 g (78 %) of product: ^{1}H NMR (DMSO-d_6): δ 8.24-8.20 (6H, m), 7.80-7.75 (4H, m), 7.28 (4H, d, *J*=7.4 Hz); IR (KBr, Nujol): ν (cm^{-1}) 2924, 2855, 1599, 1459, 1376, 1307, 1522, 1145, 1068, 1019, 968, 845, 808, 723, 630, 534, 515.

Chapter 4

Conclusions and Future Work

4.1 Conclusions

Precursor routes have been employed to prepare novel fluorenone-based copolymers with benzene (**PFB**), furan (**PFF**) and thiophene (**PFT**). Precursor polymer **PFKT** showed the highest molar masses. Its M_w was 45,000 g mol^{-1}. This result is consistent with the prediction that long aliphatic side chains will increase the solubility of oligmer and polymer intermediates so that a high molar mass polymer can be obtained.

After converting the precursor polymers to target polymers by deacetylisation of the acetal substituents to the ketone, the band gaps, which were measured by K. Loganathan [105], decreased by *ca.* 0.5 eV in each polymer. These results support the strategy that the electron donor-acceptor alternation structures can reduce the band gap.

PBIs with heteratom linkages have been prepared according to literature procedures. PBI and **PBI-1** were cast as thin films to explore their application in fuel cells. Films of **PBI-1** showed much better flexibility than PBI. The oxygen linkages on the backbone of **PBI-1** increase the flexibility of polymer. Dr Song has begun an evaluation of the performance of **PBI-1** in a fuel cell. However, no results were available at the time of submission of this thesis. The **PBI-1** film shows a conductivity of 2.06×10^{-2} S cm^{-1} at 80 °C, which was measured by Dr Song.

4.2 Future work

After over 20 years of intense investigation, electronic conducting polymers are still of immense interest to chemists and physicists. Commercial applications in PLEDs have greatly stimulated interest in polyfluorenes, and this prompted us to prepare some new members of this class. In future work polymers **PFB**, **PFF** and **PFT** can be further modified to lower band gaps. The reactive carbonyl functional groups at the C9 position of the fluorenone moieties offers the possibilities of conversion to diverse functional groups, such as esters, ethers, thioketones and thioethers. Model compounds **2-15** and **2-16** can be polymerized to copolymers with two adjacent thiophene moieties. They all are expected to be potential LED materials.

PBIs are considered prospective membrane materials for fuel cells. The present work in the ionic conducting polymers will continue with evaluation of the performance of **PBI-1**, **PBI-2** and **PBI-3** in fuel cells, and to explore the best operating conditions for PBIs. According to the literature procedures, other PBIs can be synthesized to investigate their potential application in fuel cells. Compound **3-12** can be polymerized with compound **3-6**, **3-15** and other dicarboxylates to various PBI derivatives. With more experimental results, we hope to find a suitable PBI membrane and evaluate possible further correlations between the performance and the structure of PBIs.

References

[1] Skotheim, T. A.; Elsentaumer, R. L.; Reynolds, J. R. Ed. *Handbook of Conducting Polymers* Marcel Dekker: New York, **1998**.

[2] Kudo, T.; Fueki, K. *Solid State Ionics* Kodansha: Tokyo, **1990**.

[3] Bockris, J. Ó.; Miller, D. *in Conducting Polymers, Special Applications* Alcácer, L. Ed., D. Reidel: Dordrecht, **1987**, 1-36.

[4] Kanatzidts, M. G. *Chem. Eng. News* **1990,** 36.

[5] Kreuer, K. D. *J. Membrane Sci.* **2001**, *185*, 29.

[6] Cacialli, F. *in Photonic Polymer Systems, Fundamentals, Methods and Applications* Wise, D. L.; Wnek, G. E.; Trantolo, D. J.; Cooper, T. M.; Gresser, J. D. Eds., Marcel Dekker: New York, **1998**, 103-148.

[7] Curran, S.; Stark-hauser, A.; Roth, S. *in Handbook of Organic Conductive Molecules and Polymers* Volume 2, Chapter 1, Nalwa, H. S. Ed., John Wiley & Sons, **1997**, 1-60.

[8] Ferraro, J. R.; Willams, J. M. *Introduction to Synthetic Electrical Conductors* Academic: Orlando, **1987**.

[9] Shirakawa, H.; Ito, T.; Ikeda, S. *Polym. J. (Tokyo)* **1973**, *4*, 460.

[10] Shirakawa, H.; Louis, E. J.; MacDiarmid, A. G.; Chiang, C. K.; Heeger, A. J. *J. Chem. Soc., Chem. Commun.* **1977**, 578.

[11] Chiang, C. K.; Fincher, C. R.; Park, Y. W. Jr.; Heeger, A. J.; Shirakawa, H.; Louis, E. J.; Gau, S. C.; MacDiarmid, A. G. *Phys. Rev. Lett.* **1977**, *39*, 1098.

[12] Chiang, C. K.; Druy, M. A.; Gau, S. C.; Heeger, A. J.; Louis, E. J.; MacDiarmid, A. G.; Park, Y. W.; Shirakawa, H. *J. Am. Chem. Soc.* **1978**, *100*, 1013.

[13] Lacaze, P. C.; Aeiyach, S.; Lacroix, J. C. *in Handbook of Organic Conductive Molecules and Polymers* Volume 2, Chapter 6, Nalwa, H. S. Ed., John Wiley & Sons, **1997**, 205-270.

[14] Pickup, P. G. *in Advanced Functional Molecules and Polymers* Volume 3,

Chapter 3, Nalwa, H. S. Ed., Gordon and Breach: Singapore, **2001**, 155-176.

[15] Wallace, G. G.; Spinks, G. M.; Teasdale, P. R. *Conductive Electroactive Polymers, Intelligent Materials Systems* Technomic: Pennsylvania, **1997**.

[16] Seymour, R. B. *Polymer Science and Technology* Volume 15, Seymour, R. B. Ed., **1981**, 1-6.

[17] Roncali, J. *Chem. Rev.* **1997**, *97*, 173.

[18] Liu, B.; Yu, W.-L.; Lai, Y.-H.; Huang, W. *Chem. Mater.* **2001**, *13*, 1984.

[19] Oda, M.; Nothofer, H.-G.; Scherf, U.; Šunjić, V.; Richter, D.; Regenstein, W.; Neher, D. *Macromolecules* **2002**, *35*, 6792.

[20] Herguth, P.; Jiang, X.; Liu, M. S.; Jen, A. K.-Y. *Macromolecules* **2002**, *35*, 6094.

[21] Zeng, G.; Yu, W.-L.; Chua, S.-J.; Huang, W. *Macromolecules* **2002**, *35*, 6907.

[22] Ding, J.; Day, M.; Robertson, G.; Roovers, J. *Macromolecules* **2002**, *35*, 3474.

[23] Strohriegl, P.; Grazulevicius, J. V. *in Advanced Functional Molecules and Polymers* Volume 3, Chapter 1, Nalwa, H. S. Ed., Gordon and Breach: Singapore, **2001**, 1-78.

[24] Xia, C.; Advincula, R. C. *Macromolecules* **2001**, *34*, 5854.

[25] Scherf, U.; List, E. J. W. *Adv. Mater.* **2002**, *14*, 477.

[26] Tirapattur, S.; Belletête, M.; Drolet, N.; Leclerc, M.; Durocher, G. *Macromolecules* **2002**, *35*, 8889.

[27] Belletête, M.; Beaupré, S.; Bouchard, J.; Blondin, P.; Leclerc, M.; Durocher, G. *J. Phys. Chem. B* **2000**, *104*, 9118.

[28] Arias, A. C.; Mackenzie, J. D.; Stevenson, R.; Halls, J. J. M,; Inbasekaran, M.; Woo, E. P.; Richards, D.; Friend, R. H. *Macromolecules* **2001**, *34*, 6005.

[29] Belletête, M.; Morin, J.-F.; Beaupré, S.; Ranger, M.; Leclerc, M.; Durocher, G. *Macromolecules* **2001**, *34*, 2288.

[30] Wong, K.-T.; Chien, Y.-Y.; Chen, R.-T.; Wang, C.-F.; Lin, Y.-T.; Chiang, H.-H.;

Hsieh, P.-Y.; Wu, C.-C.; Chou, C. H.; Su, Y. O.; Lee, G.-H.; Peng, S.-M. *J. Am Chem. Soc.* **2002**, *124*, 11576.

[31] Leclerc, M. J. *Polym. Sci. Part A: Polym. Chem.* **2001**, *39*, 2867.

[32] Klaerner, G.; Miller, R. D. *Macromolecules* **1998**, *31*, 2007.

[33] Xia, C.; Advincula, R. C. *Chem. Mater.* **2001**, *13*, 1682.

[34] Kreyenschmidt, M.; Klaerner, G.; Fuhrer, T.; Ashenhurst, J.; Karg, S.; Chen, W. D.; Lee, V. Y.; Scott. J. C.; Miller, R. D. *Macromolecules* **1998**, *31*, 1099.

[35] Blondin, P.; Bouchard, J.; Beaupré, S.; Belletête, M.; Durocher, G.; Leclerc, M. *Macromolecules* **2000**, *33*, 5874.

[36] Vanhee, S.; Rulkens, R.; Lehmann, U.; Rosenauer, C.; Schulze, M.; Köhler, W.; Wegner, G. *Macromolecules* **1996**, *29*, 5136.

[37] Setayesh, S.; Grimsdale, A. C.; Weil, T.; Enkelmann, V.; Müllen, K.; Meghdadi, F.; List, E. J. W.; Leising, G. *J. Am. Chem. Soc.* **2001**, *123*, 946.

[38] Johansson, D. M.; Theander, M.; Granlund, T.; Inganäs, O.; Andersson, M. R. *Macromolecules* **2001**, *34*, 1981.

[39] Donat-Bouillud, A.; Lévesque, I,; Tao, Y.; D'Iorio, M. *Chem. Mater.* **2002**, *12*, 1931.

[40] Liu, B.; Yu, W.-L.; Lai, Y.-H.; Huang, W. *Macromolecules* **2000**, *33*, 8945.

[41] Ranger, M.; Rondeau, D.; Leclerc, M. *Macromolecules* **1997**, *30*, 7686.

[42] Ranger, M.; Leclerc, M. *Macromolecules* **1999**, *32*, 3306.

[43] Uckert, F.; Setayesh, S.; Müllen, K. *Macromolecules* **1999**, *32*, 4519.

[44] Sheats, J. R.; Chang, Y.-L.; Roitman, D. B.; Stocking, A. *Acc. Chem. Res.* **1999**, *32*, 193.

[45] Tsuie, B.; Reddinger, J. L.; Sotzing, G. A.; Soloducho, J.; Katritzky, A. R.; Reynolds, J. R. *J. Mater. Chem.* **1999**, *9*, 2189.

[46] Larmat, F.; Reynolds, J. R.; Reinhardt, B. A.; Brott, L. L.; Clarson, S. J. *J. Polym.*

Sci.: Part A, Polym. Chem. **1997**, *35*, 3627.

[47] Bao, Z.; Chan, W.; Yu, L. *Chem. Mater.* **1993**, *5*, 2.

[48] Bao, Z,; Chan, W.; Yu, L. *J. Am. Chem. Soc.* **1995**, *117*, 12426.

[49] Bochmann, M.; Kelly, K.; Lu, J. *J. Polym. Sci.: Part A, Polym. Chem.* **1992**, *30*, 2511.

[50] Pei, Q.; Yang, Y. *J. Am. Chem. Soc.* **1996**, *118*, 7416.

[51] Klärner, G.; Lee, J.-I.; Davey, M. H.; Miller, R. D. *Adv. Mater.* **1999**, *11*, 115.

[52] Ranger, M.; Leclerc, M. *Chem. Commun.* **1997**, 1597.

[53] Ahn, T.; Song, S.-Y.; Shim, H. *Macromolecules* **2000**, *33*, 6764.

[54] Inaoka, S.; Advincula, R. *Macromolecules* **2002**, *35*, 2426.

[55] Kim, J. L.; Cho, H. N.; Kim, J. K.; Hong, S. I. *Macromolecules* **1999**, *32*, 2065.

[56] Pschirer, N. G.; Bunz, U. H. F.; *Macromolecules* **2000**, *33*, 3961.

[57] Jung, B.-J.; Lee, J.-I.; Chu, H. Y.; Do, L.-M.; Shim, H.-K. *Macromolecules* **2002**, *35*, 2282.

[58] Lee, S. H.; Nakamura, T.; Tsutsui, T. *Org. Lett.* **2001**, *3*, 2005.

[59] Heitner-Wirguin, C. *J. Membrane Sci.* **1996**, *120*, 1.

[60] Savadogo, O. *J. New Mat. Eletrochem. Systems* **1998**, *1*, 47.

[61] McDougall, A. *Fuel Cells* Macmillan: London, **1976**.

[62] Willis, H. L.; Scott, W. G.; *Distributed Power Generation* Marcel Dekker: New York, **2000**.

[63] Perry, M. L.; Fuller, T. F. *J. Electrochem, Soc.* **2002**, *149*, S59.

[64] Kerres, J. A. *J. Membrane Sci.* **2001**, *185*, 3.

[65] Watkins, D. S. *Fuel Cell Systems* Blomen, L. J. M. J.; Mugerwa, M. N. Eds.,

Plenum: New York, **1993**, 493-530.

[66] Yu, J.; Yi, B.; Xing D.; Liu, F.; Shao, Z.; Fu, Y.; Zhang, H. *Phys. Chem. Chem. Phys.* **2003**, *5*, 611.

[67] Eisenberg, A.; Kim, J-S. *Introduction to ionomers* John Wilty & Sons: New York, **1998**.

[68] Carrette, L.; Friedrich, K. A.; Stimming, U. *Chemphyschem.* **2000**, *1*, 163.

[69] Gray, F. M. *Solid Polymer Electrolytes: Fundamentals and Technological Applications* VCH: New York, **1991**.

[70] Beattie, D. P.; Orfino, F. P.; Basura, V. I.; Zychowska, K.; Ding, J.; Chuy, C.; Schmeisser, J.; Holdcroft, S. *J. Electroanlytical Chem.* **2001**, *502*, 45.

[71] Haubold, H.-G.; Jungbluth, T. V. H.; Hiller, P. *Electrochimica Acta* **2001**, *46*, 1559.

[72] Hasiotis, C.; Deimede, V.; Kontoyannis, C. *Electrochim. Acta* **2001**, *46*, 2401.

[73] Wang, J.-T.; Savinell, R.F.; Wainright, J.; Litt, M.; Yu, H.; *Electrochim. Acta* **1996**, *41*, 193.

[74] Gao, X.; Fang, J.; Watari, T.; Tanaka, K.; Kita, H.; Okamoto, K. *Macromolecules* **2002**, *35*, 6707.

[75] Kataoks, H.; Saito, Y.; Tabuchi, M.; Wada, Y.; Sakai, T. *Macromolecules* **2002**, *35*, 6239.

[76] Saito, Y.; Kataoka, H.; Capiglia, C.; Yamamoto, H. *J. Phys. Chem. B* **2000**, *104*, 2189.

[77] Mandal. B. K.; Walsh, C. J.; Sooksimuang, T.; Behroozi, S. J. *Chem. Mater.* **2000**, *12*, 6.

[78] Jones, D. J.; Rozière, J. *J. Membr. Sci.* **2001**, *185*, 41.

[79] Cassidy, P. E. *Thermally Stable Polymers: Syntheses and Properties* Marcel Dekker: New York, **1980**.

[80] Deimede, V.; Voyiatzis, G. A.; Kallitsis, J. K.; Qingfeng, L.; Bjerrum, N. J.

Macromolecules **2000**, *33*, 7609.

[81] Wang, J.-T.; Wainright, T. S.; Savinell, R. F.; Litt, M. *J. Appl. Electrochem.* **1996**, *26*, 751.

[82] Aharoni, S. M.; Litt, M. H. *J. Polym. Sci., Polym. Chem. Ed.* **1974**, *12*, 639.

[83] Berrada, M.; Vaultier, M.; Anbaoui, Z.; Lajrhed, N.; Berrada, M.; Knouzi, N. *Ann. Chim. Sci. Mat.* **1998**, *23*, 351.

[84] Neuse, E. W. *Adv. Polym. Sci.* **1982**, *47*, 1.

[85] Vogel, H; Marvel, C. S. *J. Polym. Sci.* **1961**, *50*, 511.

[86] Plummer, L.; Marvel, C. S. *J. Polym. Sci.: Part A* **1964**, *2*, 2559.

[87] Foster, R. T.; Marvel, C. S. *J. Polym. Sci.: Part A* **1965**, *3*, 417.

[88] Vogel,H.; Marvel, C. S. *J. Polym. Sci.: Part A* **1963**, *1*, 1537.

[89] Sivriev, H.; Borissov, G. *Eur. Polym. J.* **1977**, *13*, 25.

[90] Mitsuhashi, K.; Marvel, C. S. *J. Polym. Sci.: Part A* **1965**, *3*, 1661.

[91] Still, J. K.; Arnold, F. E. *J. Polym. Sci,: Part A-1* **1966**, *4*, 551.

[92] Iwakura, Y.; Uno, K.; Chau, N. *Makromol. Chem.* **1975**, *176*, 23.

[93] Hebderg, F. L.; Marvel, C. S. *J. Polym. Sci., Polym. Chem. Ed.* **1974**, *8*, 3199.

[94] Yamaguchi, I.; Osakada, K.; Yamamoto, T.; Katada, M. *Bull. Chem. Soc. Jpn.* **1999**, *72*, 2557.

[95] Kokelenberg, H.; Marvel, C. S. *J. Polym. Sci,: Part A-1* **1970**, *8*, 3199.

[96] Neuse, E. W.; Horlbeck, G. *Polym. Eng. Sci.* **1977**, *17*, 821.

[97] Iwakura, Y.; Uno, K.; Imai, Y. *J. Polym. Sci.: Part A* **1964**, *2*, 2605.

[98] Cameron, C. G.; Pittman, T. J.; Pickup, P. G. *J. Phys. Chem. B* **2001**, *105*, 8838.

[99] Evers, R. C.; Arnold, F. E.; Helminiak, T. E., *Macromolecules* **1981**, *14*, 925.

[100] Varma, I. K.; Veena, *J. Polym. Sci., Polym. Chem. Ed.* **1976**, *14*, 973.

[101] Srinivasan, P. R.; Mahadevan, V.; Srinivasan, M. *Makromol. Chem.* **1979**, *180*, 1845.

[102] Imai, Y.; Uno, K.; Iwakura, Y. *Makromol. Chem.* **1965**, *83*, 179.

[103] Mognonov, D. M.; Mazureskaya, Z. P.; Ul'zetueva, I. D.; Izyneev, A. A. Russ. *J. Appl. Chem.* **2000**, *73*, 1066.

[104] Levine, H. H. *Encyclopendia of Polymer Science and Technology* Vol 11; Bikales, N. M.; Conrad, J.; Ruks, A. Eds. John Wiley & Sons, **1969**, 188-232.

[105] Huang, F; Loganathan, K; Cammisa, E. G.; Pickup, P. G. Submitted to *Chemistry of Materials*.

[106] Huntress, E. H.; Hershberg, E. B.; Cliff, I. S. *J. Am. Chem. Soc.* **1931**, *53*, 2720.

[107] Rangarajan, R.; Eisenbraun, E. J. *J. Org. Chem.* **1985**, *50*, 2435.

[108] Murahashi, S.-I.; Moritani, I. *Toshikazu Nagai, Bull, CSJ* **1967**, 1655.

[109] Burnham, J. W.; Puncan, W. P.; Eisenbraun, E.J. *J. Org. Chem.* **1974**, *39*, 1416.

[110] Gilman, H.; Langhan, W.; Moore, F. W. *J. Am. Chem. Soc.* **1940**, *62*, 2327.

[111] Seitz, D. E.; Lee, S.-H. *Synth. Comm.* **1983**, *13*, 121.

[112] Meth-Cohn, O. *In Comprehensive Organic Chemistry,* Volume 4, Sammes, P. G. Ed, Pergamon: Oxford, **1979**.

[113] Trimpin, S.; Grimsdale, A. C.; Räder, H. J.; Müllen, K. *Anal. Chem.* **2002**, *74*, 3777.

[114] Sandler, S. R.; Karo, W.; Bonesteel, J.-A.; Pearce, E. M. *Polymer Synthesis and Characterization, A Laboratory Manual* Academic Press, **1998**.

[115] Billingham, N. C. *Molar Mass Measurements in Polymer Science* Kogan, **1997**.

[116] Pouchert, C. J. *The Aldrich Library of Infrared Spectra,* Edition III, Aldrich, **1981**.

[117] McOmie, J. F. W. *Protective Groups in Organic Chemistry* Plenum: London, **1973**.

[118] Rosenkranz, G.; Pataki, J.; Djerassi, C. *J. Org. Chem.* **1952**, *17*, 290.

[119] Cameron, C. *"Enhanced Rateds of Electron Transport in Conjugated-Redox Polymer Hybrids"*, Doctoral dissertation, Memorial University of Newfoundland **2000**.

[120] Adámek, M.; Novák, J. *Chem. Abstr,* **1961**, *55*, 22205i.

[121] Stille, J. K.; Arnold, F. E. *J. Polym. Sci.:Part A-1* **1966**, *4*, 551.

[122] Narayan, T. V. L.; Marvel, C. S. *J. Polym. Sci.: Part A-1* **1967**, *5*, 1113.

[123] Samms, S. R.; Wasmus, S.; Savinell, R. F. *J. Electrochem. Soc.* **1996**, *143*, 1225.

[124] Wainright, J. S.; Wang, J.-T.; Weng, D.; Savinell, R. F.; Litt, M. *J. Electrochem. Soc.* **1995**, *142*, L121

[125] Linkous, C. A.; Anderson, H. R.; Kopitzke, R. W.; Nelson, G. L. *Int. J. Hydrogen Energy* **1998**, *23*, 525.

[126] Colson, J. G.; Michel, R. H.; Paufler, R. M. *J. Polym. Sci.: Part A-1* **1996**, *4*, 59.

Appendix I

^{1}H NMR Spectra

Introduction

This appendix includes the ^{1}H NMR spectra in this thesis.

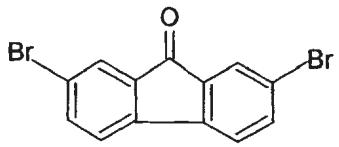

2-4

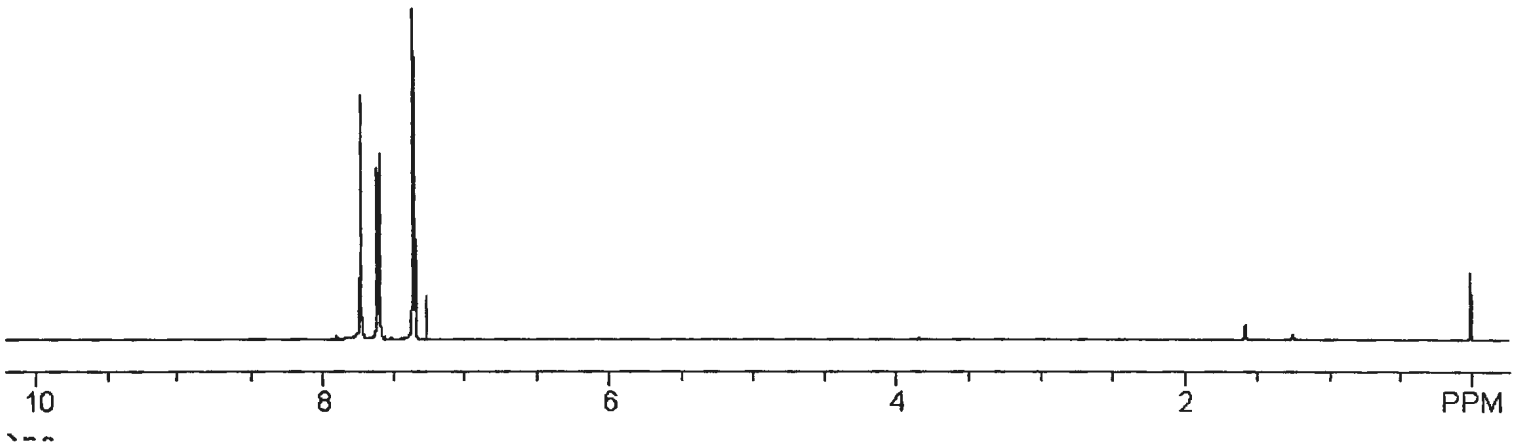

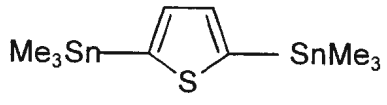

2-5

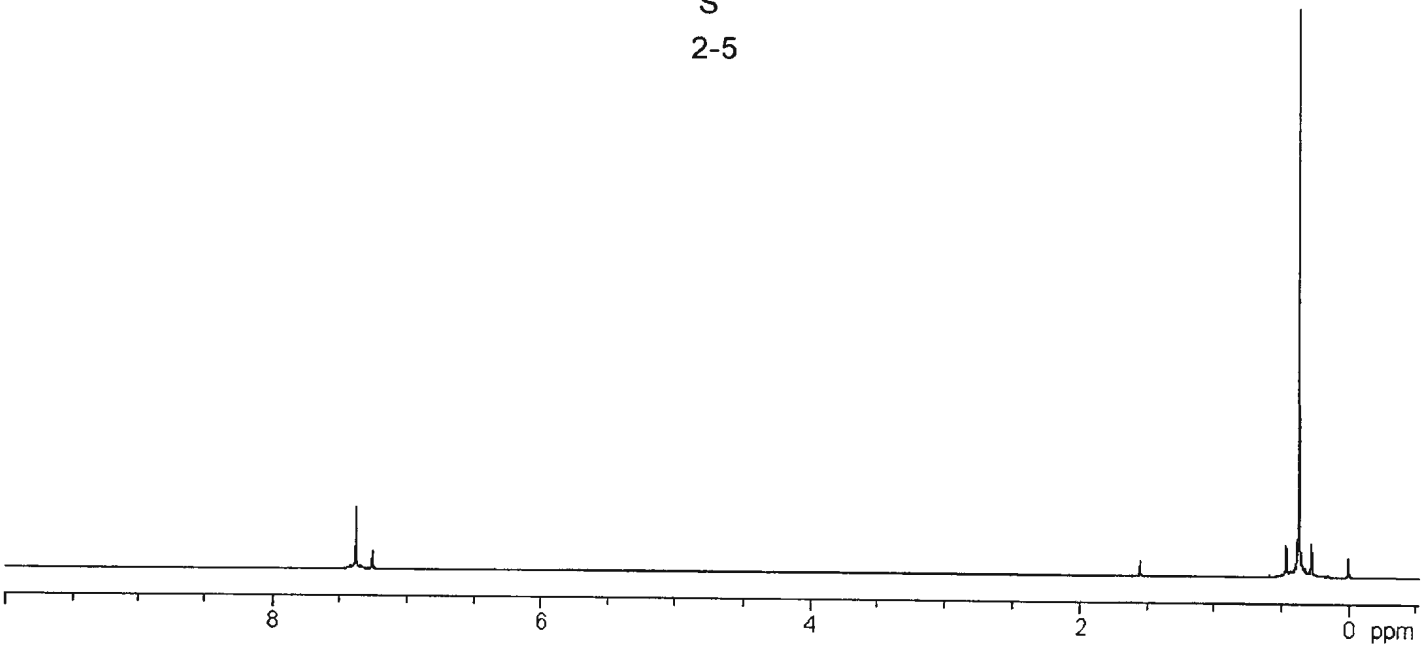

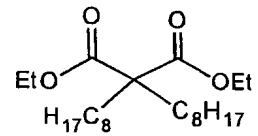

2-7

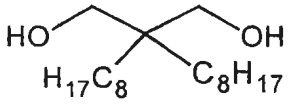

2-8

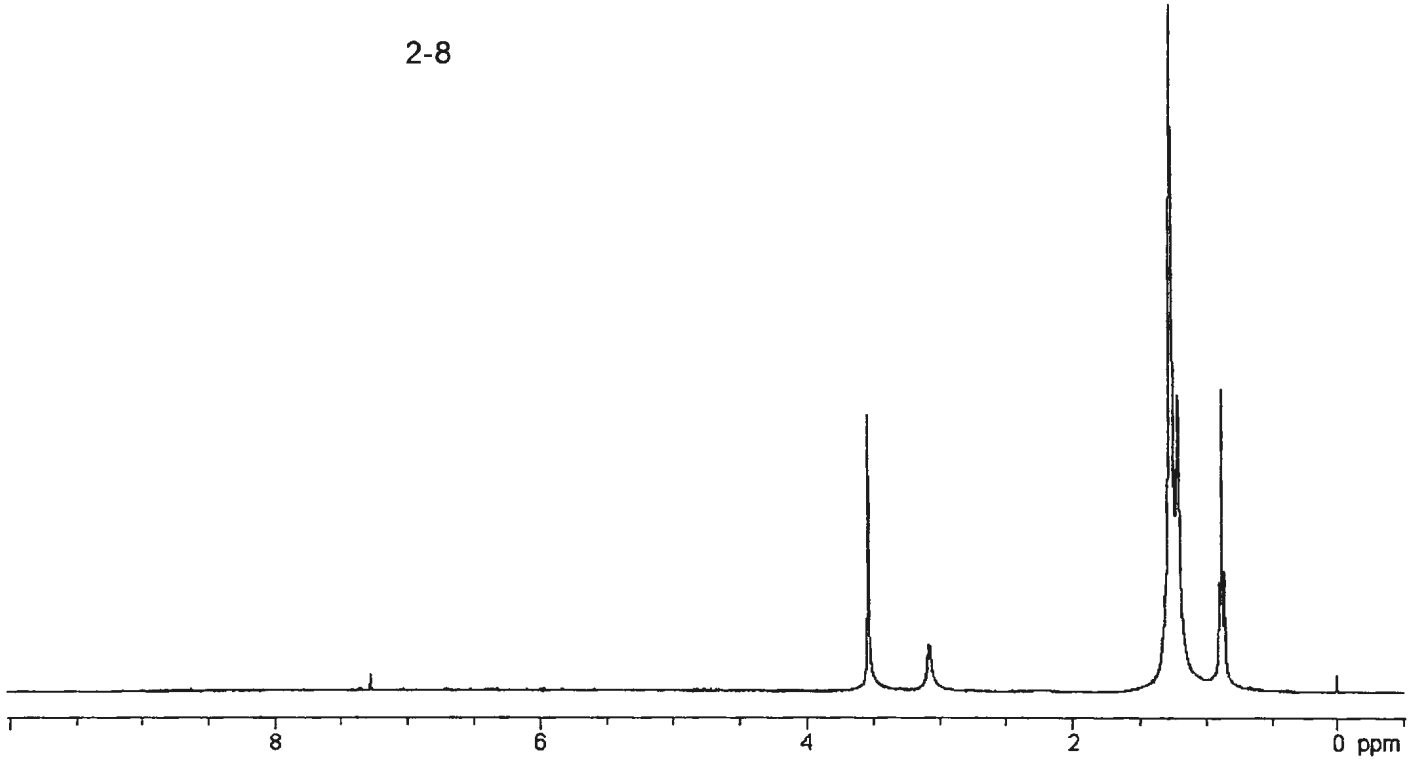

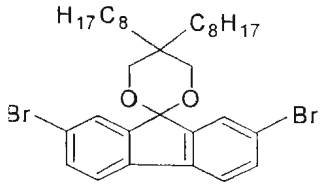

2-9

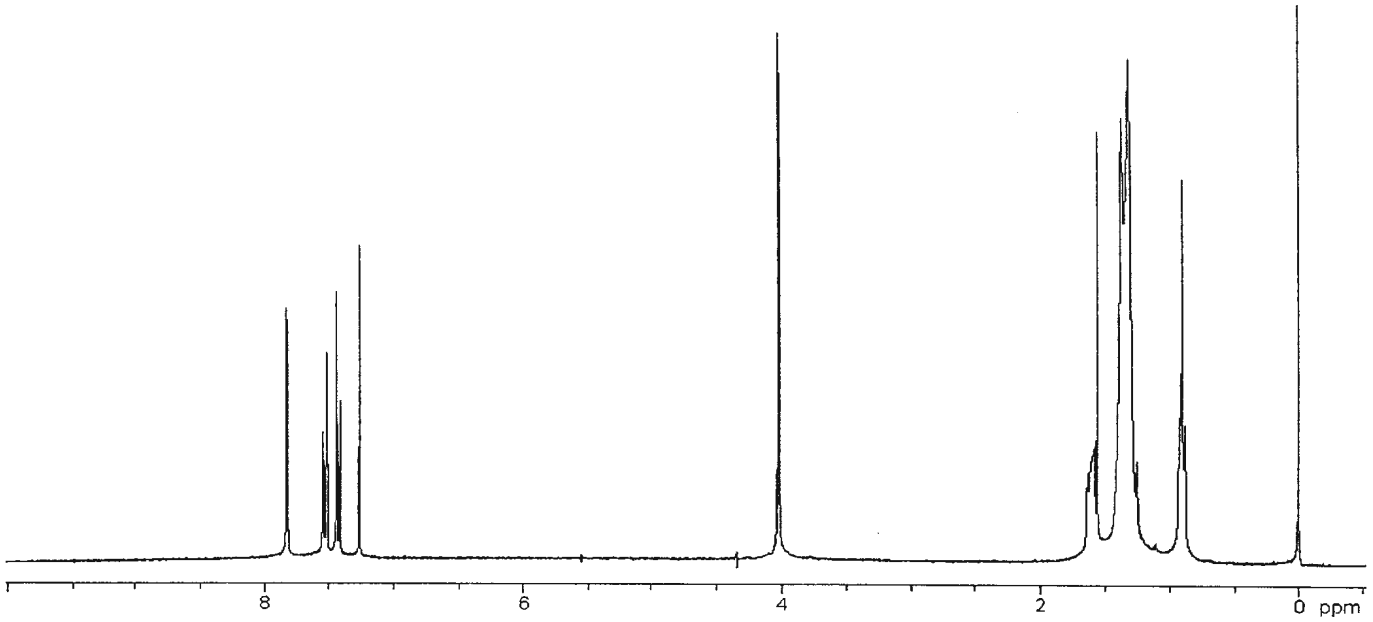

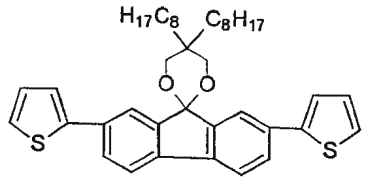

2-15

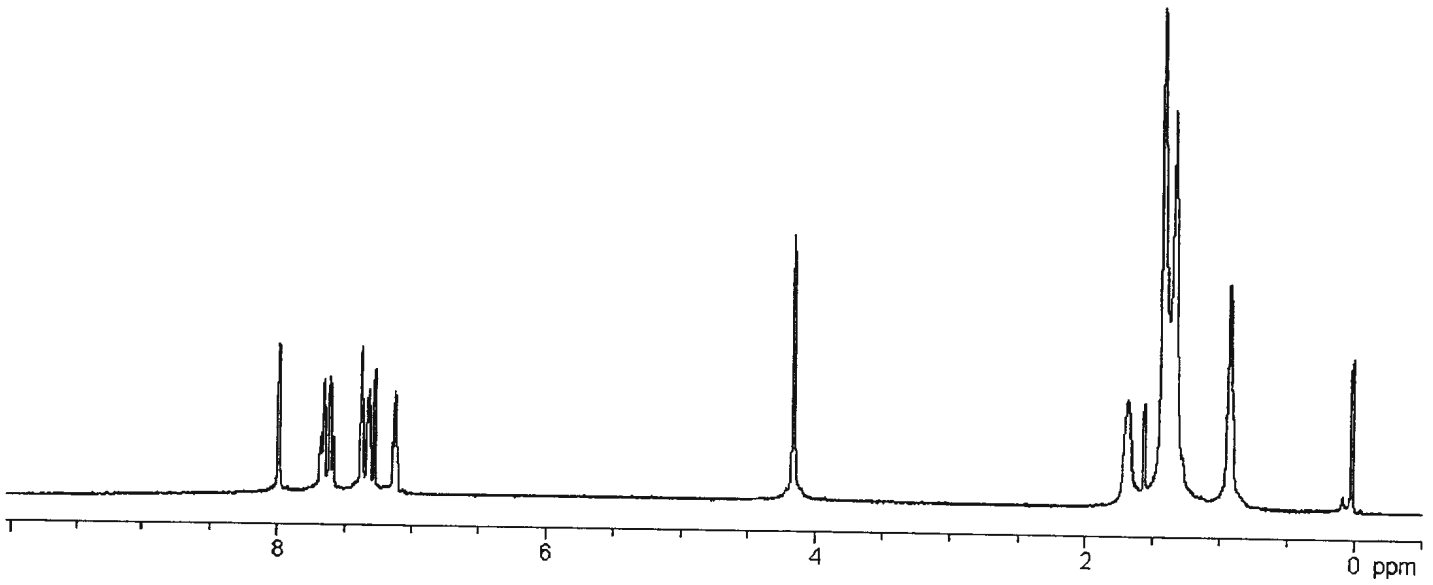

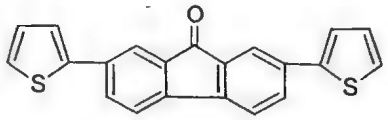

2-16

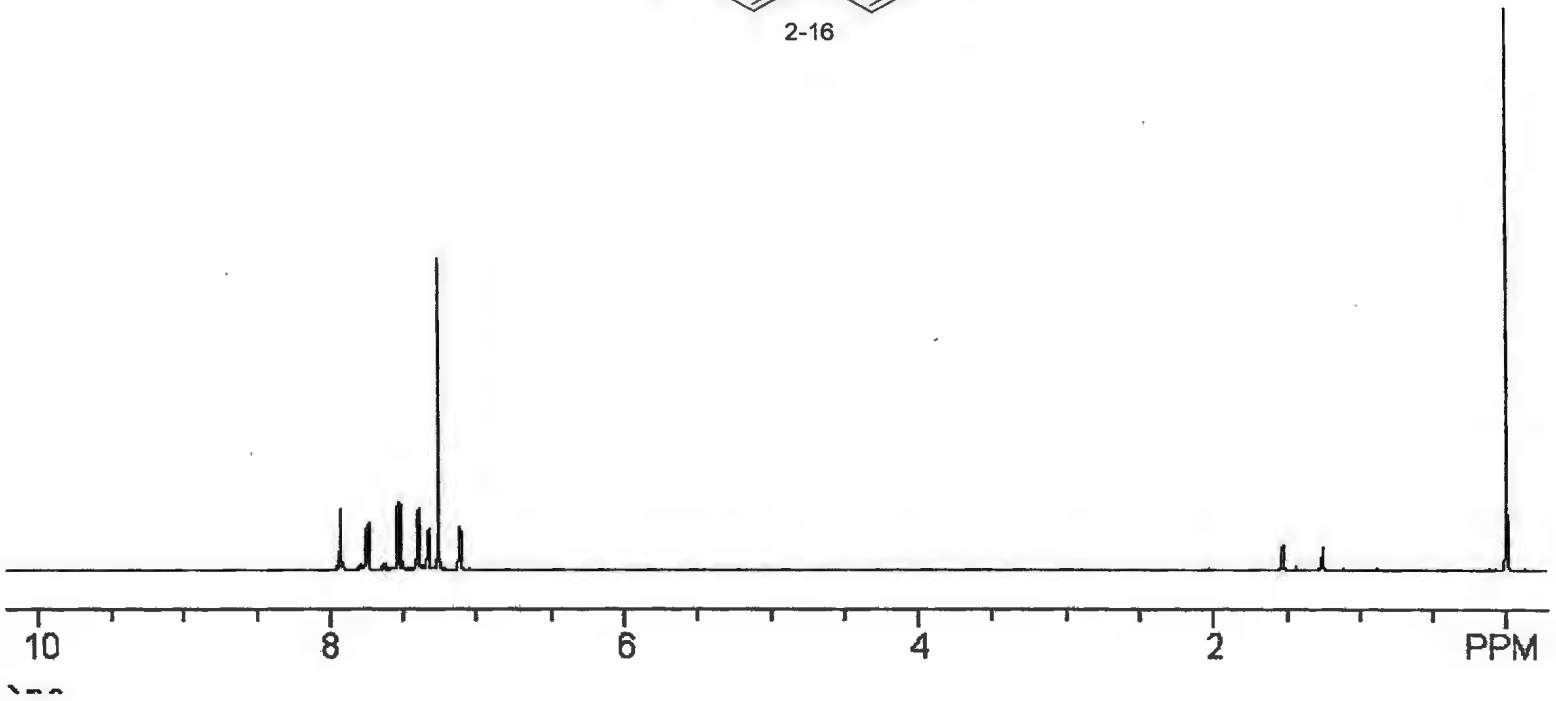

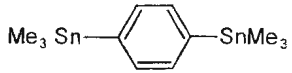

2-20

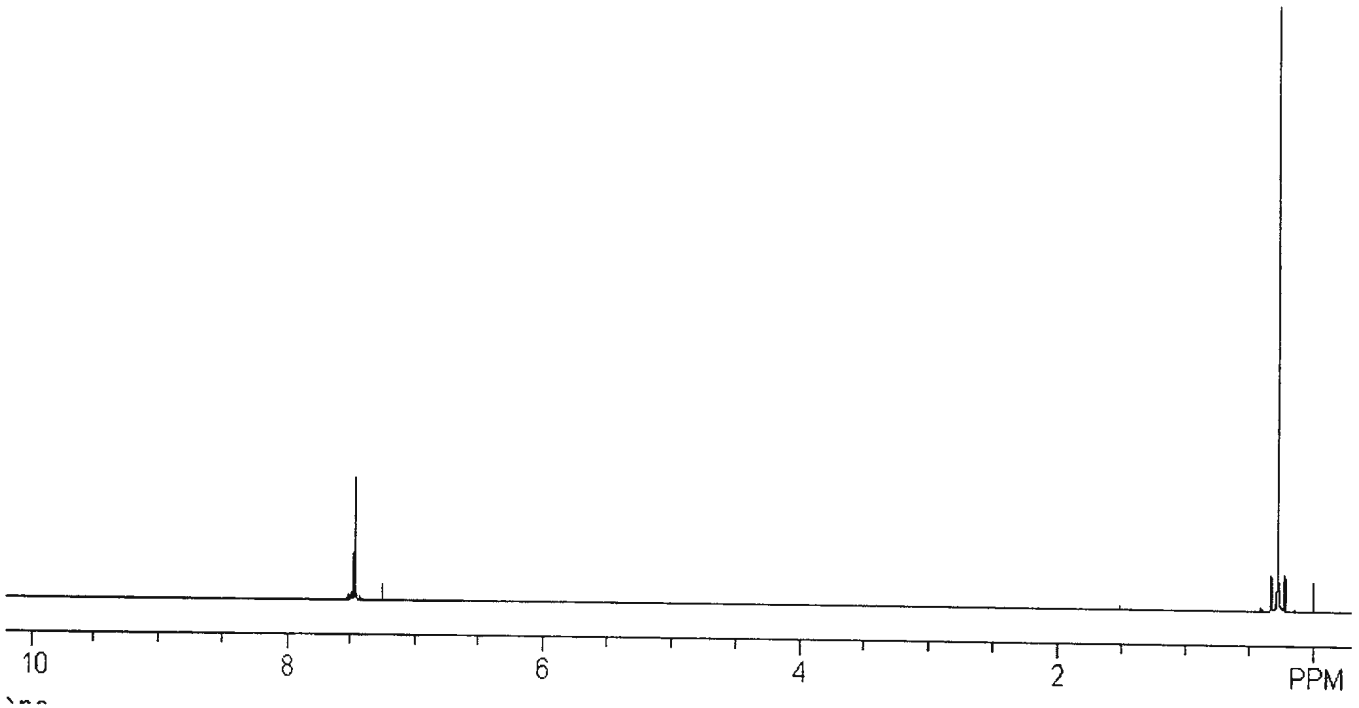

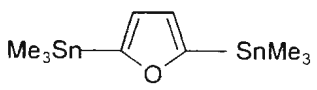

2-28

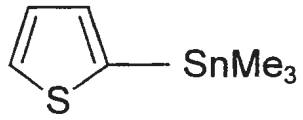

2-32

n
$H_{17}C_8$
C_8H_{17}
O
O
PFKB
8
6
4
2
0 ppm

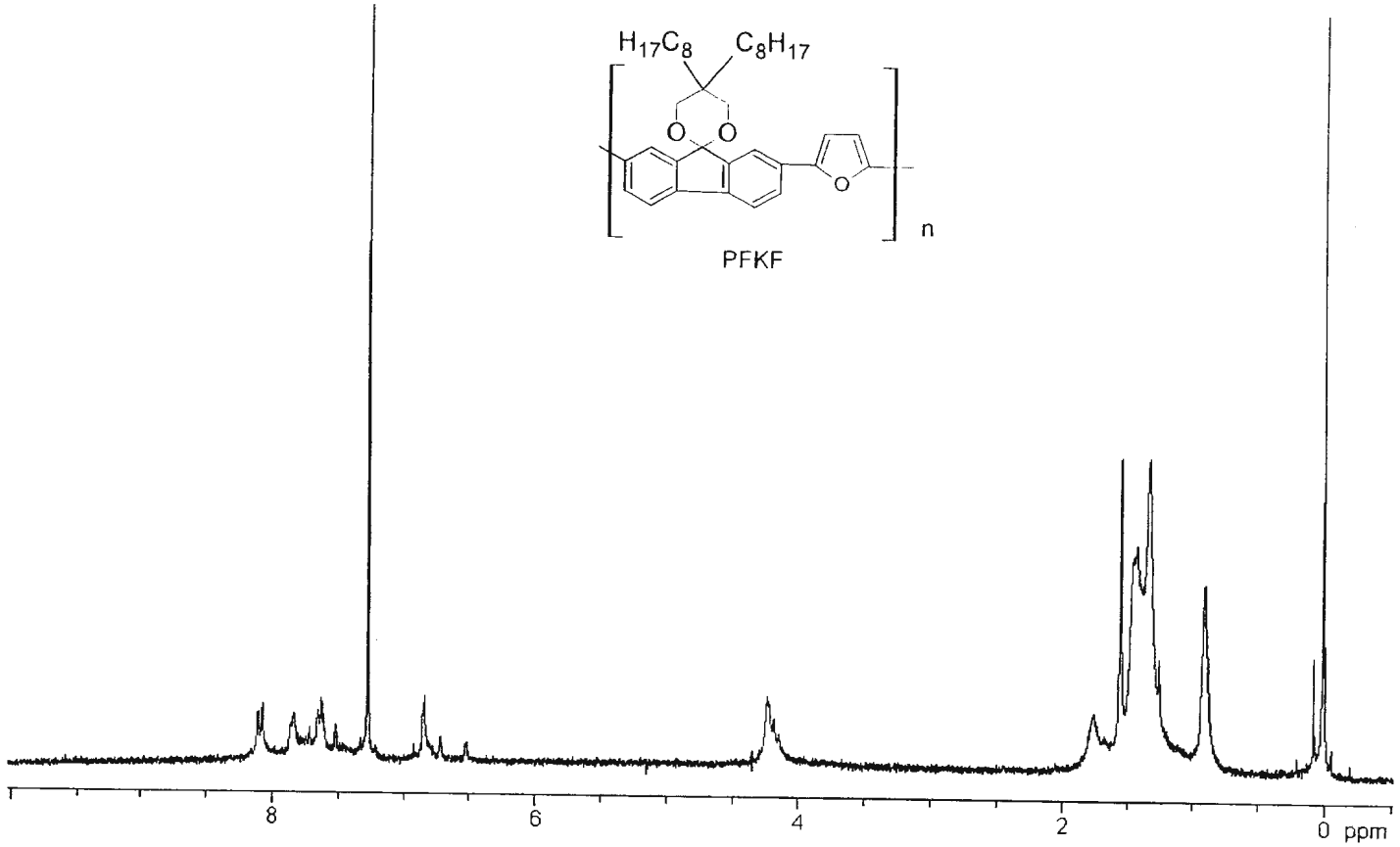
H17C8
C8H17
O
O
O
n
PFKF
8
6
4
2
0 ppm

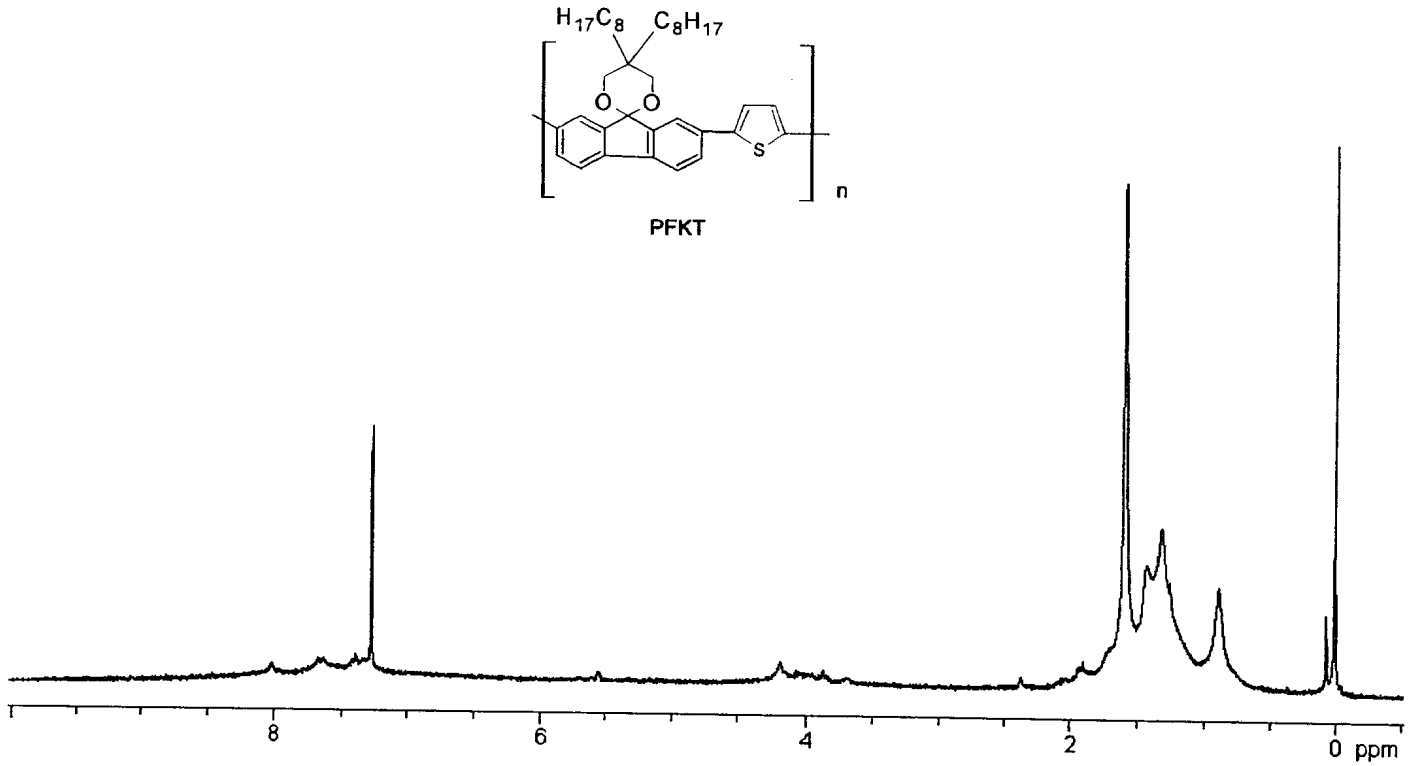
H17C8
C8H17
O
O
S
n
PFKT
8
6
4
2
0 ppm

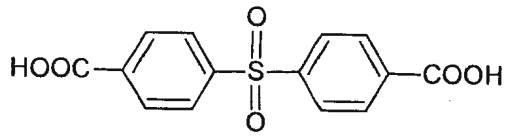

3 -6

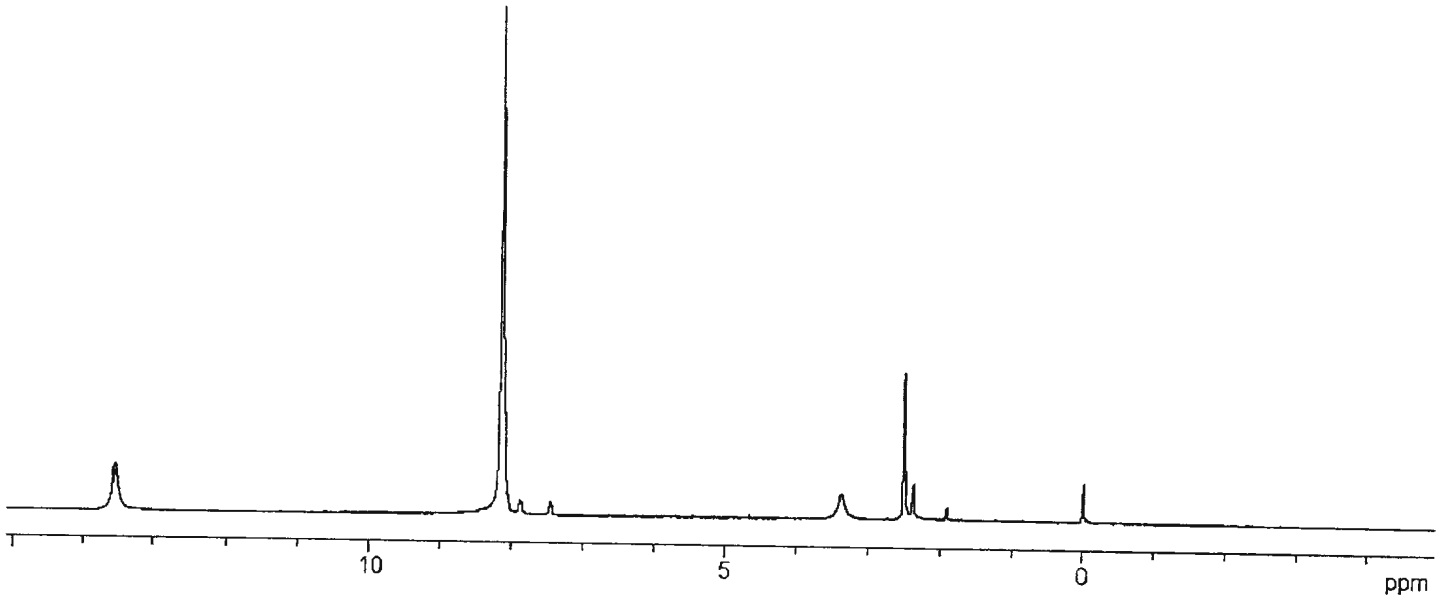

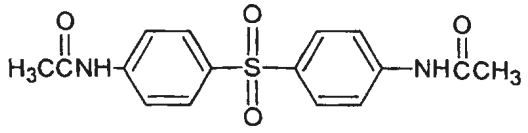

3 -9

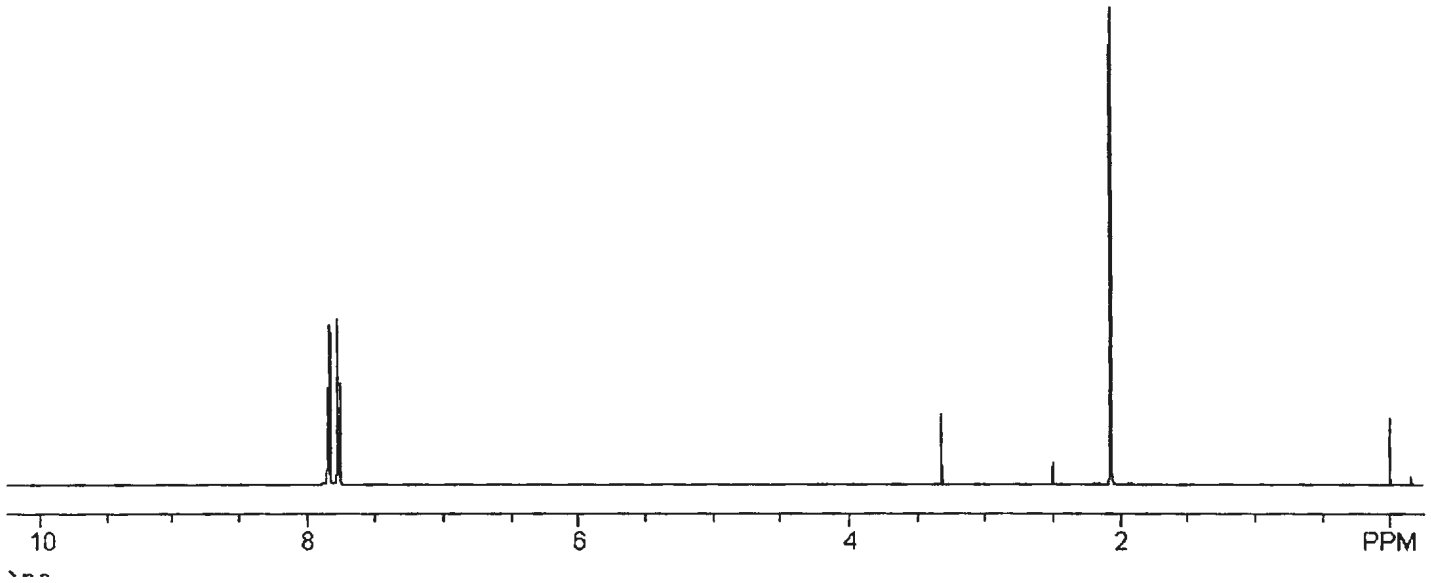

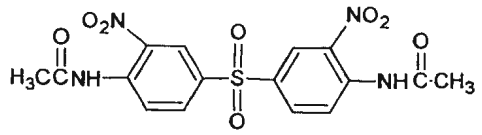

3 -10

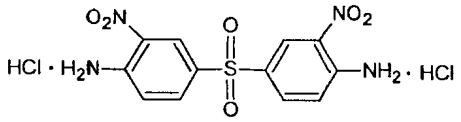

3 -11

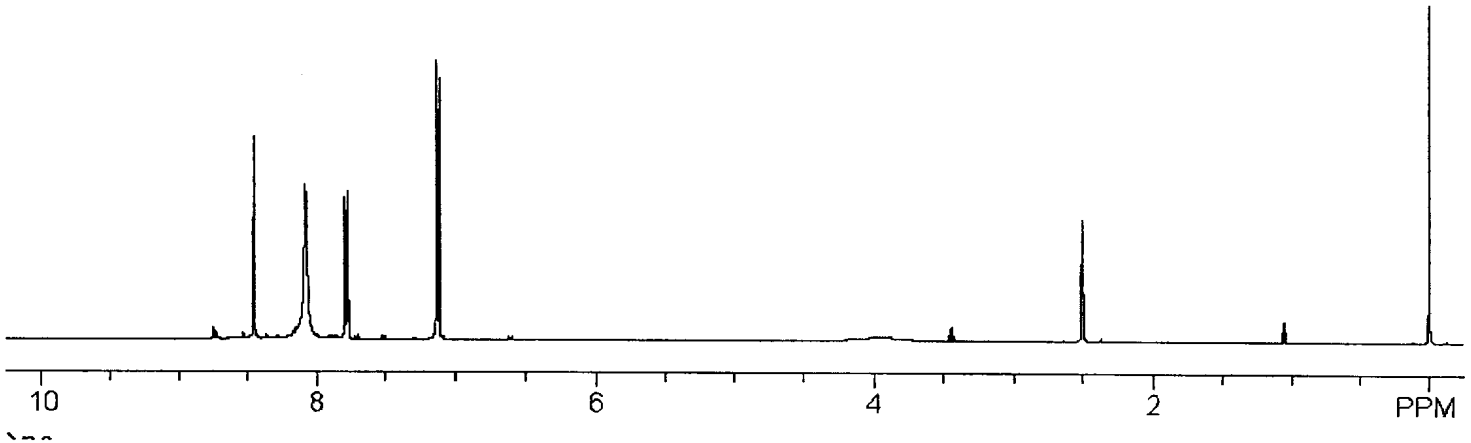

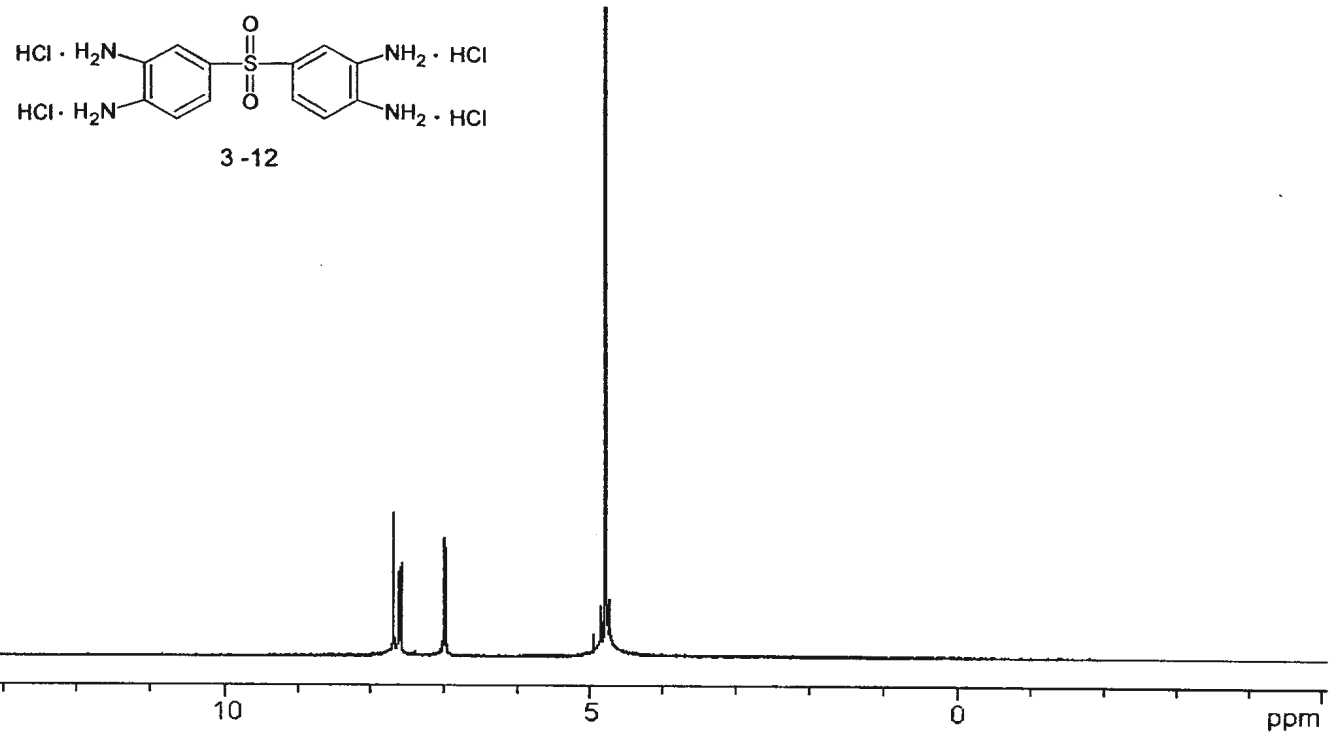
HCl · H2N
HCl · H2N
O
S
O
NH2 · HCl
NH2 · HCl
3 -12
10
5
0
ppm

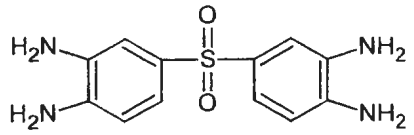

3 -13

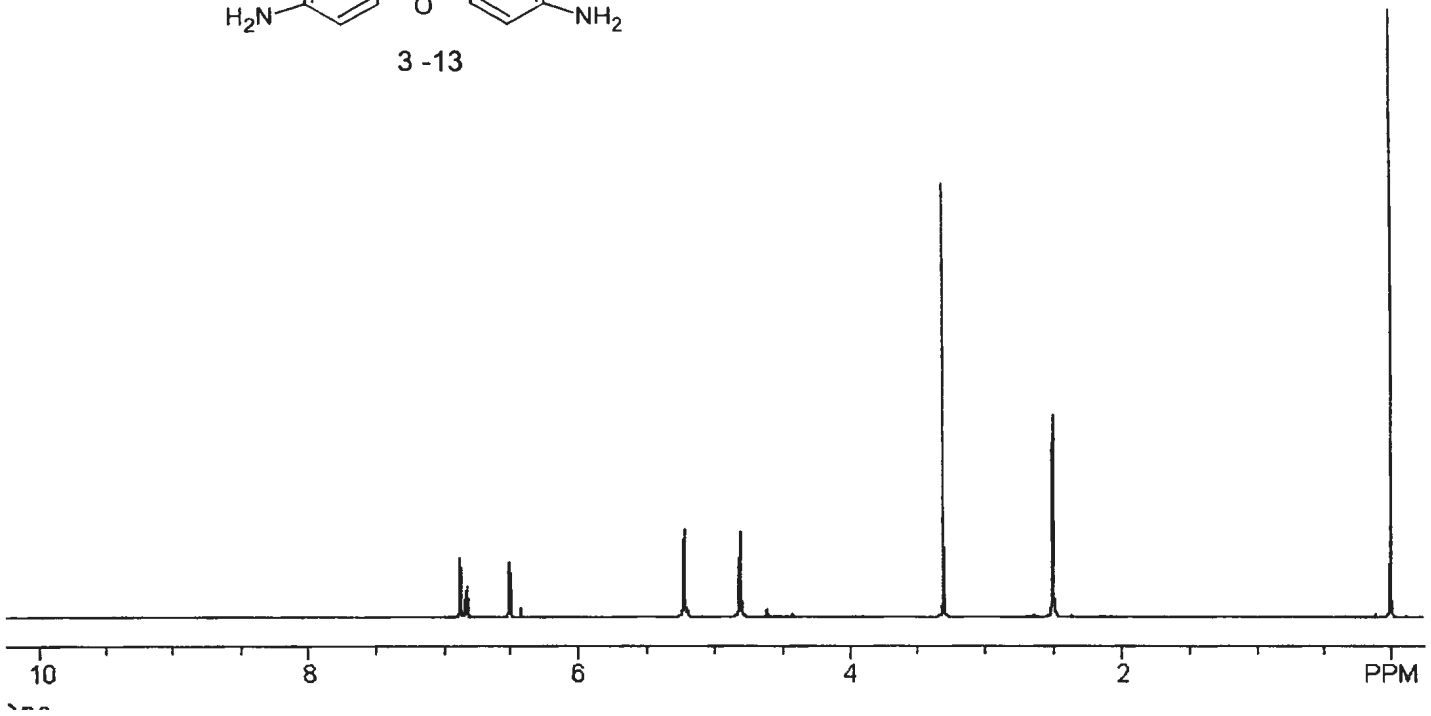

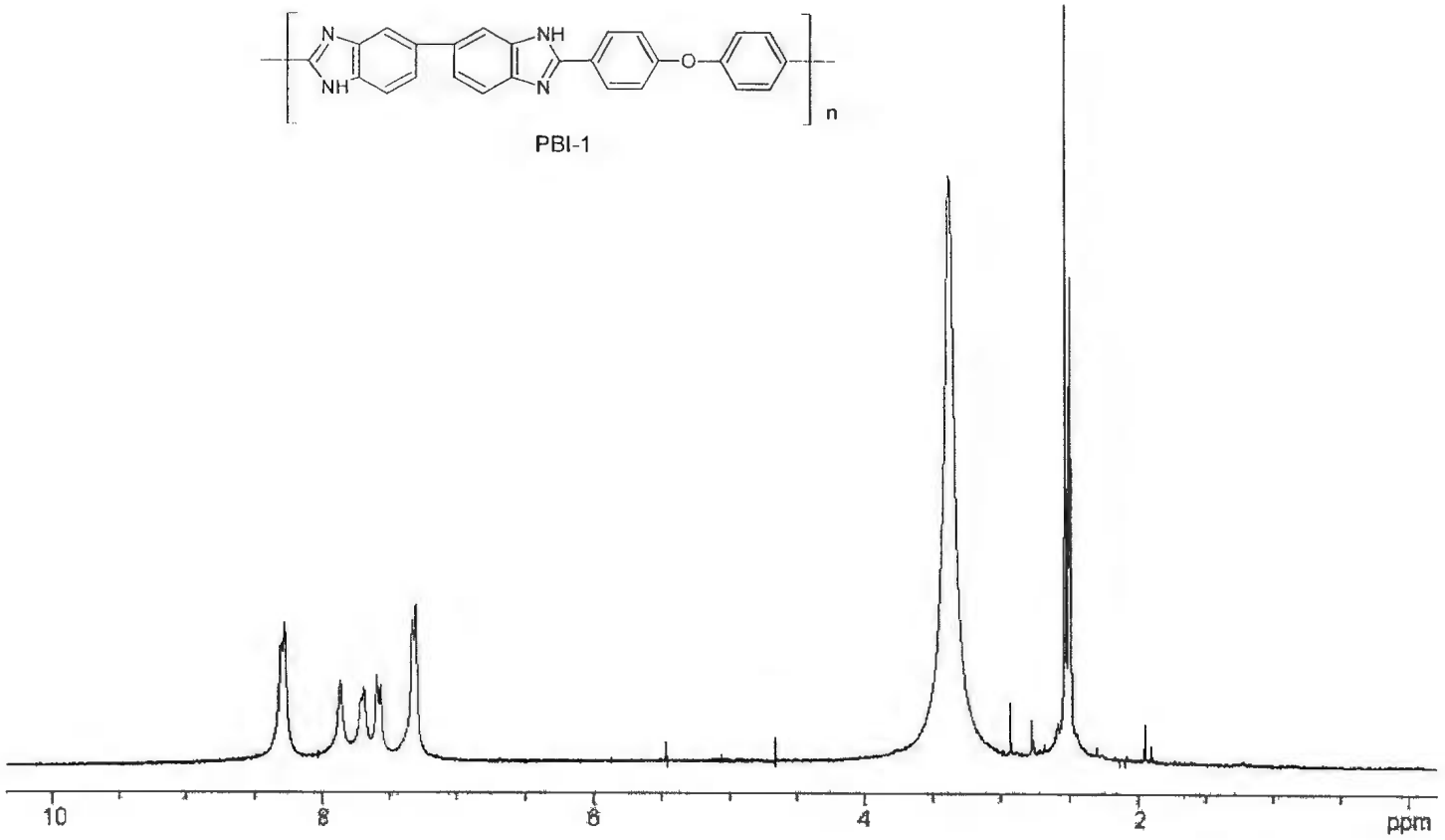
N
NH
NH
N
O
n
PBI-1
10
8
6
4
2
ppm

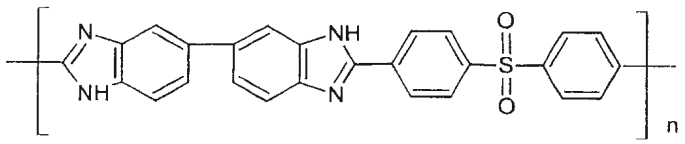

PBI-2

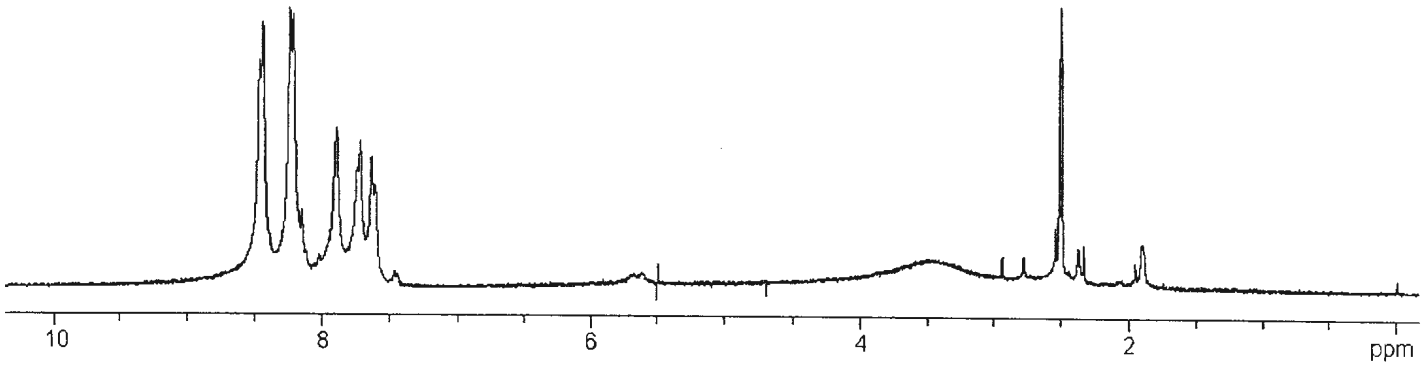

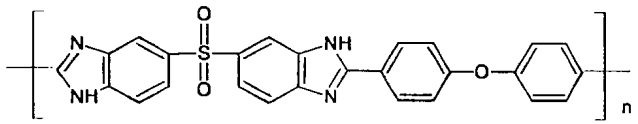

PBI-3

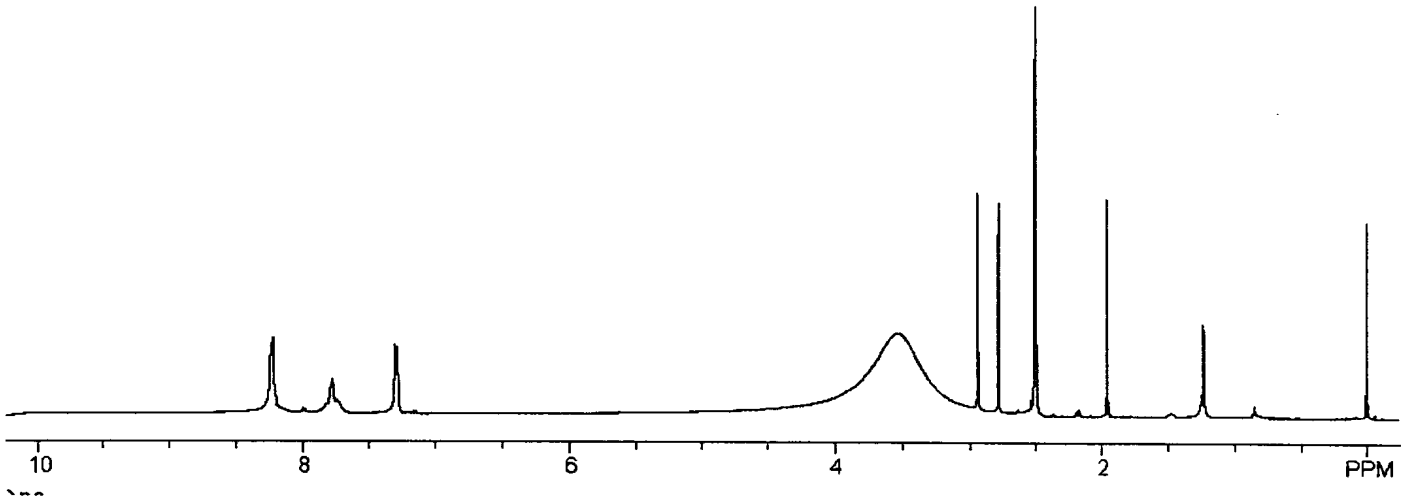

Appendix II

IR Spectra

Introduction

This appendix includes the IR spectra in this thesis.

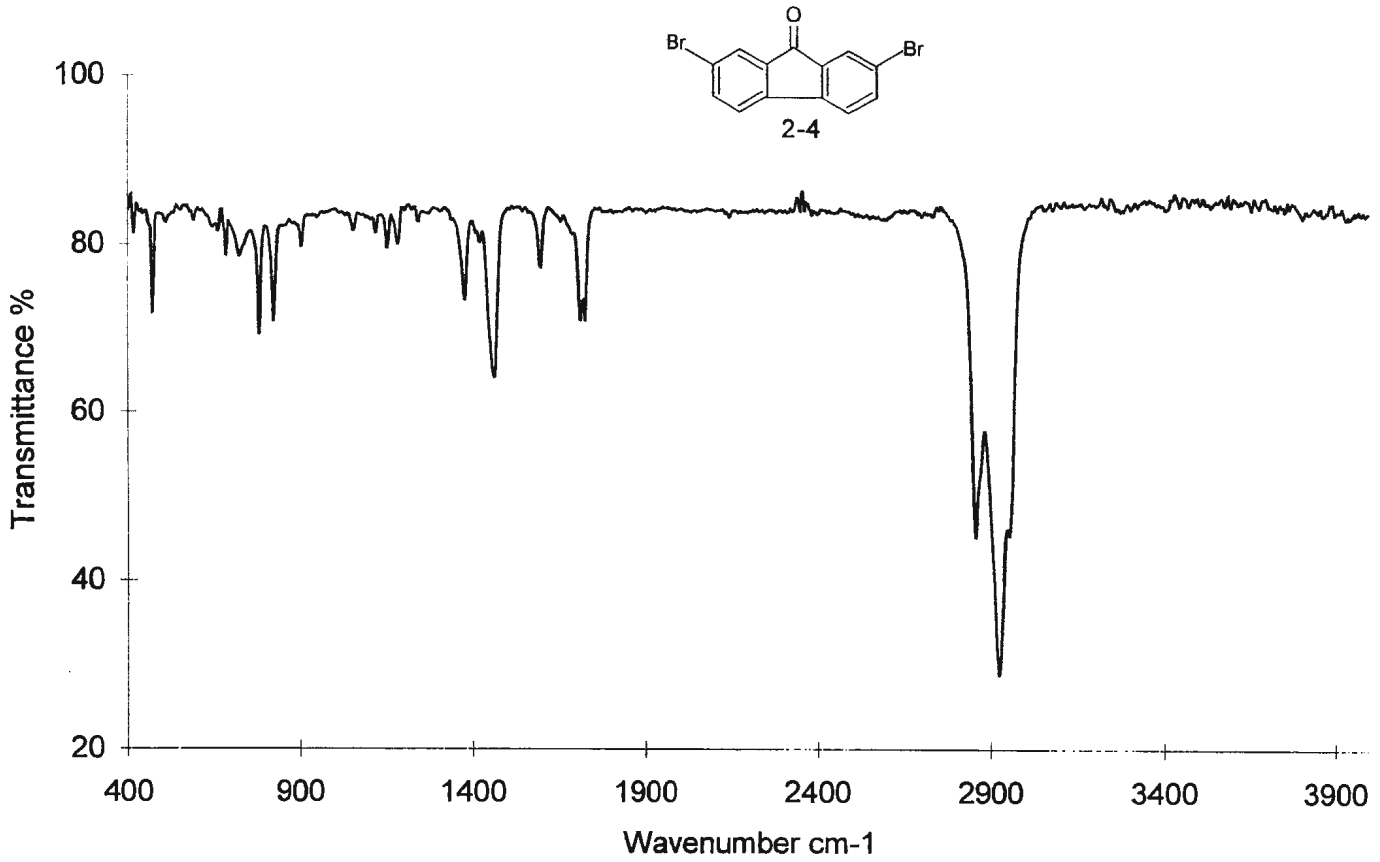
O
Br
Br
2-4
100
80
60
40
20
Transmittance %
400
900
1400
1900
2400
2900
3400
3900
Wavenumber cm-1

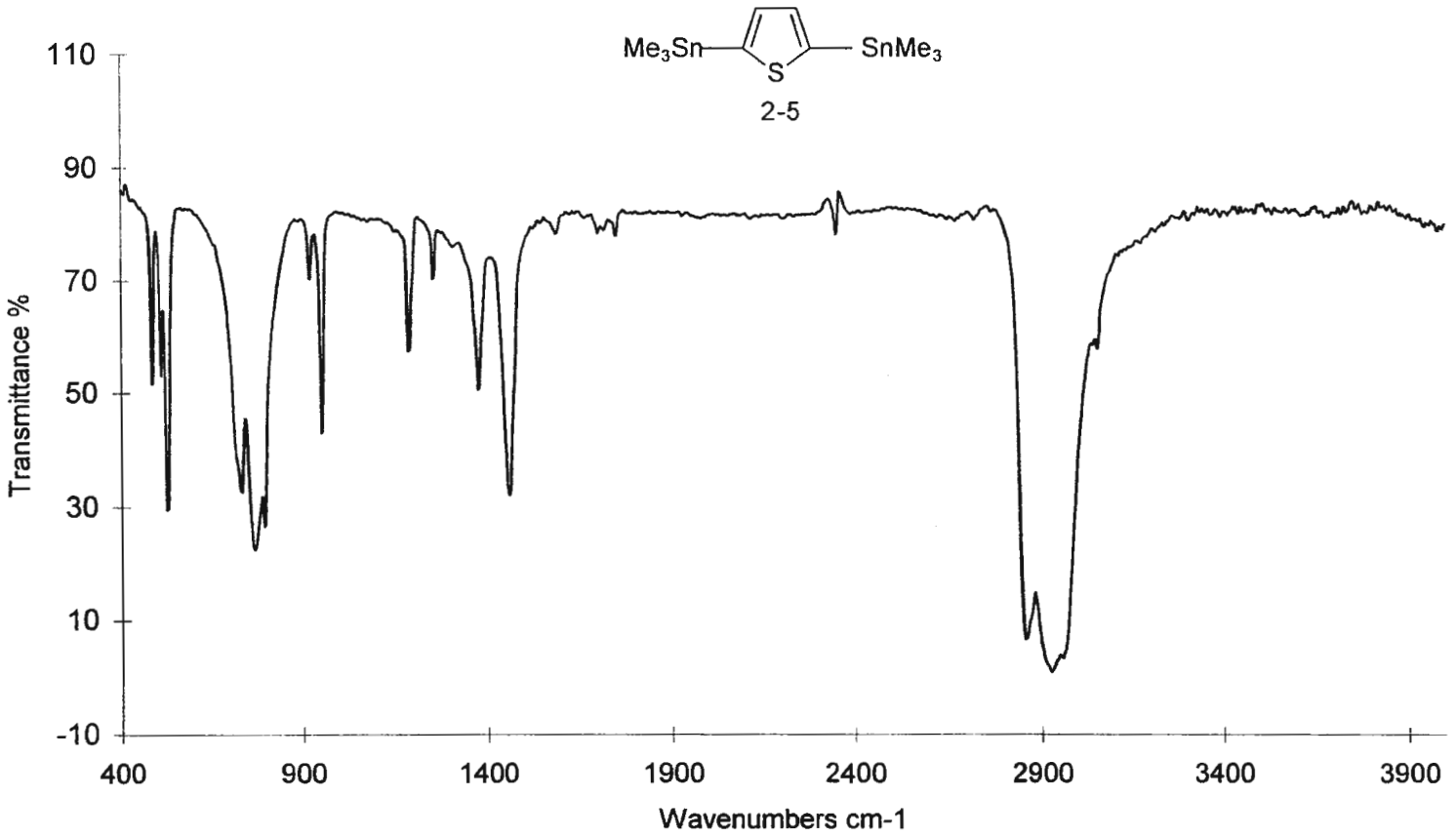
Me3Sn
SnMe3
S
2-5
110
90
70
50
30
10
-10
Transmittance %
400
900
1400
1900
2400
2900
3400
3900
Wavenumbers cm-1

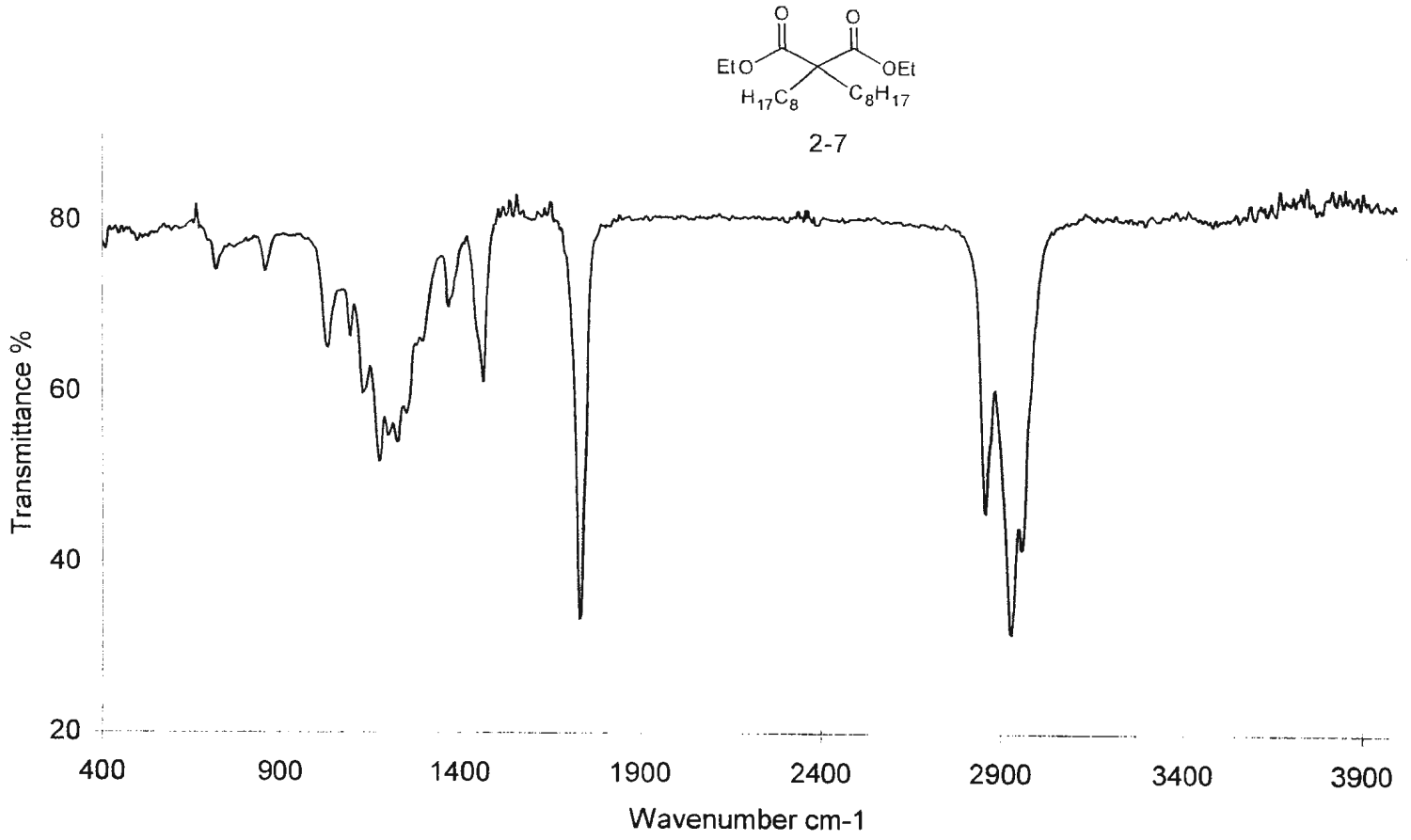
O
O
EtO
OEt
H17C8
C8H17
2-7
Transmittance %
80
60
40
20
400
900
1400
1900
2400
2900
3400
3900
Wavenumber cm-1

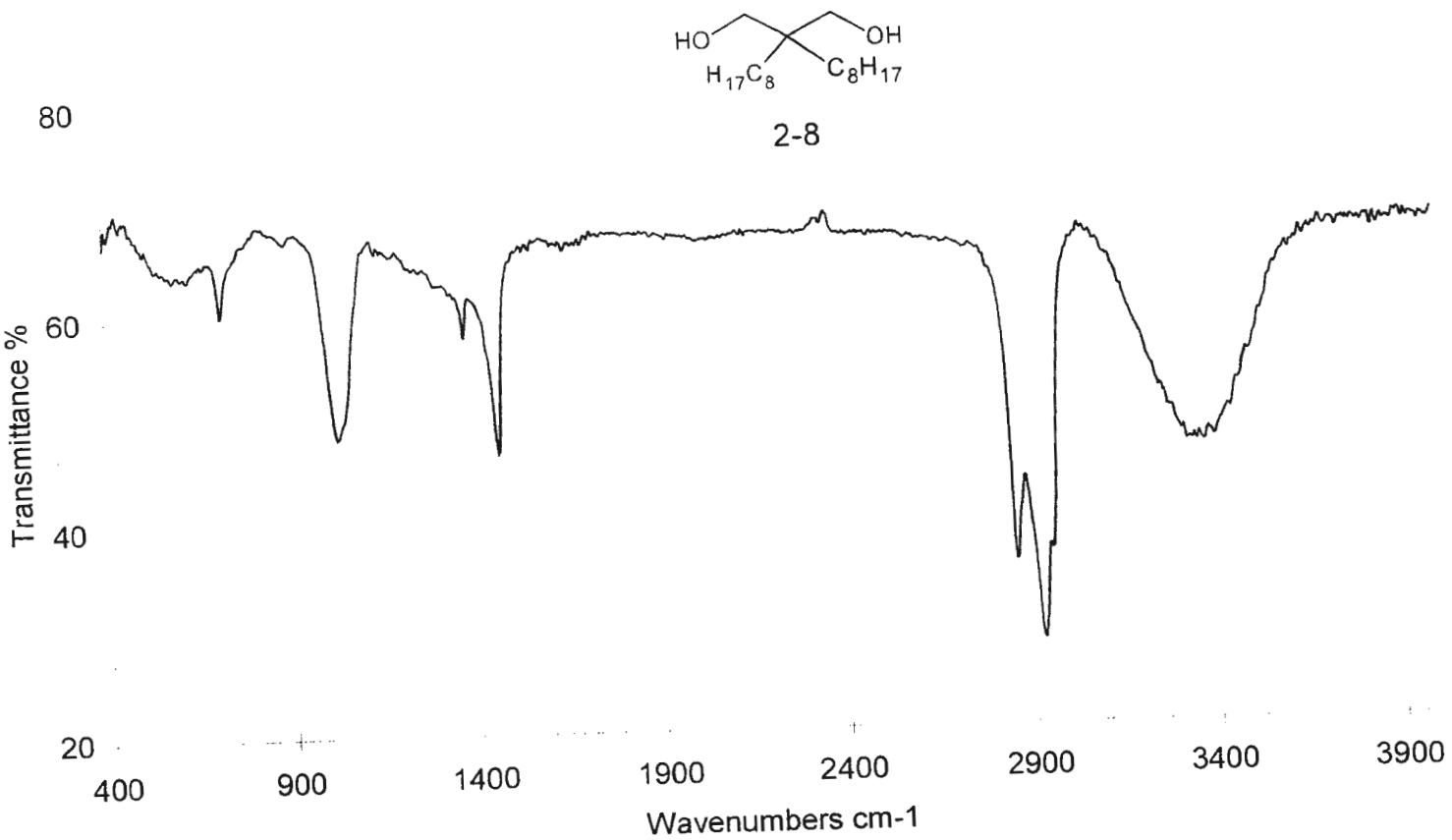
HO
OH
$H_{17}C_8$
C_8H_{17}
2-8
80
60
40
20
Transmittance %
400
900
1400
1900
2400
2900
3400
3900
Wavenumbers cm-1

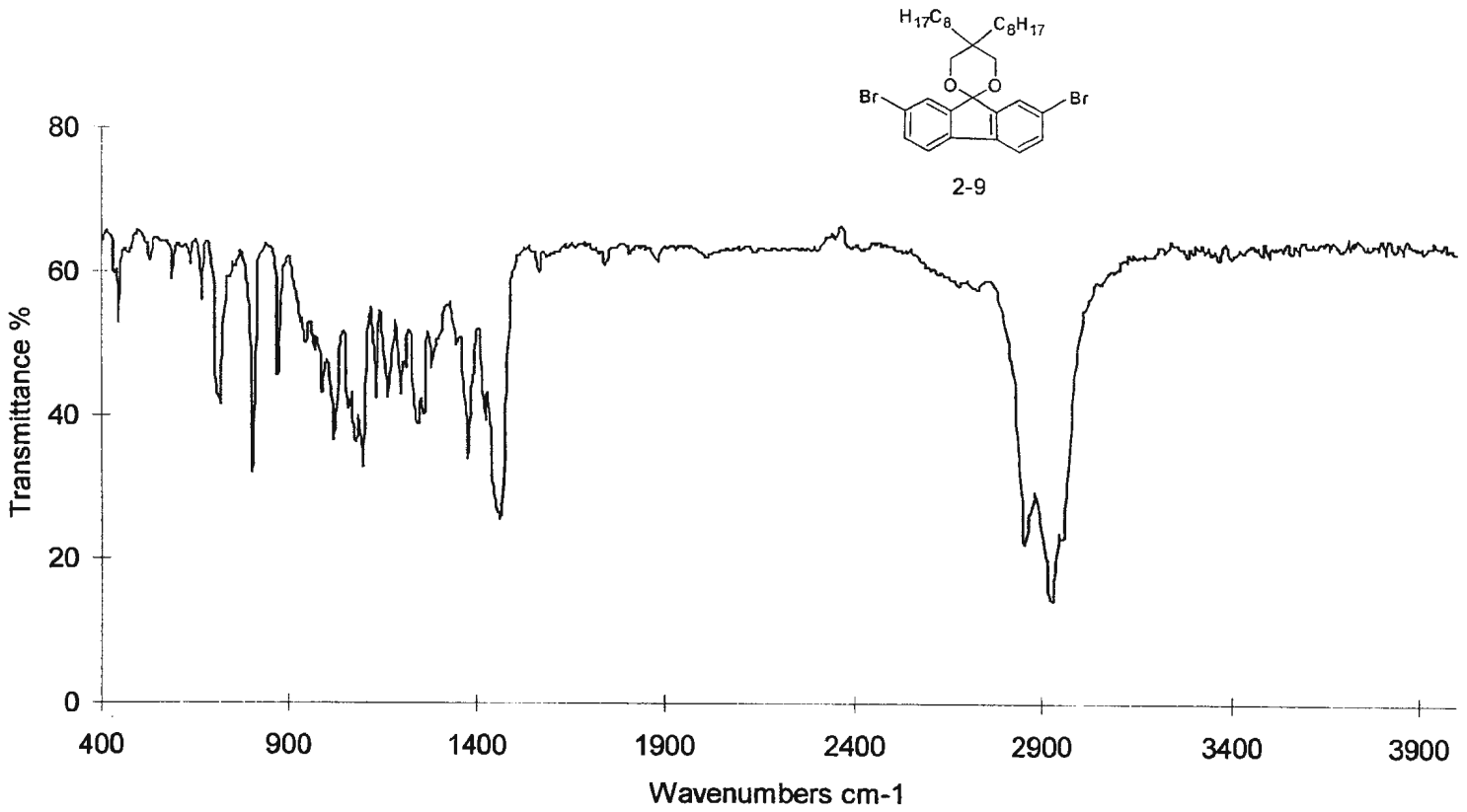
H17C8
C8H17
O
O
Br
Br
2-9
80
60
40
20
0
Transmittance %
400
900
1400
1900
2400
2900
3400
3900
Wavenumbers cm-1

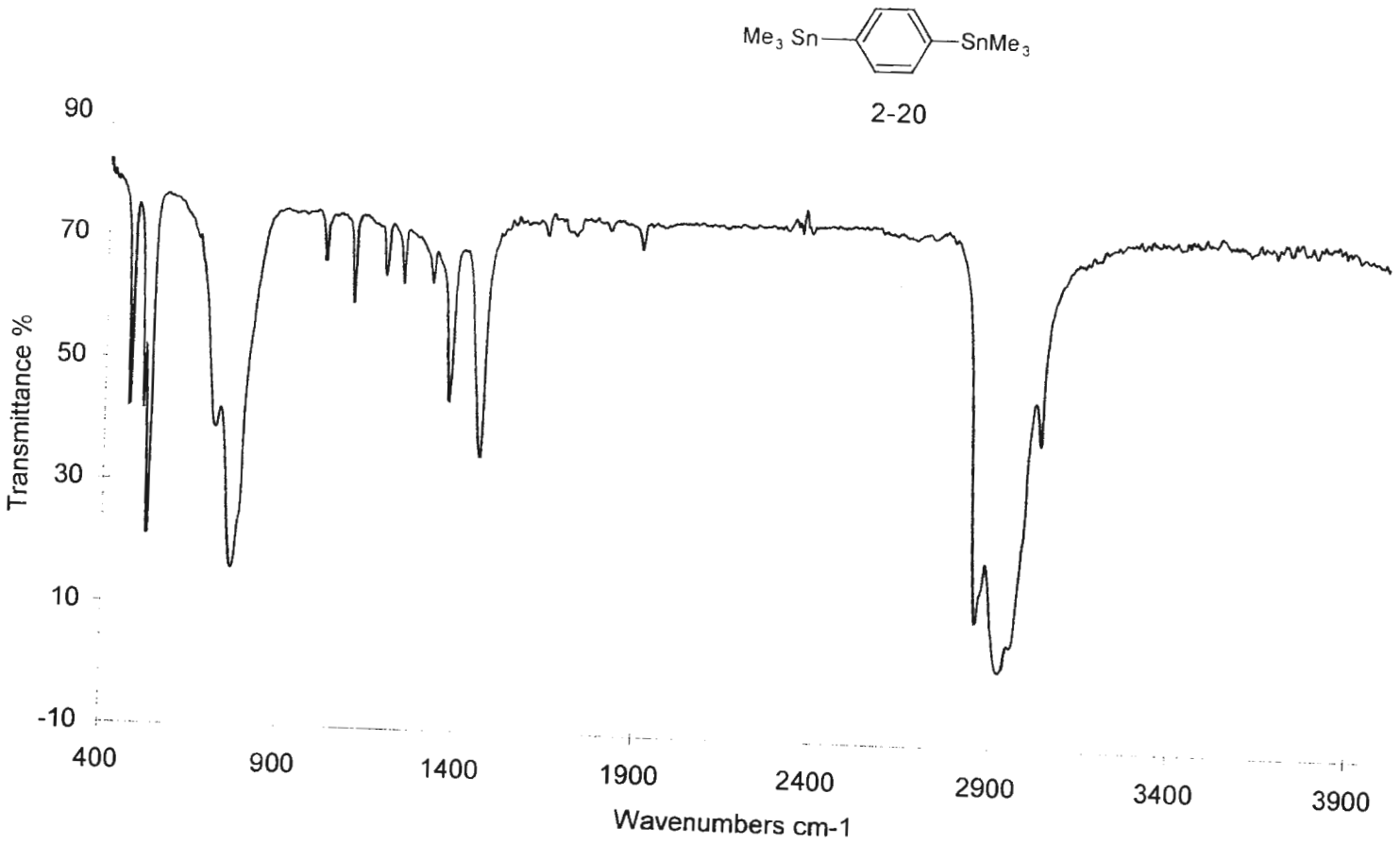
Me3 Sn
SnMe3
2-20
90
70
50
30
10
-10
Transmittance %
400
900
1400
1900
2400
2900
3400
3900
Wavenumbers cm-1

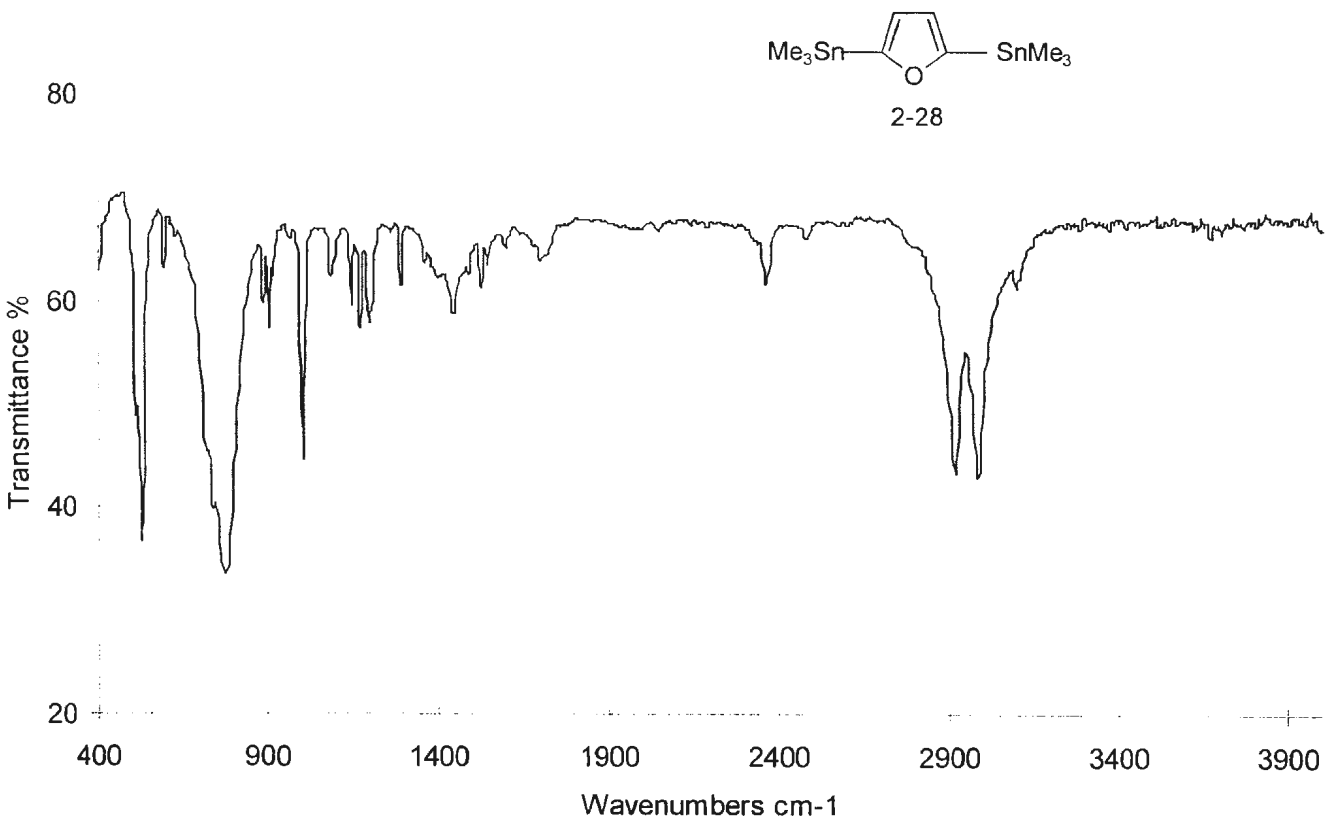
Me3Sn
SnMe3
O
2-28
80
60
40
20
Transmittance %
400
900
1400
1900
2400
2900
3400
3900
Wavenumbers cm-1

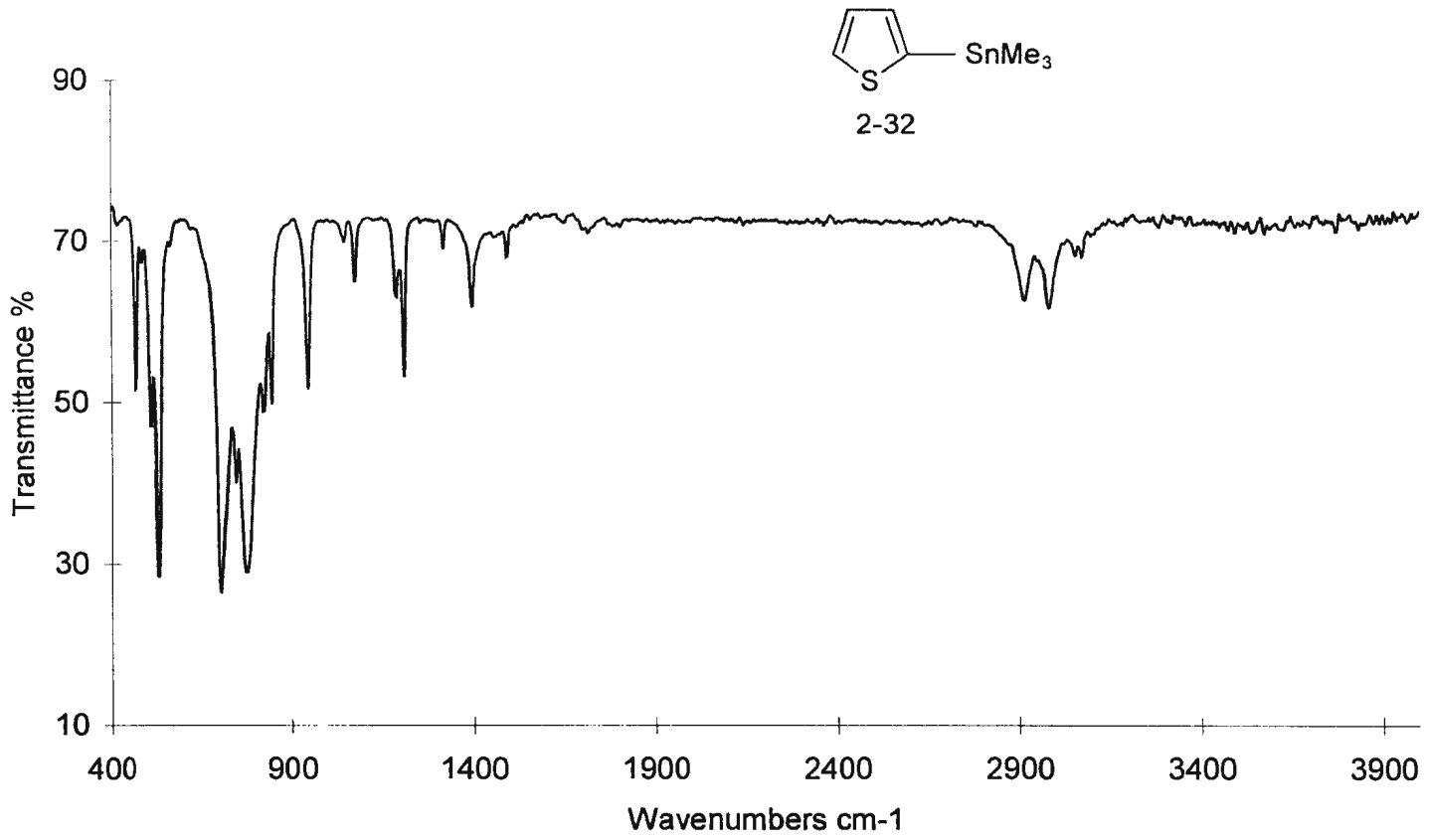
SnMe3
S
2-32
90
70
50
30
10
Transmittance %
400
900
1400
1900
2400
2900
3400
3900
Wavenumbers cm-1

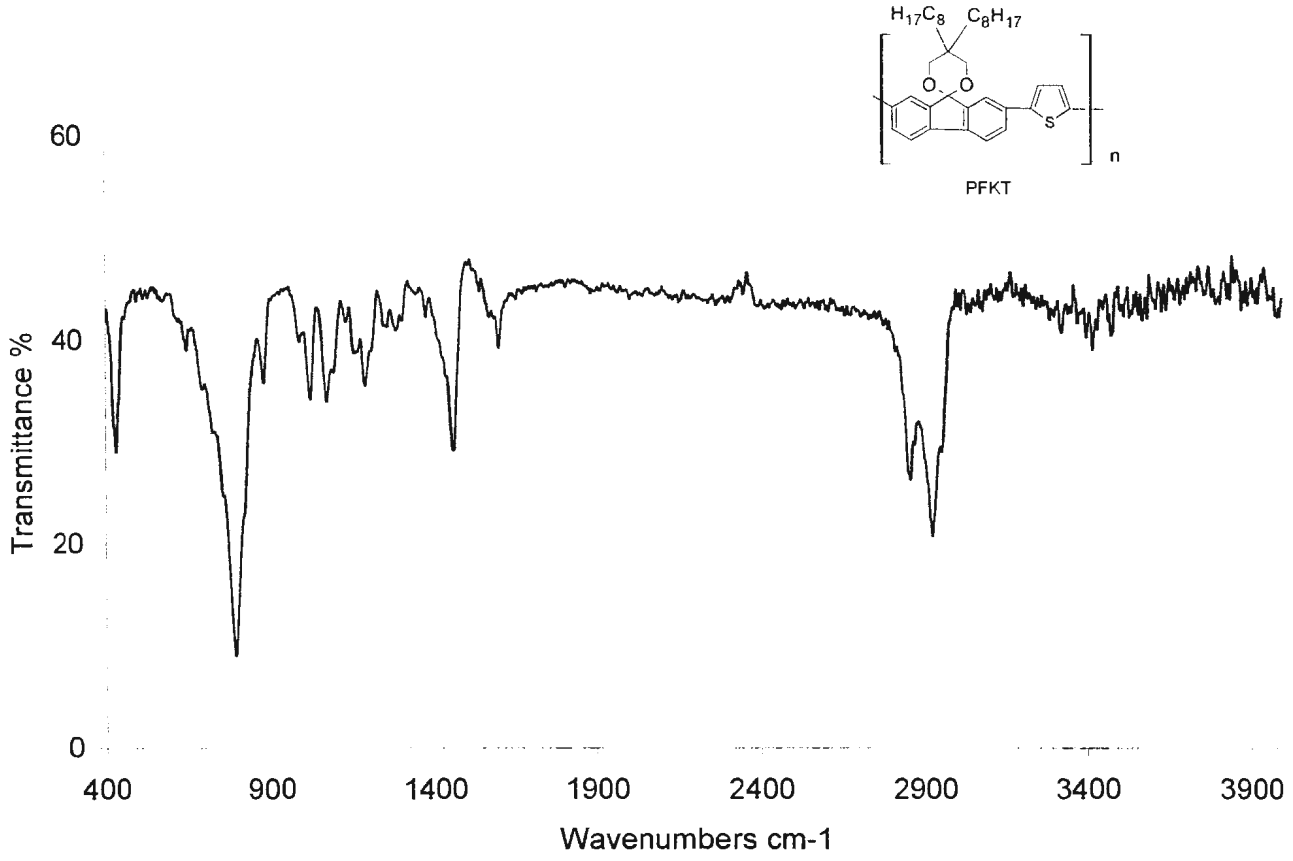
H17C8 C8H17
O
O
S
n
PFKT
60
40
20
0
Transmittance %
400
900
1400
1900
2400
2900
3400
3900
Wavenumbers cm-1

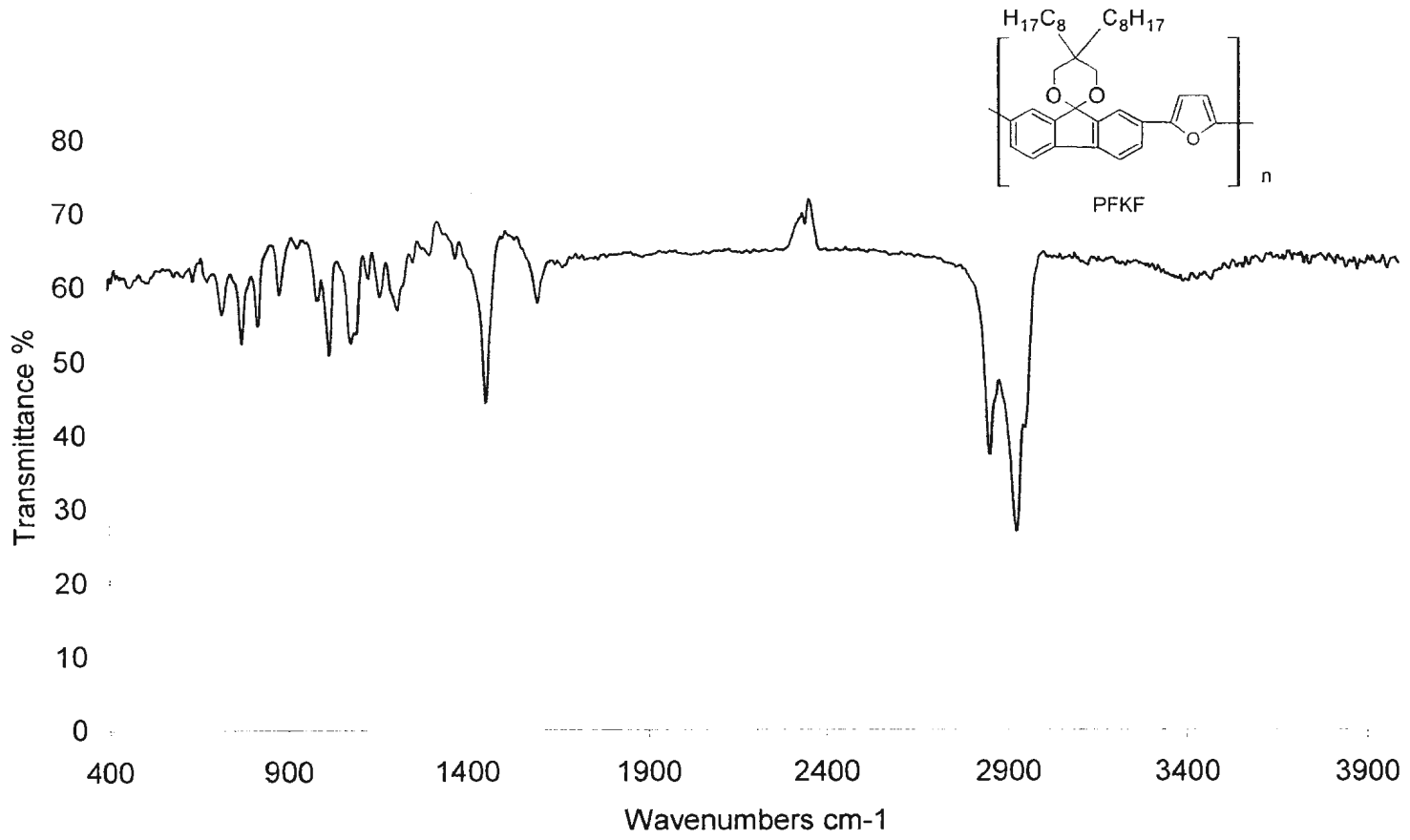
H17C8
C8H17
O
O
O
n
PFKF
80
70
60
50
40
30
20
10
0
Transmittance %
400
900
1400
1900
2400
2900
3400
3900
Wavenumbers cm-1

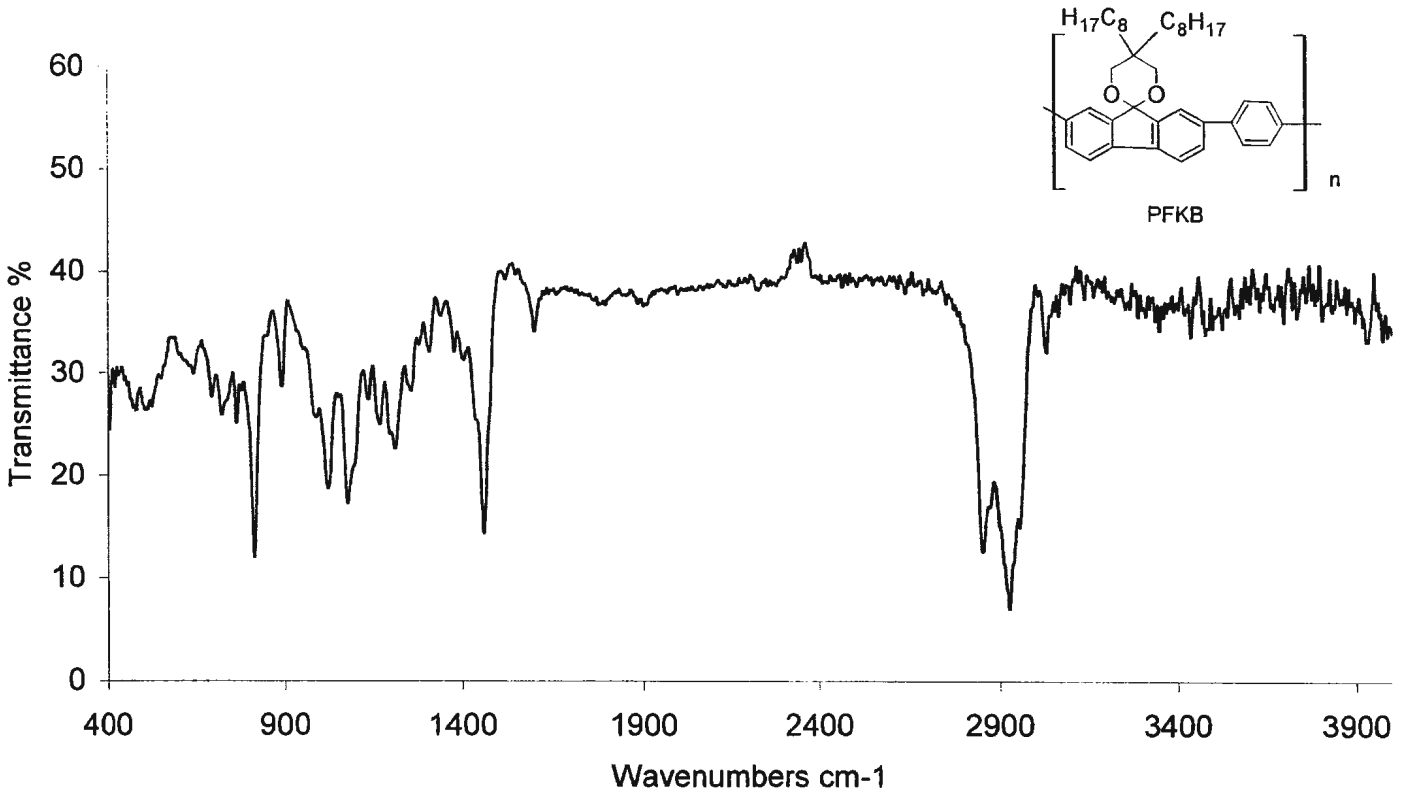
H17C8
C8H17
O
O
n
PFKB
60
50
40
30
20
10
0
Transmittance %
400
900
1400
1900
2400
2900
3400
3900
Wavenumbers cm-1

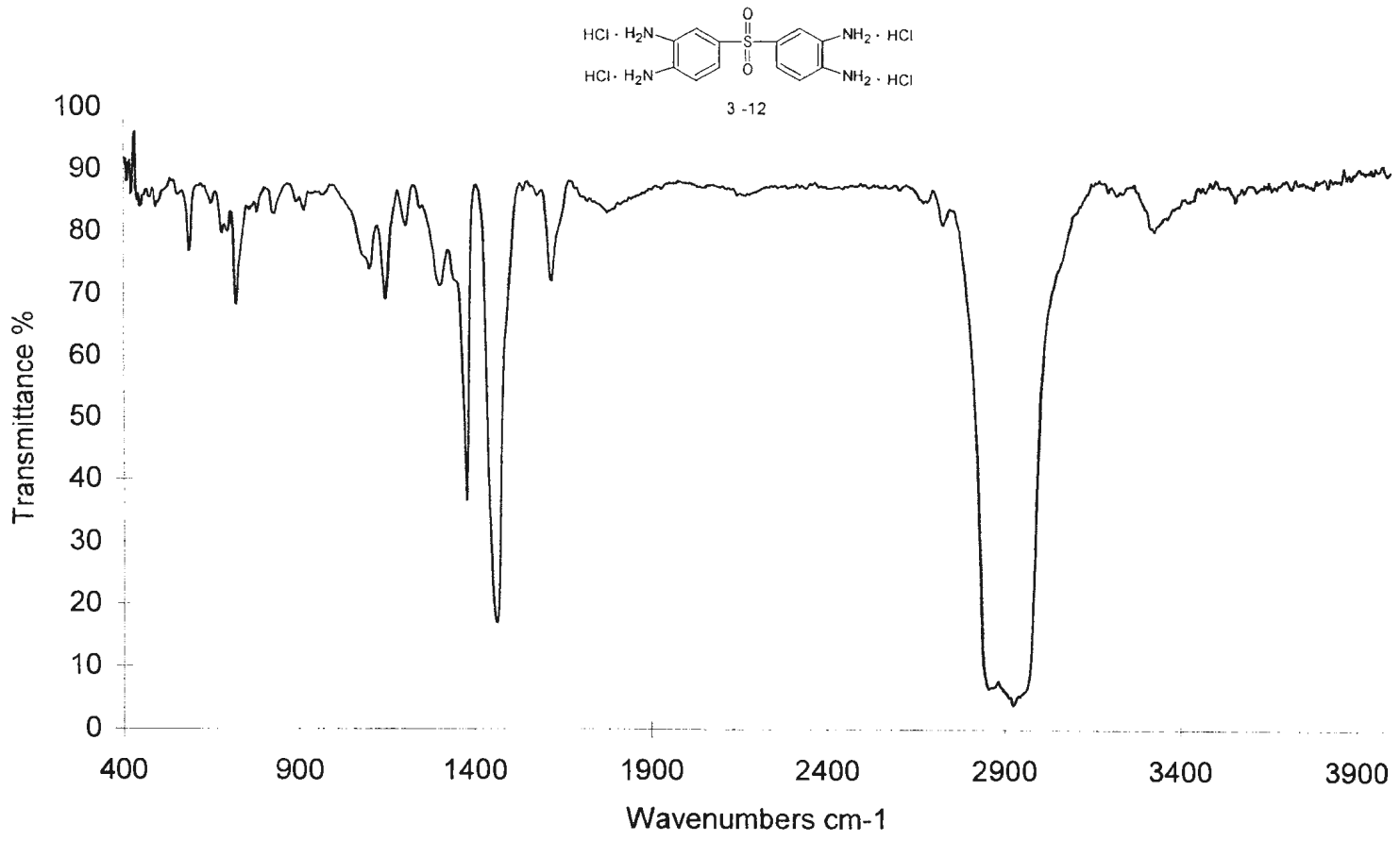
HCl · H2N
HCl · H2N
NH2 · HCl
NH2 · HCl
3 -12
Transmittance %
100
90
80
70
60
50
40
30
20
10
0
400
900
1400
1900
2400
2900
3400
3900
Wavenumbers cm-1

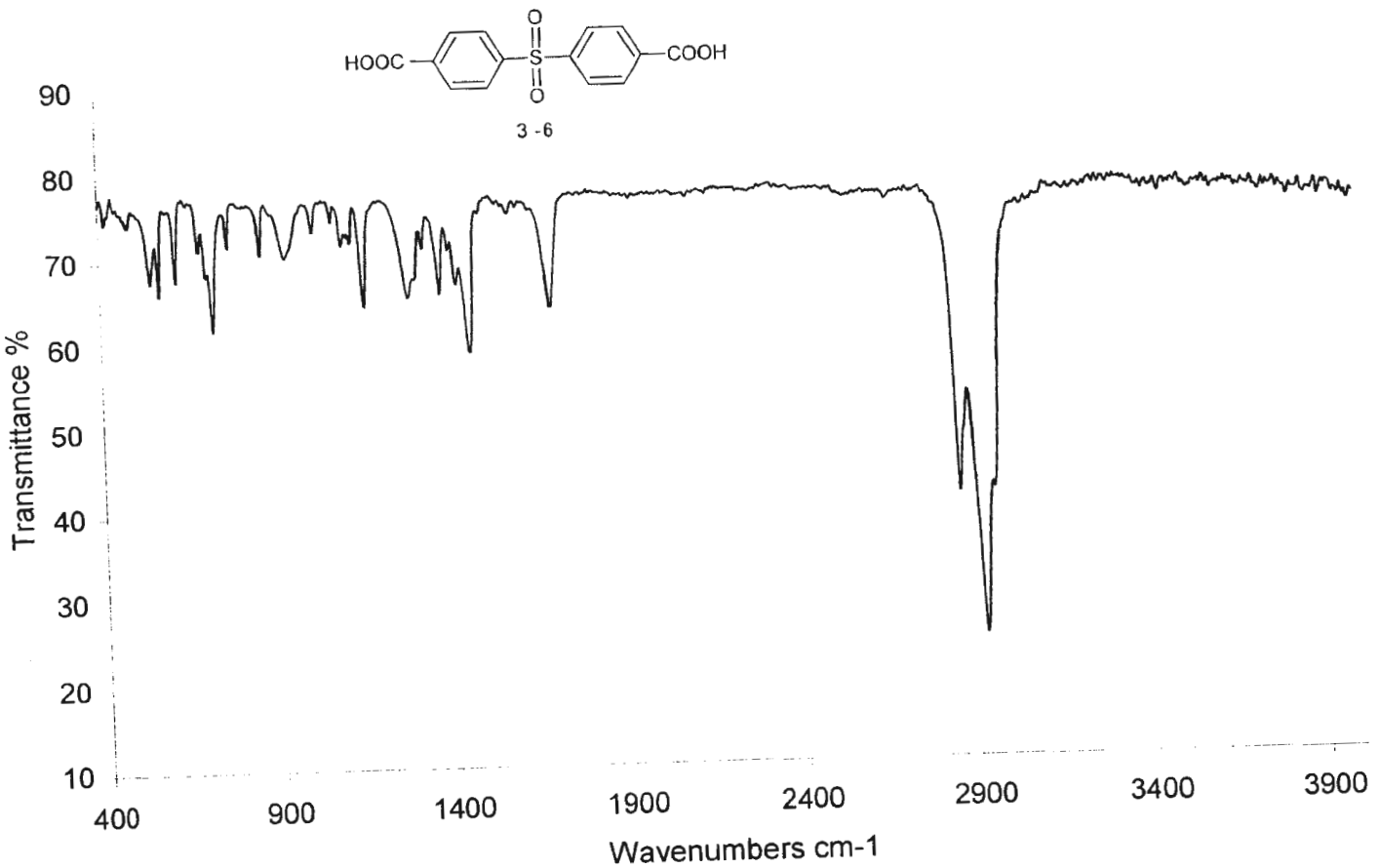
HOOC
COOH
O
S
O
O
3 -6
90
80
70
60
50
40
30
20
10
Transmittance %
400
900
1400
1900
2400
2900
3400
3900
Wavenumbers cm-1

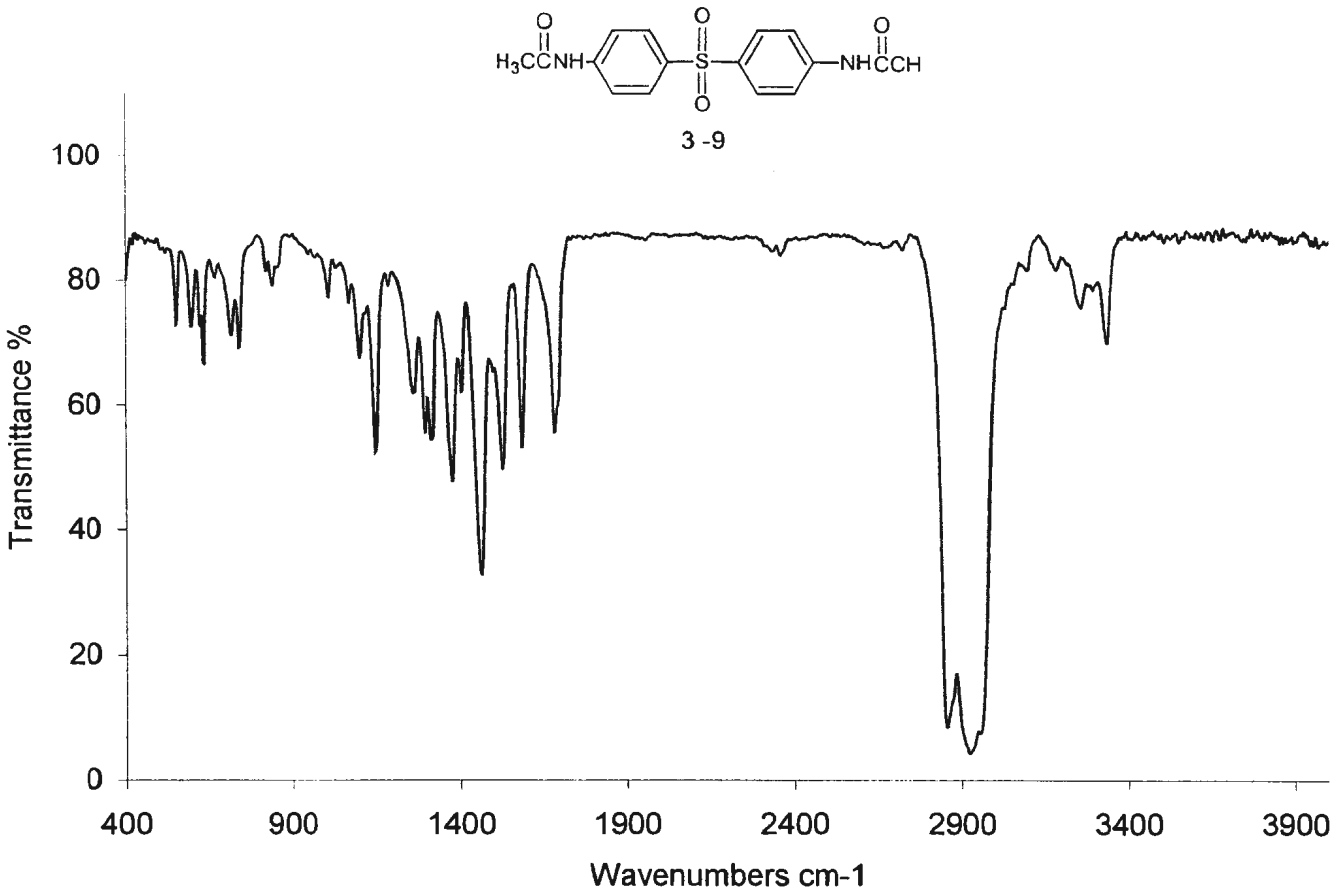
H3CCNH
NHCCH
3 -9
Transmittance %
100
80
60
40
20
0
400
900
1400
1900
2400
2900
3400
3900
Wavenumbers cm-1

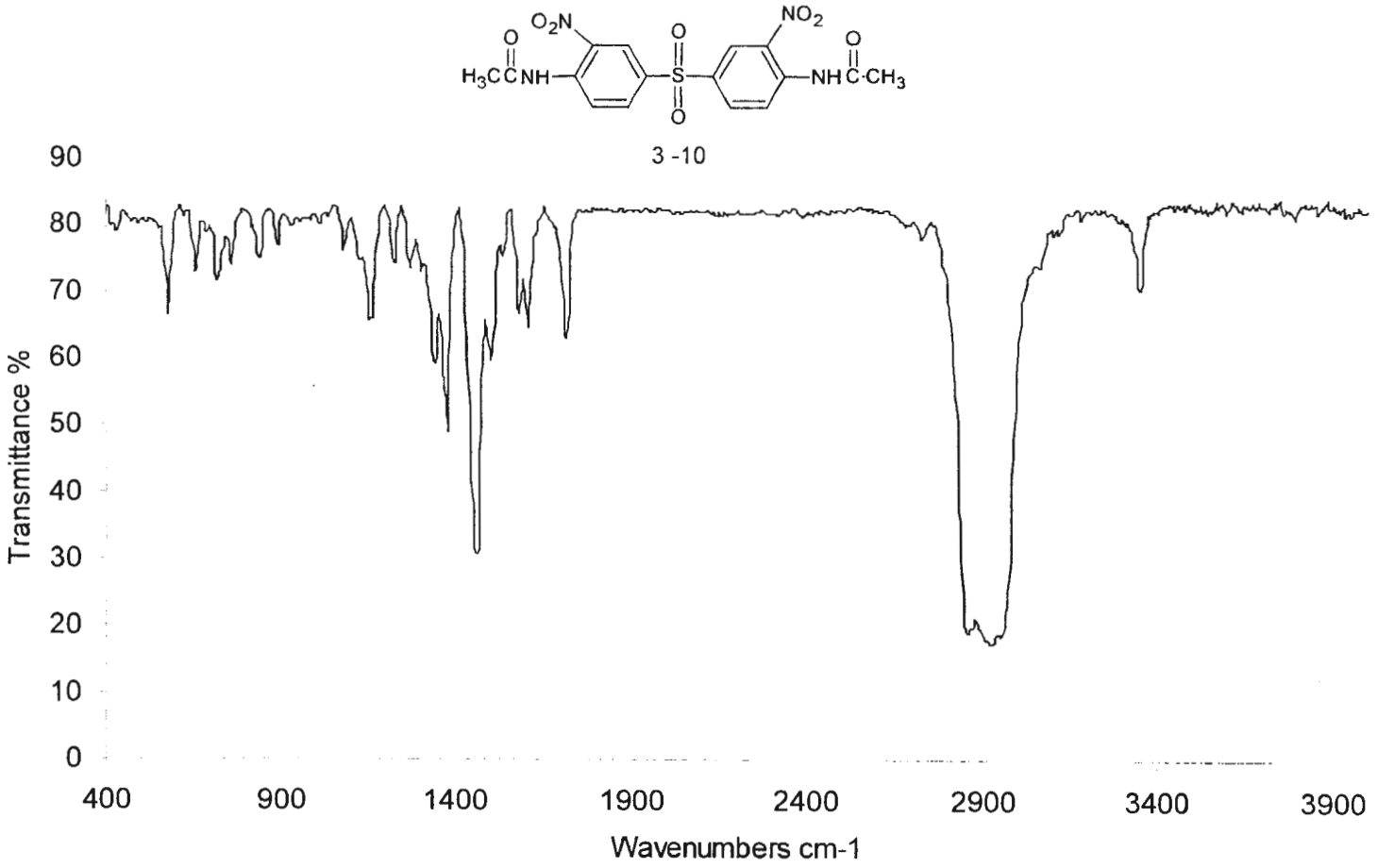
3 -10
Transmittance %
90
80
70
60
50
40
30
20
10
0
400
900
1400
1900
2400
2900
3400
3900
Wavenumbers cm-1

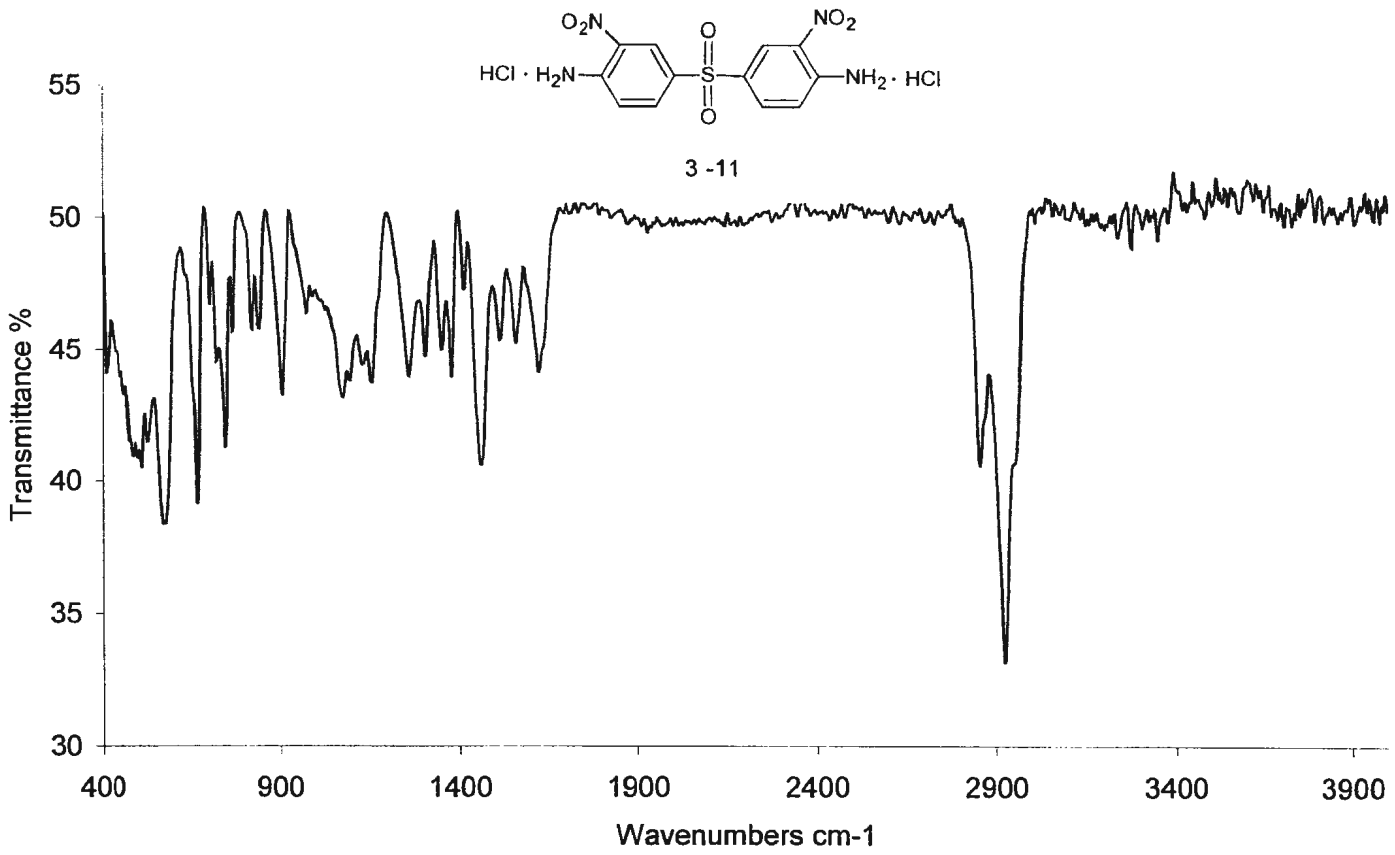
O_2N
NO_2
$HCl \cdot H_2N$
$NH_2 \cdot HCl$
O
S
O
3 -11
55
50
45
40
35
30
Transmittance %
400
900
1400
1900
2400
2900
3400
3900
Wavenumbers cm-1

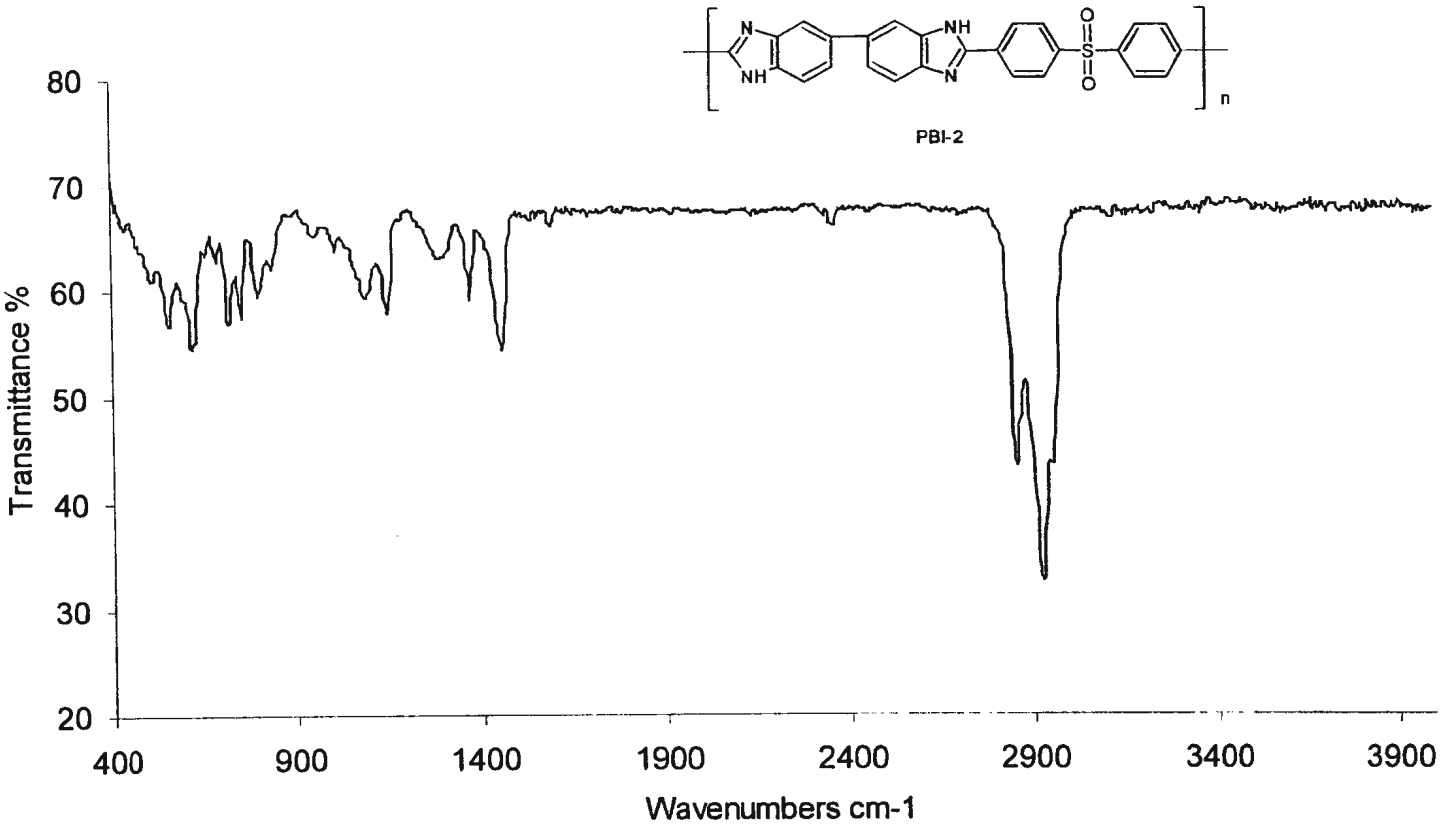
PBI-2
Transmittance %
80
70
60
50
40
30
20
400
900
1400
1900
2400
2900
3400
3900
Wavenumbers cm-1

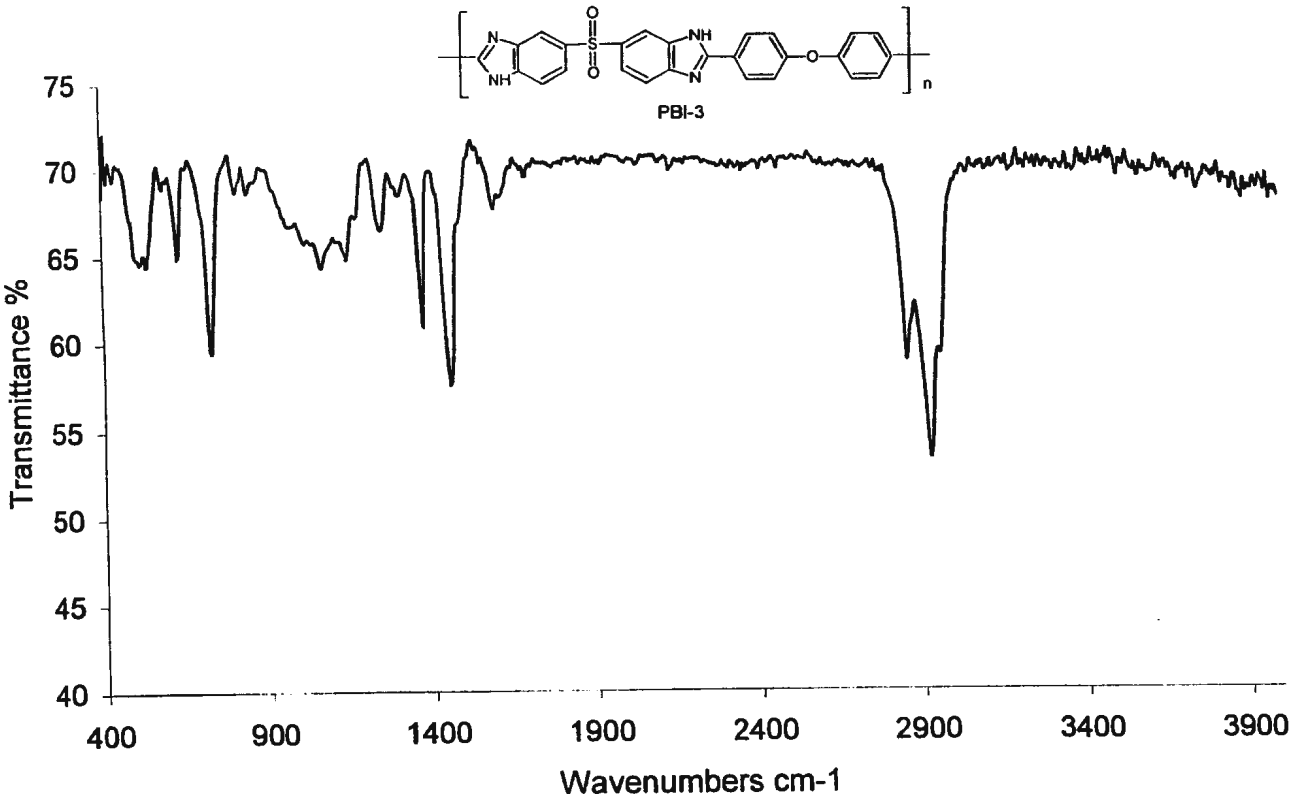
PBI-3
Transmittance %
75
70
65
60
55
50
45
40
400
900
1400
1900
2400
2900
3400
3900
Wavenumbers cm-1